
Editorial Office of *Earth's Cryosphere (Kriosfera Zemli)*
Institute of Geography, Russian Academy of Sciences
37 Vavilov str., office 22, Moscow, 117312 Russia
Editorial staff: *N.V. Arutyunyan, N.G. Belova, O.M. Lisitsyna, G.E. Oblogov*
Phone: 007(985) 957-10-01, e-mail: kriozem@gmail.com
Editor of the English translation: *D.E. Konyushkov*

Journal promoted by
Russian Academy of Sciences, Siberian Branch, Novosibirsk
Earth's Cryosphere Institute, Tyumen Scientific Centre SB RAS, Tyumen
Melnikov Permafrost Institute, SB RAS, Yakutsk

Editorial Manager *M.A. Trashkeeva*
Designed by *N.F. Suranova*
Typeset by *N.M. Raizvikh*

Photo by *V.A. Gabyshev*.
Delta of Lena River, Sokol bay. August 17, 2017.

RUSSIAN ACADEMY OF SCIENCES
SIBERIAN BRANCH
EARTH'S CRYOSPHERE INSTITUTE, TYUMEN SCIENTIFIC CENTRE
MELNIKOV PERMAFROST INSTITUTE

EARTH'S CRYOSPHERE
SCIENTIFIC JOURNAL

Founded in January 1997	6 issues per year	Vol. XXVII, No. 2	March–April 2023

CONTENTS

EARTH'S CRYOSPHERE
SCIENTIFIC JOURNAL

Earth's Cryosphere, 2023, vol. XXVII, No. 2, pp. 3–13

GEOTHERMAL FIELDS AND THERMAL PROCESSES IN CRYOSPHERE

GROUND TEMPERATURE AT THE DEPTH OF ZERO ANNUAL AMPLITUDE IN THE AREA OF SUPRAPERMAFROST TALIKS IN CENTRAL YAKUTIA

L.S. Lebedeva[1,*], N.E. Baishev[1], N.A. Pavlova[1], V.S. Efremov[1], V.V. Ogonerov[1], A.M. Tarbeeva[2]

[1]*Melnikov Permafrost Institute, Siberian Branch of the Russian Academy of Sciences, Merzlotnaya St. 36, Yakutsk, 677010 Russia*
[2]*Lomonosov Moscow State University, Faculty of Geography, Makkaveev Research Laboratory of Soil Erosion and Channel Processes, Leninskie Gory 1, Moscow, 119991 Russia*

**Corresponding author; e-mail: lyudmilaslebedeva@gmail.com*

Despite the low mean annual air temperature and low precipitation, subaerial suprapermafrost aquifer taliks are formed in some cases in the continuous permafrost zone of Central Yakutia. The paper presents an analysis of the seasonal and interannual dynamics of ground temperature in contrasting geocryological conditions – in areas of permafrost spread from the surface and in suprapermafrost subaerial taliks – of the key site Levaya Shestakovka 20 km southwest of Yakutsk. The permafrost table in this area occurs at depths from 0.5 to 20 m. The highest ground temperatures are typical of the aquiferous suprapermafrost taliks confined to gentle slopes composed of sandy sediments and covered with pine woodland. The thickness of the seasonally frozen layer reaches 3 m, and the depth of zero annual amplitudes varies from 6 to 12 m. Thawed deposits are preserved due to the continuous filtration of groundwater in them. The lowest ground temperatures are characteristic of the mire and the river floodplain. The depth of seasonal thawing varies from 0.5 to 1.0 m, and the depth of zero annual amplitudes exceeds 15 m. In recent years, slow freezing of the taliks from below has been noted due to mild cooling of the strata underlying the thawed aquifers. Beyond the area of taliks, weak multidirectional changes in ground temperature have been recorded.

Keywords: *suprapermafrost taliks, temperature at the depth of zero annual amplitude, Central Yakutia, sand deposits, groundwater, seasonally thawed layer, seasonally frozen layer, continuous permafrost*.

Recommended citation: Lebedeva L.S., Baishev N.E., Pavlova N.A., Efremov V.S., Ogonerov V.V., Tarbeeva A.M., 2023. Ground temperature at the depth of zero annual amplitude in the area of suprapermafrost taliks in Central Yakutia. *Earth's Cryosphere* XXVII (2), 3–13.

INTRODUCTION

Permafrost, common in Central Yakutia, has a thickness of 200 to 700 m [*Anisimova, 2003*]. The continuity of the permafrost zone is interrupted by through taliks under large lakes and the Lena River bed. The depth of seasonal thawing of rocks varies from 0.3 to 4.5 m and depends on the type of landscape [*Pavlov, 1979; Anisimova et al., 2005; Varlamov, Scryabin, 2012*]. In the basins of the Lena and Vilyui rivers, the existence of local subaerial suprapermafrost aquifers is known [*Ponomareva, 1999; Boitsov, 2002*]. The temperature regime of the rocks in them differs from the surrounding area. Under natural conditions, near the city of Yakutsk, the temperature of water-bearing sandy sediments of the suprapermafrost talik in the depth interval of 3–6 m is about 0°C throughout the year [*Lebedeva et al., 2019*]; outside the talik, it reaches –6.6°C [*Varlamov, Skryabin, 2012*]. In the Vilyui River basin, in areas composed of eolian sediments from the surface and covered with bearberry-lichen pine forest, the thickness of the seasonally frozen layer (SFL) above the taliks is 2.5–4.5 m [*Ponomareva, 1999; Lytkin et al., 2018*]. The seasonal and interannual regime of rock temperature in the areas of talik development and beyond remains poorly studied to date. Questions of the genesis, distribution, geometry, and seasonal and interannual dynamics of taliks are rarely raised [*Shepelev, 2011; Anisimova, Pavlova, 2014; Galanin, 2015; Semernya et al., 2018*]. The response of rock temperature in areas with widespread suprapermafrost taliks to climate warming has not been determined.

It is known that the current increase in air temperature leads to uneven degradation of the upper part of permafrost. Over 25 years of observation at the end of the 20th century, no increase in the thickness of the seasonally thawed layer (STL) was found in the peatlands of the north of Western Siberia [*Moskalenko, 1998*]. According to [*Vasiliev et al., 2020*], in the southern tundra and forest tundra of Western Siberia, the permafrost table subsided by 2–10 m; in the north-

ern taiga zone, by 4–6 m: in some areas, suprapermafrost taliks were formed. In the northeast of the European territory of Russia, observations on hummocky peatlands over a five-year period showed that the thickness of the STL is increasing [*Kaverin et al., 2019*]. In the Timan-Pechora region, the retreat of the southern permafrost boundary to the north has taken place since the 1970s. By 2008, it shifted to the north by 30–40 km in the Pechora Lowland, and up to 80 km on the denudation plains of the Cis-Ural region [*Oberman, Lygin, 2009*]. The area of continuous permafrost has decreased due to the appearance of new taliks and transition to discontinuous permafrost.

In northern Yakutia, there has been a tendency for an increase in the temperature of rocks in the tundra and taiga since the late 1990s [*Fedorov-Davydov et al., 2018*]. According to [*Boike et al., 2019*], the temperature of the rocks at the bottom of the annual heat transfer layer has increased since the early 2000s by 2–3°C. In some years (2007–2008 and 2010–2011), the depth of seasonal thawing of rocks increased by 10–20% of the norm.

An intensive increase in air temperature has been observed in Central Yakutia since the mid-1960s [*Gorokhov, Fedorov, 2018; Neradovskii, 2020*]. Meanwhile, some researchers note that an increase in the thickness of the STL and in the temperature of frozen rocks is weakly expressed [*Pavlov et al., 2002; Varlamov et al., 2020*]. The modern period as a whole is characterized by sufficient thermal stability of both high-temperature and low-temperature permafrost [*Varlamov et al., 2021*]. Other authors show that rock temperature in open (forestless) areas has increased by up to 0.5°C over the past three decades with a simultaneous increase in the depth of seasonal thawing, activation of thermokarst subsidence in areas of the development of wedged ice and suffusion processes in areas of discharge of intrapermafrost waters [*Fedorov et al., 2014; Gagarin et al., 2016*].

In south Yakutia, the thickness of the STL does not change significantly [*Zabolotnik S., Zabolotnik P., 2014*]. In many other regions of the permafrost zone, against the background of global climate warming, the mean annual permafrost temperature decreases, the ice content of rocks increases, and the thickness of the STL decreases [*Konishchev, 2009; Biskaborn et al., 2019*]. The aim of this work is to analyze the seasonal and interannual dynamics of rock temperature in contrasting geocryological conditions – in areas of permafrost spread from the surface and of suprapermafrost subaerial taliks within the key site of Levaya Shestakovka 20 km southwest of Yakutsk.

OBJECT OF STUDY

The Levaya Shestakovka site with an area of about 1 km^2 is located in the basin of the Shestakovka River, a small left tributary of the Lena River, on a gentle slope of a denudation plain with absolute heights of 190–210 m asl [*Shepelev et al., 2002*] (Fig. 1).

The climate of the study area is sharply continental with severe long winters and short hot summers. The mean annual air temperature at the nearest weather station in Yakutsk for the period of 1920–2019 is –9.5°C; the mean monthly air temperature in January is –40.5°C; in July, +19.1°C. The mean annual precipitation from 1937 to 2015 is 268 mm/yr, including 160 mm/yr of rainfall, 100 mm/yr of snow, and 8 mm/yr of mixed (liquid/solid) precipitation [*Bulygina et al., 2022a,b*].

Larch-birch forests grow in ravines and depressions and on level surfaces. Pine forests occupy mainly slopes and divides. Mires and swamps are developed along streams and lakes.

The upper part of the geological section down to a depth of 30 m is composed of loose sandy sediments with few clayey interlayers [*Boitsov, 1985*]. On the slopes and divides, fine- and medium-grained sands predominate. Their volumetric moisture content in the aeration zone does not exceed 2–8%. Sandy sediments have a quartz–feldspar composition; their bulk density is more than 1.70 g/cm^3, and their porosity is 33–35% [*Boitsov, 2002*]. Moistened (15–25%) sands are overlain by an organogenic layer in the bottoms of the valleys of streams and ravines [*Skryabin et al., 1999*].

The territory under consideration belongs to the area of development of non-stationary frozen strata, the thickness of which in the modern period reaches 400–500 m. The temperature of rocks at a depth of 100 m is from –0.6 to –1.0°C [*Boitsov, 1985*], and at the bottom of the layer of zero annual amplitudes, depending on the landscape, it varies from positive (close to 0°C) values to –2...–3°C and below [*Varlamov, Skryabin, 2012*]. The thickness of the STL varies from 4 m on gentle slopes and divides under pine forests to 0.5 m in mires. On the right-bank terrace of the Levaya Shestakovka River, a suprapermafrost subaerial aquifer talik 180–200 m in width and more than 500 m in length was discovered by drilling. According to the results of geophysical studies, the talik has a complex spatial pattern with several water-conducting branches, and its thickness varies from 3 to 20 m [*Lebedeva et al., 2019*]. In landscape terms, it is confined to a flat area with a bearberry-lichen pine forest.

Thin (up to 3 m) water-bearing subaquatic taliks are distributed under bead-like widenings of the Levaya Shestakovka River channel. They are confined to areas where, due to the great depth of the river (up to 4 m), a layer of water remains under the ice in winter [*Tarbeeva et al., 2019*].

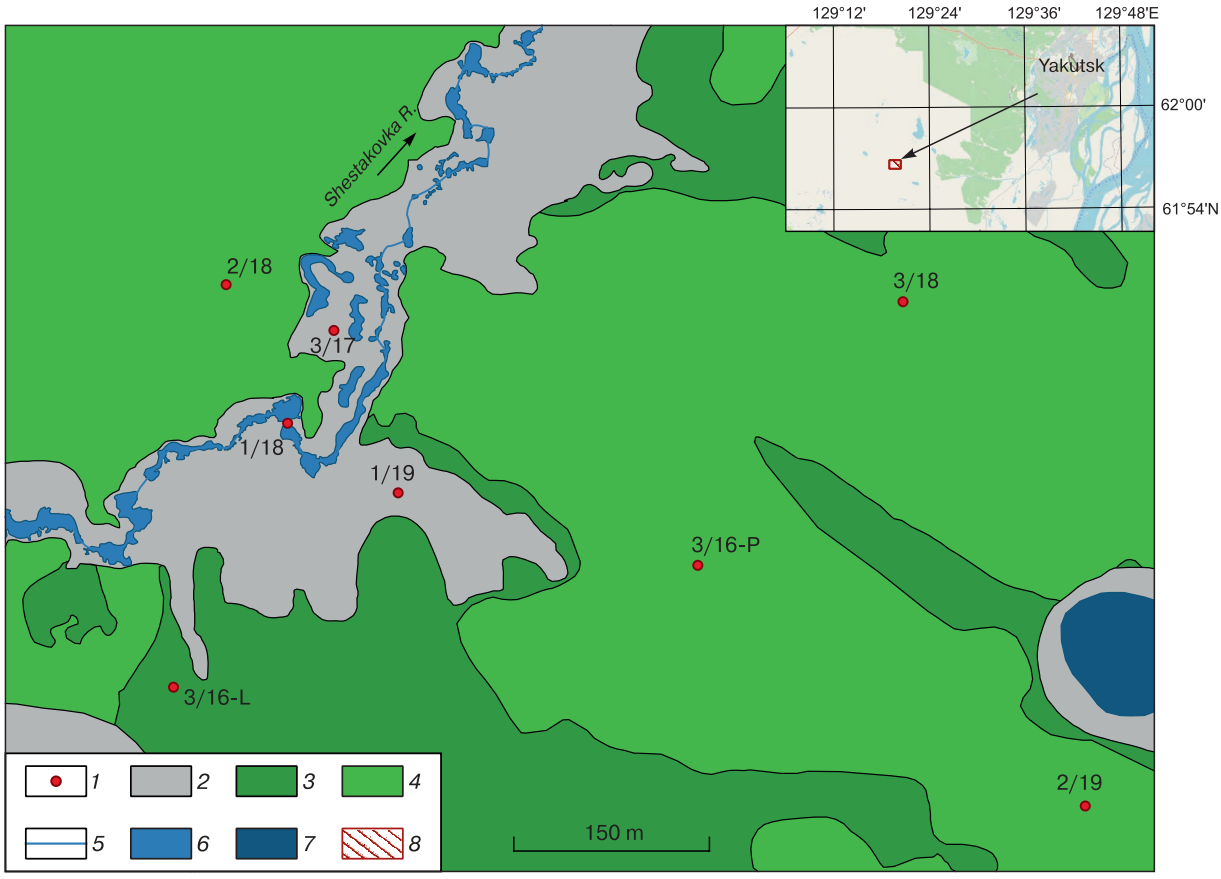

Fig. 1. Location of thermometric boreholes in the Levaya Shestakovka River basin:

1 – well, *2* – floodplain of the river and mire, *3* – larch forest, *4* – pine forest, *5* – river, *6* – widening of the river bed, *7* – lake, *8* – study area on the inset map.

RESEARCH METHODS

Drilling. Eight thermometric boreholes were drilled in different landscape and geomorphic conditions at the Levaya Shestakovka site in 2016–2019. Drilling works were carried out in April, when the layer of seasonal freezing reaches its maximum. Four boreholes were located under pine forests (Fig. 1; Table 1). The birch-larch forest, mire, flooded floodplain, and the Shestakovka River channel were characterized by one thermometric borehole each. Drilling was accompanied by core sampling to determine the moisture content of the rocks by the thermostatic-weight method. The texture of sediments from boreholes 3/16-P and 3/16-L was determined in the field; particle-size distribution of sediment samples from other boreholes was determined by the aerometric and sieve methods in laboratory conditions.

Monitoring of rock temperature within the Shestakovka River catchment. Six thermometric boreholes were equipped with temperature braids fitted with Maxim Integrated DL18B20 sensors. Temperature sensors were installed every 0.5 m up to a depth of 5 m and every meter in deeper layers (Table 1). Temperature measurement accuracy with DL18B20 thermistors is ±0.5°C. Readings were taken manually once a month. Two boreholes (3/16-P and 3/16-L) were equipped with Onset HOBO U12 temperature loggers. Recordings were made every three hours. The temperature measurement accuracy of Onset thermistors is ±0.25°C in the temperature range of 0–50°C and ±0.5°C at –20°C. As a rule, the thermistor error does not go beyond ±0.1°C [*Konstantinov et al., 2011*].

At the Onset HOBO weather station installed 2.5 km from the key site, the surface air temperature, the amount of liquid precipitation, and other basic meteorological parameters were recorded.

RESULTS

The structure of the upper part of the geological section in the key area. The main landscape units in the key area are represented by gentle slopes covered by pine forests, ravines and depressions with a predominance of larch forests and moss-herb mires, and the bottom of the Levaya Shestakovka River val-

Table 1. **Characteristics of temperature boreholes**

Borehole no.	Depth, m	Presence of talik	STL, m	SFL, m	Depth of zero annual amplitude, m	Soil composition	Location	Availability of data	Installed sensors
3/16-P	6	Yes	–	<3.0	<6	Fine and medium sand	Pine forest	Apr. 2016–Sep. 2019	Logger, 4 sensors at depths of 0.5, 1.0, 3.0, and 6.0 m
3/16-L	3	No	>1.0	–	*	Fine- and medium sand	Larch forest	Apr. 2016–Sep. 2019	Logger, 4 sensors at depths of 0.5, 1.0, 2.0, and 3.0 m
3/17	20	No	0.5–1.0	–	20	Peat, loam, loamy sand, sand	Floodplain	Apr. 2017–Oct. 2020	26 sensors: every 0.5 m from 0 to 5 m and every meter from 5 to 20 m
1/18	12	No	2.5	–	15	Peat, sandy loam, fine and medium sand	Riverbed	Apr. 2018–Oct. 2020	18 sensors: every 0.5 m from 0 to 5 m and every meter from 5 to 12 m
2/18	15	No	4.5	–	5	Loam, sandy loam, fine and medium sand	Pine forest	Apr. 2018–Oct. 2020	21 sensors: every 0.5 m from 0 to 5 m and every meter from 5 to 15 m
3/18	11.6	Yes	–	3.0	10	Fine and medium sand	Pine forest	Apr. 2018–Oct. 2020	16 sensors: every 0.5 m from 0 to 5 m and every meter from 5 to 10 m
1/19	16.8	No	<1.0	–	>15	Peat, silt loam, sandy loam, fine and medium sand	Mire	Apr. 2019–Oct. 2020	21 sensors: every 0.5 m from 0 to 5 m and every meter from 5 to 15 m
2/19	21	Yes	–	3.0	>11.5	Medium- and coarse sand	Pine forest	Apr. 2019–Oct. 2020	17 sensors: every 0.5 m from 0 to 4.5 m and every meter from 4.5 to 11.5 m

Note: Dash – not applicable; asterisk – no data.

ley (floodplain and river channel). Absolute heights vary from 200–204 m asl on gentle slopes to 189–192 m asl on the floodplain and in the bottoms of ravines.

In areas with pine forests, the ground cover is sparse and consists of pine needle litter and separate thickets of lingonberry and bearberry. The geological section down to a depth of 21 m is represented by silty to coarse-grained sands (Fig. 2). Thus, on the right bank of the Levaya Shestakovka River, 640 m from its channel, on a very gentle slope (1°–2°), 21-m-deep borehole 2/19 penetrated medium-grained sands (4.9 m from the top) underlain by gray coarse-grained sands.

In borehole 3/16-P, 300 m from the edge of the floodplain, yellowish gray medium-grained sands with signs of ferrugination and few inclusions of organic matter were exposed throughout the section (to a depth of 10 m). Near the border of the pine and larch forests, according to the drilling data of borehole 3/18 with a depth of 11.6 m, the geological section is represented by fine-grained sands. In its upper part (up to a depth of 40 cm) sands are humified and contain inclusions of plant roots; to a depth of 2.2 m, they are ferruginous red and light gray; dove-gray sands lie beneath them, at the base of the section with inclusions of silt fraction and organic matter.

Boreholes 2/19, 3/16-P, and 3/18 encountered an aquifer at depths of 2.5–18.0, 1.7–7.2, and 2.2–7.7 m, respectively. The ice content of the SFL sands in April increased down the section from 1.5–2 to 8.3–10 wt.%, and it was 17.6–20 wt.% directly at the top of the aquifer. Permafrost immediately above the talik had the ice content from 18.3–19.6 to 33–35 wt.%.

On the left bank of the river in a pine forest, borehole 2/18 with a depth of 16.85 m revealed fine-grained sands. Light yellow sands with signs of ferrugination and rare inclusions of loam lie in the upper 2-m-thick layer. They are underlain to a depth of 7 m by fine- and very fine-grained silty light yellowish gray and bluish gray sands with horizons of ferrugination. Deeper, fine-grained gray sands with remains of organic matter, thin interlayers of greenish gray bluish sandy loams and silty loams with signs of ferrugination at depths of 11.1–13.5 m were exposed. The rocks throughout the section were frozen. Borehole 3/16-L, 3.9 m deep, uncovered uniform frozen gray and brown medium-grained sands with organic inclusions in the area of the birch-larch forest, The ice content of the permafrost ranged from 16.3 to 22.3 wt.%.

The geological structure of the low left-bank floodplain in the expansion of the river valley was described in detail by A.M. Tarbeeva [*2019*] according to drilling data from borehole 3/17 with a depth of 21 m. Fine- and medium-grained sands with interlayers of gravel and peat occur under the peaty litter from the surface to a depth of 4.7 m. They are underlain by silty sandy loams with peat interlayers. Beneath them, at the depth interval of 7.8–16.9 m, fine-grained sands with interlayers of plant remains are exposed. Silty sandy loams and silty sands occur at

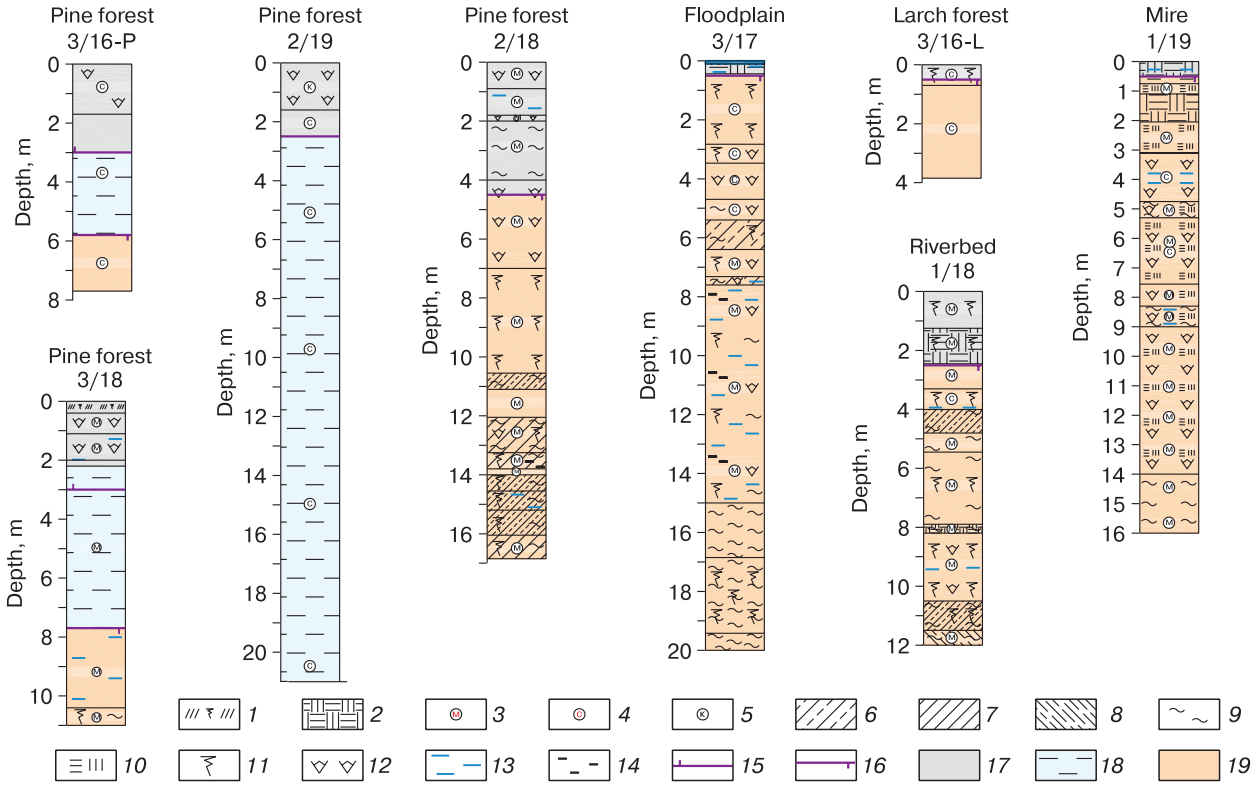

Fig. 2. Geological columns from boreholes in the upper reaches of the Shestakovka River basin:

1 – soil-vegetative layer, *2* – peat, *3* – fine sand, *4* – medium sand, *5* – coarse sand; *6* – loamy sand, *7* – loam, *8* – interlayering of loamy sand and loam, *9* – silt; *10* – peat admixture, *11* – organic residues, *12* – ferrugination, *13* – ice, *14* – charcoal, *15* – lower boundary of the seasonally frozen layer; *16* – permafrost table, *17* – active layer, *18* – water-bearing talik, *19* – permafrost.

the base of the section. The entire thickness was in the frozen state at the time of drilling. The ice content was maximum in the surface peaty horizon (>40%), varied from 17 to 35% at depths of 1–14 m, and decreased to 14–15% at depths of 18 and 20 m.

In borehole 1/18 under the river channel, gray, brown, and yellowish fine- and medium-grained sands with inclusions and thin interlayers of organic matter and peat were found in the surface (to a depth of 4 m) layer; below, to a depth of 4.8 m, there was a layer of silty bluish gray sandy loam with numerous ice lenses. At the depth interval of 4.8–10.5 m, silty fine-grained sands with organic interlayers and signs of ferrugination were exposed. They were underlain to a depth of 12 m by silty bluish gray sandy loams with interlayers of light loam and gray silty fine-grained sands. In April, the rocks throughout the section were in the frozen state. The ice content varied from 16 to 25.6 wt.% increasing at depths of 0.3–0.5 m (29.0–49.5 wt.%) and 4.0–4.5 m (31.0–59.4 wt.%).

The section under the mire on the right bank of the river was studied to a depth of 16 m in borehole 1/19. The upper 0.7-m-thick layer of ice-rich peat is underlain by interlayering ferruginous fine- and medium-grained sands with peat are exposed. The thickness of this layer is 3.1 m. Deeper, medium-grained bluish gray sands with ferruginous mottles and organic matter inclusions extend to a depth of 4.8 m; the layer of 4.8–5.3 m is represented by silty sand; the layer of 5.3–8.3 m, by fine- and medium-grained sands with interlayers of organic matter and ferrugination; in the lower part, they contain inclusions of loam and ice. Deeper, to the bottom of the well, fine-grained silty sands with interlayers of organic matter and ferrugination are exposed. Sediments of the entire section were in the frozen state.

Thus, according to the results of drilling on the right bank of the Levaya Shestakovka River performed in 2016–2019, the presence of water-bearing taliks was established in the areas of pine forest in sections with sandy sediments. In the analogous landscape positions on the left bank, sediments were frozen. Probable reasons for the absence of talik on the left bank are a finer texture of the sediments (the presence of fine-grained sands, loamy sands, loams, and silty sands) and a steeper slope ensuring more rapid runoff of surface and supra-permafrost waters into the river. Beyond the area of pine forests, talik zones were not found regardless of the composition of the sediments. Earlier, when studying subaerial taliks

in the area of Malaya Chabyda Lake, 5 km from the study area, A.V. Boitsov established an important role of the intra-annual redistribution of moisture in sandy rocks of the aeration zone: the water content of thawed sand is always higher than that of frozen sand, which leads to the formation of a positive temperature shift at the bottom of the STL due to the difference in the thermal conductivity coefficients of sediments in the frozen and thawed states [*Boitsov, 2002*].

Temperature regime of rocks. The course of rock temperatures over time at depths of 3, 6, and 10 m is shown in Fig. 3; the thicknesses of the active layer (STL or SFL) and the depth of zero annual amplitudes are given in the Table 1.

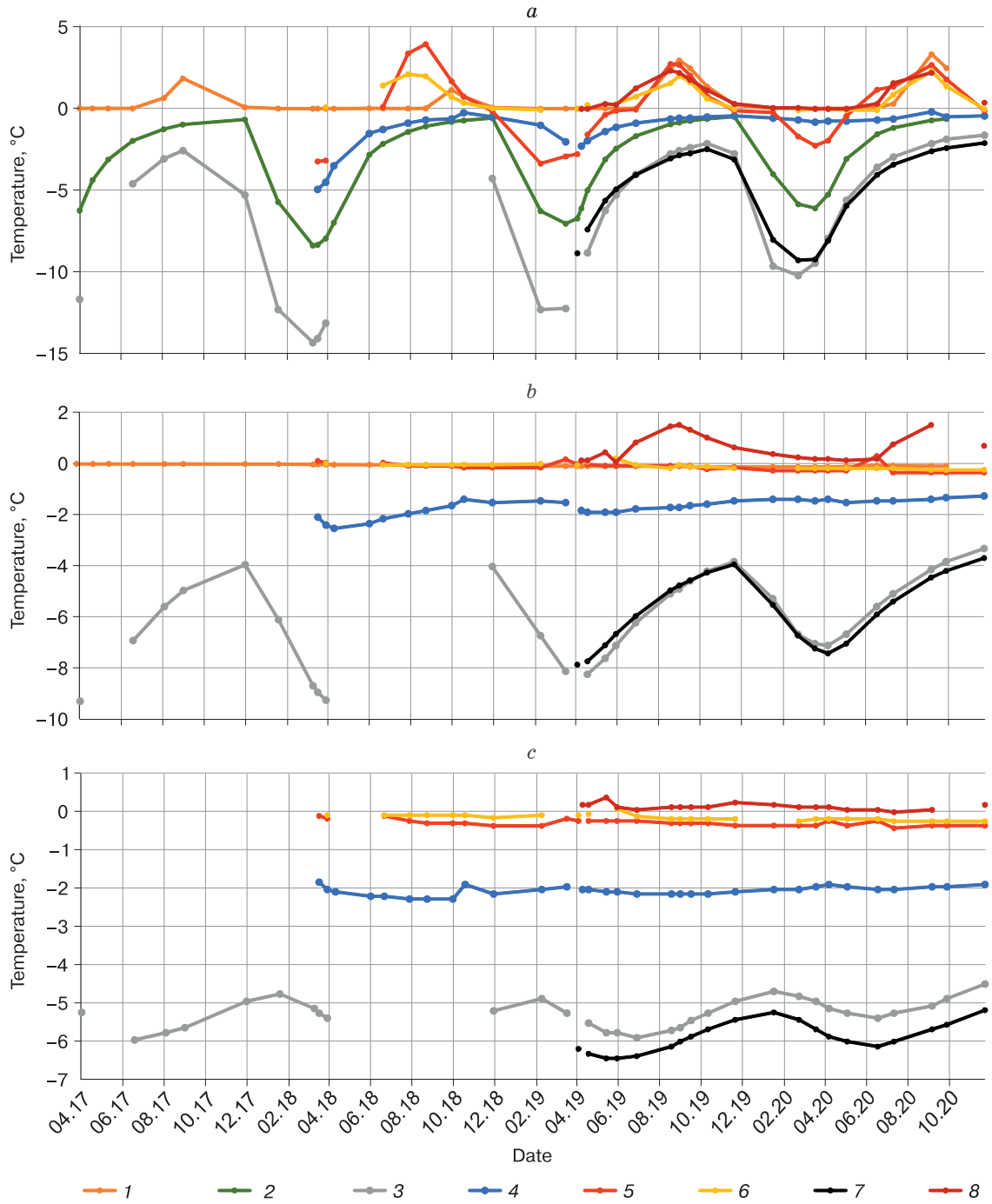

Fig. 3. Change in rock temperature at depths of (*a*) 3, (*b*) 6, and (*c*) 10 m from April 2017 to November 2020 in boreholes:

1 – 3/16-P, *2* – 3/16-L, *3* – 3/17, *4* – 1/18, *5* – 2/18, *6* – 3/18, *7* – 1/19, *8* – 2/19.

According to geothermal observations in borehole 3/17 on the river floodplain, the thickness of the STL does not exceed 1 m. At this depth, the temperature varies from –0.4°C in November–December to –18.6°C in February. The seasonally thawed layer begins to form in the late April–early May and completely freezes in October. At depths of 10 and 20 m, the temperature of the rocks varies from –4.7 to –6.0°C and from –3.6 to –3.9°C, respectively. The delay time of temperature fluctuations at a depth of 16–18 m (as compared with the surface) is 9–10 months. At a depth of 20 m, seasonal fluctuations are not fixed. In borehole 1/18 under the freezing narrow riverbed, thawing of rocks begins in the late April–early May, and they become fully frozen in November–December. The thickness of the STL is 2.5 m. At this depth, the temperature varies from 0 to –4.7°C; at a depth of 10 m, from –1.9 to –2.3°C; and at a depth of 12 m, from –2.1 to –2.5°C. The time of passage of the temperature wave from the surface to the depth of 10–12 m is about 10 months. The thickness of the layer of annual heat exchange is 15 m. There was a slight tendency towards an increase in the rock temperature at depths of 6–12 m over two years of measurements. Under the lake-like widenings of the river, where a layer of water over 2 m is preserved under the ice in winter, there are local taliks of up to 8 m in thickness under the channel [*Tarbeeva et al., 2019*]. The connection between underchannel and slope subaerial taliks, apparently, is absent in the winter season. This is evidenced by the merging of the surface freezing layer with permafrost on the floodplain of the Levaya Shestakovka River and under the mire at the footslope in October.

According to the results of geothermal measurements in borehole 1/19, the thickness of the STL under the mire is less than 1 m. At this depth, the temperature of the rocks varies from –0.7 to –12.4°C; at depths of 10 and 15 m it varies from –5.3 to –6.5°C and from –5.3 to – 5.6°C, respectively. Annual temperature fluctuations reach a depth of 15 m (the same depth as on the floodplain) with a lag of 9–10 months. The depth of the layer of zero annual amplitudes is 17–18 m.

According to the results of measurements in the larch forest (borehole 3/16-L), the thickness of the STL is slightly more than 1 m. At this depth, the rock temperature ranges from +0.2 to –11.3°C; at a depth of 3 m, from –0.6 to –8.4°C. The section is in the frozen state.

In borehole 2/18 on the left bank of the river valley in the pine forest, the STL thickness reaches the maximum: 4.5 m. At the depths of 5, 10, and 15 m, the temperature during the observation period varied within 0...–0.2, –0.3...–0.4 and –0.3...–0.5°C, respectively. From August 2018 to October 2020, soil cooling by 0.2–0.3°C was observed throughout the section. In warm and snowy winters after a wet summer, overwintering of thawed rocks is possible in this area.

Temperature regime of rocks in the area of suprapermafrost subaerial talik. In boreholes 3/18, 2/19, and 3/16-P, which exposed the suprapermafrost subaerial talik, the SFL thickness during the observation period was 2.0–3.5 m.

The maximum penetration depth of the isotherm –0.1°C was recorded in borehole 2/19, and the minimum one was recorded in borehole 3/16-P. In summer, the rocks at the base of the SFL warmed up to a temperature of 2.1–2.9°C. In the interval of occurrence of the water-bearing talik, the temperature of the rocks varied from 0°C in the winter months to 2.3°C in September–October. The permafrost underlying the talik had a high subzero temperature (–0.1... –0.3°C). The thickness of the layer of annual heat exchange is 6–12 m.

In general, in the areas of the suprapermafrost subaerial talik, the SFL thickness remained stable over the observation period; however, the timing of its formation and rock temperature extremes varied from year to year. Thus, according to the data obtained from borehole 3/16-P, the front of seasonal freezing reached a depth of 0.5 m in October 2016 and in November 2017–2020 (Fig. 4). Mean daily temperatures at this depth in winter usually did not fall below –14°C. Only the winter of 2017/18 was different, when the mean daily temperature of rocks at a depth of 0.5 m dropped to –17°C. As a result, in the subsequent summer season of 2018, the underlying

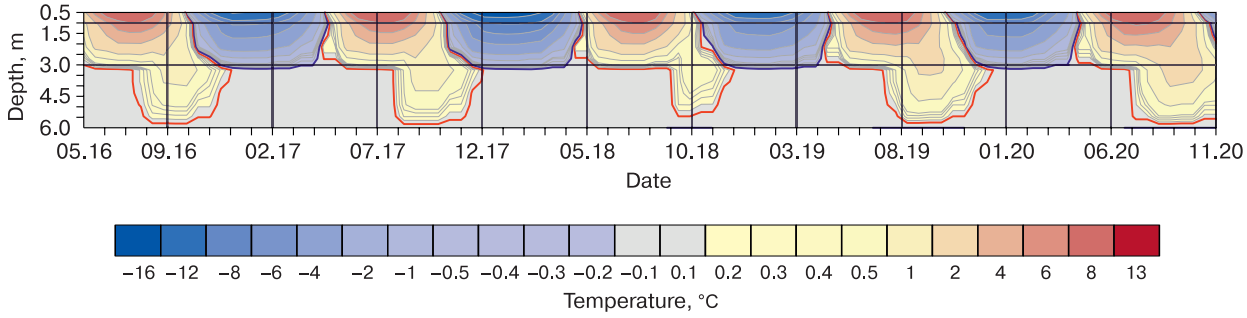

Fig. 4. Dynamics of rock temperature in borehole 3/16-P from May 2016 to November 2020.

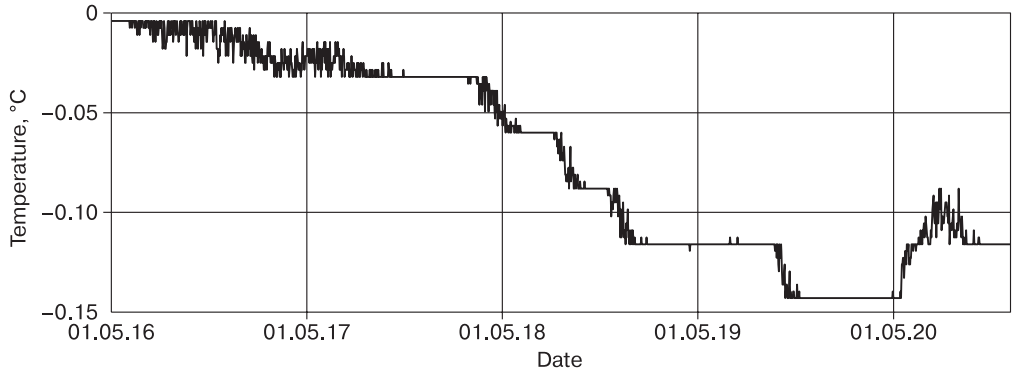

Fig. 5. Change in the mean daily temperature of rocks at a depth of 6 m in borehole 3/16-P.

thawed aquifers warmed up to a lower temperature and for a shorter time than in the previous years, but this effect was leveled in 2019–2020.

The thawing of SFL during the observation period began in mid-April and reached a depth of 0.5 m in May. Positive mean monthly temperatures of rocks in the aeration zone at a depth of 0.5 m were observed from May to September or October; at a depth of 1 m, from May to October; and at a depth of 3 m, from August to December in all years of observation, except for 2018, when the temperature was above 0°C only from October to December.

During the rest of the year, the temperature of rocks at a depth of 3 m was 0°C. At a depth of 6 m, from May 2016 to November 2020, gradual cooling of the rocks by 0.2°C took place (Fig. 5), and permafrost aggradation was observed; in 2020, rock temperature began to rise again.

DISCUSSION

The lowest values of rock temperature, low thickness of the STL (about 1 m), and a great depth of penetration of annual temperature fluctuations (>15 m) were observed in boreholes 3/17 and 1/19 on the floodplain and within the mire, respectively. Similar permafrost conditions were noted in the area of borehole 3/16-L in larch forest. In general, rock temperature patterns on the floodplain and under the mire were almost identical from the surface to a depth of 6–7 m. From a depth of 8 m, rock temperatures under the mire were 0.5–1.0°C lower than on the floodplain. In a depression occupied by larch forest, the temperature of the rocks was higher than that under the mire and on the floodplain: at a depth of 1 m, by 7–9°C in winter and by 0.2–0.5°C in summer; at a depth of 3 m, by 5–6°C in winter and by 1.5–2.0°C in summer. The low temperatures of the rocks in these landscapes were due to the presence of a wet organic (peat) horizon, the thermal conductivity of which is higher in winter than in summer. Thus, the thickness of ice-rich peat in the mire was 0.75 m, on the floodplain, 0.32 m; in the larch forest, a continuous moss cover of up to 0.3 m in thickness was developed on the surface.

In addition, at the end of autumn and at the beginning of winter, when the freezing of rocks begins and a snow cover forms, the discharge of suprapermafrost water on the surface was observed in the mire and on the floodplain. The resulting water-snow mass froze in the form of thin ice. In April 2017, in the area of borehole 3/17, the thickness of surface ice layer reached 8 cm. The presence of ice reduces the warming effect of the snow cover and favors deep and intense cooling of the rocks in winter. In the larch forest, snow cover accumulates throughout the cold season, which may explain the relatively high temperatures of the rocks there, especially in winter.

On gentle slopes under pine woodland with an almost absent ground cover, the thickness of the active layer reaches 4.5 m, and the depth of zero annual amplitude is 5–12 m. The geological section is represented here almost entirely by sandy sediments. Three boreholes exposed water-bearing taliks. Apparently, the warming of rocks is associated both with the absence of an organic horizon on the surface and with intensive filtration of suprapermafrost water of the STL and suprapermafrost groundwater in thawed sands with a high hydraulic conductivity. The temperature of water-saturated sands in the talik zone is about 0°C throughout the year; these sands do not freeze both because of the large costs of cold required to transform all liquid water into ice, and because of the continuous filtration of water through the pores and convective heat transfer. Probably, the thickness of the aeration zone and the depth of the aquifer table in the talik play an important role in the formation of the temperature regime. In boreholes 3/18 and 2/19 drilled in the upper part of the talik slope, seasonal temperature fluctuations penetrate to depths of 9–11 m, while in other boreholes of this group (3/16-P and 2/18), seasonal fluctuations decay at depths of 5–6 m. This can be explained by a shallower depth of suprapermafrost water in the upper part of the slope.

An intermediate position between "warm" and "cold" sites is occupied by the riverbed. The thickness of the STL here is 2.5 m, and the depth of zero annual amplitude is about 15 m. Apparently, river flow from May to October and the absence of an organic horizon contribute to higher temperatures in the section compared to those within the floodplain and mire. At the same time, loamy sands and loams present in the section limit groundwater filtration, convective heat transfer, and the formation of thawed horizons. As a rule, the rocks that have thawed during the warm period are completely frozen by February–March. As shown in Fig. 6, rock temperature in borehole 3/16-P at a depth of 6 m slightly decreased from zero values in 2016 to –0.1°C in 2020. A weakly pronounced tendency to temperature decrease at depths of 10–20 m is also characteristic of "warm" sites in the talik area (boreholes 3/18 and 2/19) and beyond it (borehole 2/18). The length of the series of observations is insufficient to draw definite conclusions about the trend of temperature changes; however, the consistency of the noted changes over 2–4 years for four boreholes allows us to conclude that in these years the permafrost table somewhat ascended. At the "cold" sites, multidirectional trends were observed. Under the river channel (borehole 1/18) and on the river floodplain (borehole 3/17), a slight decrease in rock temperature by 0.1–0.3°C took place, whereas linear approximation for the mire site attests to some rise in the permafrost temperature over the past year and a half. The absence of a pronounced increase in permafrost temperature is consistent with the results of the analysis of long-term (39 years) geothermal observations in the area of research by S.P. Varlamov [*Varlamov et al., 2021*], who came to the conclusion that the thermal state of the permafrost remains stable, regardless of the type of terrain and the nature of the deposits.

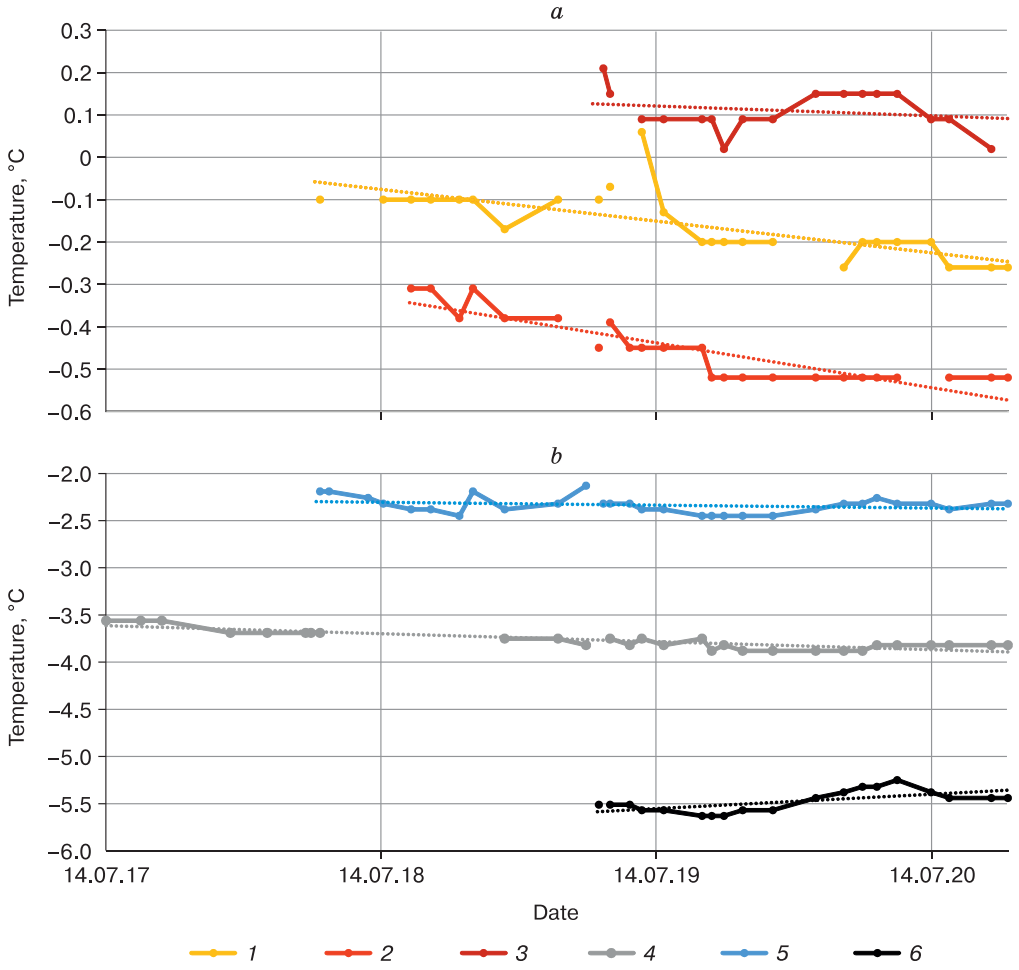

Fig. 6. Change in rock temperature at depths of 10–20 m in boreholes and linear approximation trend:

a: *1* – borehole 3/18, 10 m; *2* – borehole 2/18, 15 m; *3* – borehole 2/19, 12 m; *b*: *4* – borehole 3/17, 20 m; *5* – borehole 1/18, 12 m; *6* – borehole 1/19, 15 m.

CONCLUSIONS

In the key area of about 1 km^2 in the Levaya Shestakovka River basin, geothermal conditions are different under the same meteorological background. The depth of permafrost table varies from 0.5 to 20 m. Both seasonally frozen and seasonally thawed conditions are observed in the upper part of the geological section depending on the composition and properties of the sediments. The highest rock temperatures are characteristic of the area of aquiferous suprapermafrost taliks confined to gentle slopes composed of sandy sediments and covered with sparse pine forests. In such areas, the thickness of the seasonally frozen layer reaches 3 m, and the depth of zero annual amplitude varies from 6 to 12 m. The thawed rocks are preserved due to the constant filtration of groundwater in them. The presence of sediments with lower infiltration capacity (loamy sands and loams) in the upper part of the section does not favor the formation of talik zones.

The lowest rock temperatures are characteristic of the mire site and the floodplain. The thickness of the seasonally thawed layer varies from 0.5 to 1.0 m, and the depth of zero annual amplitudes exceeds 15 m. The formation of the low-temperature sediments is facilitated by the presence of an organic horizon in the upper part of the section and by the small snow depth because of the formation of icings.

In the period from 2016 (2018) to 2020, slow freezing of the taliks from below was noted due to a weakly pronounced cooling of the strata underlying the thawed aquifers. Beyond the areas of taliks, weak multidirectional changes in rock temperature were recorded.

The established wide distribution of suprapermafrost subaerial taliks in a small area of research within the continuous permafrost zone suggests the possibility of their existence in similar landscape-permafrost conditions in Central Yakutia.

Acknowledgments. *Rock temperature monitoring was carried out with the financial support of the Russian Foundation for Basic Research (project 20-05-00670). Borehole drilling and study of the geological section was carried out within the framework of state assignment 122012400106-7 "Cryolithozone groundwater: patterns of formation and regime, features of interaction with surface water and frozen rocks, prospects for use".*

References

Anisimova N.P. (ed.), 2003. *Groundwaters in Central Yakutia and Prospects of Their Use*. Novosibirsk, Acad. Publ. Geo, 117 p. (in Russian).

Anisimova N.P., Pavlova N.A., 2014. *Hydrogeochemical Studies of Permafrost in Central Yakutia*. Novosibirsk, Acad. Publ. Geo, 198 p. (in Russian).

Anisimova N.P., Pavlova N.A., Stambovskaya Ya.V., 2005. The chemical composition of the water of valley taliks in the middle reaches of the Lena River. *Nauka i obrazovanie* **4** (40), 92–96.

Biskaborn B.K., Smith S.L., Noetzli J. et al., 2019. Permafrost is warming at a global scale. *Nat. Commun.* 10, p. 264. doi: 10.1038/s41467-018-08240-4.

Boike J., Nitzbon J., Anders K. et al., 2019. A 16-year record (2002–2017) of permafrost, active-layer, and meteorological conditions at the Samoylov Island Arctic permafrost research site, Lena River delta, northern Siberia: an opportunity to validate remote-sensing data and land surface, snow, and permafrost models. *Earth Syst. Sci. Data* **11**, 261–299. doi: 10.5194/essd-11-261-2019.

Boitsov A.V., 1985. Conditions of formation and the regime of slope taliks in Central Yakutia. In: *Hydrogeological Studies*. Yakutsk, Izd. Melnikov Permafrost Inst. SB RAS, p. 44–55 (in Russian).

Boitsov A.V., 2002. The Conditions of Formation and the Regime of Groundwater in Suprapermafrost and Intrapermafrost Runoff in Central Yakutia. Cand. Sci. (Geol.) Diss., Yakutsk, 176 p. (in Russian).

Bulygina O.N., Razuvaev V.N., Korshunova N.N., Shvets N.V., 2022a. Description of the Data Array of Monthly Precipitation at Weather Stations of Russia: Certificate of State Registration of the Database No. 2015620394. http://meteo.ru/data/158-total-precipitation#opisanie-massiva-dannykh (last visited: March 15, 2022).

Bulygina O.N., Razuvaev V.N., Trofimenko L.T., Shvets N.V., 2022b. Description of the Data Array of the Mean Monthly Air Temperature at Weather Stations of Russia: Certificate of State Registration of Database No. 2014621485. http://meteo.ru/data/156-temperature#opisanie-massiva-dannykh (last visited: March 15, 2022).

Fedorov A.N., Ivanova R.N., Park H. et al., 2014. Recent air temperature changes in the permafrost landscapes of northeastern Eurasia. *Polar Sci.* **8** (2), 114–128. doi: 10.1016/j.polar.2014.02.001.

Fedorov-Davydov D.G., Davydov S.P., Davydova A.I. et al., 2018. The temperature regime of soils in the Northern Yakutia. *Earth's Cryosphere* XXII (4), 12–19.

Gagarin L.A., Semernya A.A., Lebedeva L.S., 2016. Assessment of thermosuffosion processes in Central Yakutia on the example of the Ulakhan-Taryn site. *Inzhenern. Geol. Gidrogeol. Geokriol.* 3, 252–262.

Galanin A.A., 2015. Cryogenic-eolian mechanism of formation of aquiferous interpermafrost taliks in Central Yakutia. In: *Proc. XXI Conf. on Groundwater in Siberia and the Far East*. Yakutsk, Izd. Melnikov Permafrost Inst. SB RAS, p. 80–84 (in Russian).

Gorokhov A.N., Fedorov A.N., 2018. Current trends of climate change in Yakutia. *Geograf. Prirodn. Res.* 2, 111–119.

Kaverin D.A., Pastukhov A.V., Novakovskiy A.B. et al., 2019. Landscape and climatic factors impacting the thaw depth in soils of permafrost peat plateaus (on the example of CALM R52 site). *Earth's Cryosphere* XXIII (2), 53–60.

Konishchev V.N., 2009. Response of permafrost to climate warming. *Byull. Mosk. Gos. Univ. Ser. 5: Geogr.* 4, 10–20.

Konstantinov P.Ya., Fedorov A.N., Machimura T., Iwahana G., Yabuki H., Iijima Y., Costard F., 2011. Use of automated recorders (data loggers) in permafrost temperature monitoring. *Kriosfera Zemli* XV (1), 23–32.

Lebedeva L.S., Bazhin K.I., Khristoforov I.I. et al., 2019. Suprapermafrost subaerial taliks, Central Yakutia, the Shestakovka River basin. *Earth's Cryosphere* XXIII (1), 35–44.

Lytkin V.M., Galanin A.A., Shaposhnikov G.I. et al., 2018. Temperature regime of dune massifs in Central Yakutia. In: *Geo-*

logy and Mineral Resources of the Northeast of Russia (Proc. VIII All-Russia Sci.-Pract. Conf.). Yakutsk, Izd. Melnikov Permafrost Inst., vol. 2, 237–240 (in Russian).

Moskalenko N.G., 1998. Investigation of the seasonal thaw of peatlands in the West Siberian cryolithozone. *Kriosfera Zemli* II (1), 32–35.

Neradovskii L.G., 2020. Changes in the background permafrost temperature in Yakutsk during current period of climate warming in Siberia (1976–2011). *Earth's Cryosphere* XXIV (4), 40–49.

Oberman N.G., Lygin A.M., 2009. Forecasting the degradation of permafrost on the example of the Northeast of European Russia. *Razvedka i Okhrana Nedr* 7, 15–20.

Pavlov A.V., 1979. *Thermal Physics of Landscapes*. Novosibirsk, Nauka, 284 p. (in Russian).

Pavlov A.V., Anan'eva G.V., Drozdov D.S. et al., 2002. Monitoring of active layer and the temperature of frozen grounds in the North of Russia. *Kriosfera Zemli* VI (4), 30–39.

Ponomareva O.E., 1999. Aquiferous taliks in sandy sediments on the lower reaches of the Vilyui River. *Kriosfera Zemli* III (4), 84–89.

Semernya A.A., Gagarin L.A., Bazhin K.I., 2018. Cryohydrogeological features of the site of intrapermafrost aquifer distribution in the Eruu Spring area (Central Yakutia). *Earth's Cryosphere* XXII (2), 26–34.

Shepelev V.V., 2011. *Suprapermafrost Waters in the Cryolithozone*. Novosibirsk, Acad. Publ. Geo, 169 p. (in Russian).

Shepelev V.V., Boytsov A.V., Oberman N.G. et al., 2002. *Groundwater Monitoring in Permafrost*. Yakutsk, Izd. Melnikov Permafrost Inst. SB RAS, 172 p. (in Russian).

Skryabin P.N., Skachkov Yu.B., Varlamov S.P., 1999. Climate warming and thermal state of ground in Central Yakutia. *Kriosfera Zemli* III (3), 32–40.

Tarbeeva A.M., Lebedeva L.S., Efremov V.S. et al., 2019. Conditions and processes of formation of a beaded channel of a small river in permafrost, Shestakovka River (Central Yakutia). *Earth's Cryosphere* XXIII (2), 33–44.

Varlamov S.P., Skachkov Y.B., Skryabin P.N., 2020. Influence of climate change on the thermal condition of Yakutia's permafrost landscapes (Chabyda station). *Land* **9** (5), p. 132. doi: 10.3390/land9050132.

Varlamov S.P., Skachkov Yu.B., Skryabin P.N., 2021. *Monitoring of the Thermal Regime of Soils in Central Yakutia*. Yakutsk, Izd. Melnikov Permafrost Inst. SB RAS, 156 p. (in Russian).

Varlamov S.P., Skryabin P.N., 2012. Dynamics of the thermal state of soils in permafrost landscapes of Central Yakutia. *Izvest. Samarsk. Nauchn. Tsentra RAN* 14 (1–8), 2040–2044.

Vasiliev A.A., Gravis A.G., Gubarkov A.A. et al., 2020. Permafrost degradation: results of long-term geocryological monitoring in the Western sector of the Russian Arctic. *Earth's Cryosphere* XXIV (2), 14–26.

Zabolotnik S.I., Zabolotnik P.S., 2014. Conditions of ground seasonal thawing and freezing in South Yakutia. *Kriosfera Zemli* XVIII (1), 23–30.

Received May 6, 2022
Revised December 11, 2022
Accepted February 1, 2023

Translated by A.V. Muravyev

EARTH'S CRYOSPHERE
SCIENTIFIC JOURNAL

Earth's Cryosphere, 2023, vol. XXVII, No. 2, pp. 14–20

SURFACE AND GROUND WATERS IN TERRESTRIAL PERMAFROST REGION

THE CHEMICAL COMPOSITION OF WATER OF LARGE EAST SIBERIAN RIVERS AND ITS DEPENDENCE ON THE THICKNESS OF SEASONALLY THAWED LAYER IN THE CATCHMENTS

O.I. Gabysheva[1,*], V.A. Gabyshev[1], I.A. Yakshina[2]

[1] *Institute for Biological Problems of Cryolithozone, Yakutsk Science Center, Siberian Branch of the Russian Academy of Sciences, prosp. Lenina 41, Yakutsk, 677980 Russia*
[2] *Lena Delta Nature Reserve, Akad. Fedorova St. 28, Tiksi, 678400 Russia*

**Corresponding author; e-mail: g89248693006@yandex.ru*

The main features of the chemical composition and physical characteristics of water in twelve largest rivers of East Siberia (Lena, Vilyui, Kolyma, Aldan, Olenek, Vitim, Indigirka, Amga, Olekma, Anabar, Yana, and Chara) were determined on the basis of observations during summer low-water runoff in 2007–2011. It was found that favorable oxygen regime, relatively high values of the chemical oxygen demand and water color, higher concentration of total iron and ammonium ions, and moderate salinity are characteristic of the studied rivers. East Siberia is a region with a ubiquitous distribution of permafrost. The thickness of seasonally thawed layer within river catchments is extremely variable. Using canonical-correlation analysis, it was found that concentrations of specific components of ionic constituents (water hardness, calcium, magnesium, bicarbonates, sulfate ions, and salinity) depend on the active layer thickness (ALT). Herewith, the deeper the active layer in a catchment, the higher the concentrations of these ionic constituents in river water. This is explained by the fact that permafrost serves as a barrier preventing infiltration of surface water into deep mineral horizons and thus limiting water saturation with mineral ions.

Keywords: *physico-chemical composition of water, major ions, salinity, permafrost, seasonally thawed layer, large rivers, East Siberia.*

Recommended citation: Gabysheva O.I., Gabyshev V.A., Yakshina I.A., 2023. The chemical composition of water of large East Siberian rivers and its dependence on the thickness of seasonally thawed layer in the catchments. *Earth's Cryosphere* XXVII (2), 14–20.

INTRODUCTION

East Siberia is characterized by a ubiquitous distribution of permafrost. Permafrost thickness is found to be 350–450 m in the central part of the region and reaches 1500 m further to the north, in the Olenek River basin [*Shepelev, 2009*]. The seasonally thawed layer (STL) varies in thickness from 0.1 to 1.5 m in coastal areas in the north of the region and increases to 3 m in the southern part, in the boreal zone [*Desyatkin et al., 2009*]. In the central part of the region, seasonal thawing begins at the end of April and reaches its maximum at the end of August. In October, freezing occurs simultaneously from the top and from the bottom; upper and lower freezing layers together at a depth of 0.7–0.8 m at the end of November or in December [*Matveev et al., 1989*].

The STL has a significant potential to influence the chemical composition of surface water in permafrost areas [*Smith et al., 2005; Frey, McClelland, 2009*]. The mechanisms of such influence may be quite different. First, soluble chemical components in the upper permafrost become labile, when they are found in the STL. Second, in catchments with a deep STL, the depth of surface runoff and the duration of water being in the soil differ from those in the areas with a thin STL. These factors cannot but influence the surface water chemistry through exchange reactions between water and soil. Finally, the chemical composition of river water is influenced by the balance between precipitation and groundwater in river alimentation, which depends on the STL thickness in river catchments.

In modern conditions of global climate change, the relevance of issues related to the study of the STL impact on the chemical composition of river water is increasing. According to the results of STL dynamics modeling [*Stendel, Christensen, 2002*], it is likely that STL thickness will increase by 30–40% in a larger part of permafrost areas in the northern hemisphere by 2100. For some regions, such as East Siberia, where permafrost is ubiquitous, transformations caused by permafrost degradation processes can be most dramatic due to their scale, since they will cover the entire territory. Therefore, understanding of the mechanisms of the STL influence on the chemical

composition of river water is quite significant for predicting the chemical composition of Arctic rivers and the rate of runoff of dissolved substances into the Arctic Ocean.

The purpose of this study is to characterize the main features of the chemical composition and physical characteristics of the water of large rivers in East Siberia and to measure an impact of STL thickness in river catchments on the formation of the chemical composition of river water.

MATERIALS AND METHODS

This study focuses on catchments of twelve largest rivers in East Siberia: Lena, Vilyui, Kolyma, Aldan, Olenek, Vitim, Indigirka, Amga, Olekma, Anabar, Yana, and Chara (Fig. 1). Water samples were taken from the upper water layer (0–0.3 m) near the banks and along the fairway during summer low water (June–August) in 2007–2011. Conservation and storage of water samples were carried out in accordance with generally accepted methods [*Semenov, 1977*].

Water transparency was determined using a Secchi disk; color, by photometric method on an SF-26 device; pH value, by the potentiometric method using a Multitest IPL-101 device; suspended substances, by gravimetric method; oxygen concentration, by titrimetric method; oxygen saturation percentage, by calculation method; carbon dioxide concentration, by titrimetric method with phenolphthalein; water hardness and calcium concentration, by titrimetric method; magnesium concentration, by calculation method; sodium and potassium concentrations, by atomic emission spectrometry using an AAnalyst400 AAS device; bicarbonates, by back titration method; chloride ions, by the mercurimetric method; sulfate ions, by the turbidimetric method on an SF-26 device; mineralization (sum of dissolved salts), by calculation method; ammonium ions, by the photometric method with Nessler reagent on an SF-26 device; nitrite ions, by the photometric method with Griess reagent on an SF-26 device; nitrate ions, by the photometric method with salicylic acid on an SF-26 device; phosphate ions and silicon, by the photometric method with ammonium molybdate on an SF-26 device; total phosphorus, by the photometric method with ammonium persulfate on an SF-26 device; total iron, by the photometric method with sulfosalicylic acid on an SF-26 device; biological oxygen demand (BOD_5), by the titrimetric method (iodometric determination); chemical oxygen consumption (COD), by the photometric method using a Fluorate-02 device; petroleum products, phenols, and anionic surfactants (AS), by the fluorimetric method on a Fluorat-02 device. Classifications generally accepted in hydrochemistry were used to characterize river water [*Alekin, 1953, 1970*]. A system of maximum permissible concentrations for piscicultural water use MPCpw was applied to assess water quality.

Full data on the physical and chemical properties of water at each sampling point of the studied rivers were published previously [*Gabyshev, Gabysheva, 2018*].

Data on the STL thickness (minimum, average, and maximum) were extracted using ArcGIS software in accordance with the coordinates of observation points (Fig. 1) from a georeferenced dataset. This dataset is based on materials from 1960–1987 and was published as an appendix to the work of K. Beer with coauthors [*Beer et al., 2013*]; it is available in the PANGEA repository as a NetCDF file. The Russian map "*Seasonal Freezing and Thawing of Soils*" was also used [*National Atlas..., 2001*].

The data array generated by the authors includes two groups of quantitative variables: physical and chemical indicators of water (28 variables) and characteristics of the seasonally thawed layer (3 variables). The total number of observations in the array is 303.

The method of canonical correlations for a paired set of quantitative characteristics [*Afifi, Azen, 1982*] describing the STL and the physicochemical parameters of river water was applied to analyzing multiple correlations. The use of a multidimensional model for the analysis of canonical values also made it possible to distinguish data of the studied array according to a grouping characteristic of the studied rivers. When testing statistical hypotheses, the critical level of statistical significance was assumed to be 5%. Statistical analysis procedures were performed in the Statistica 10 software package.

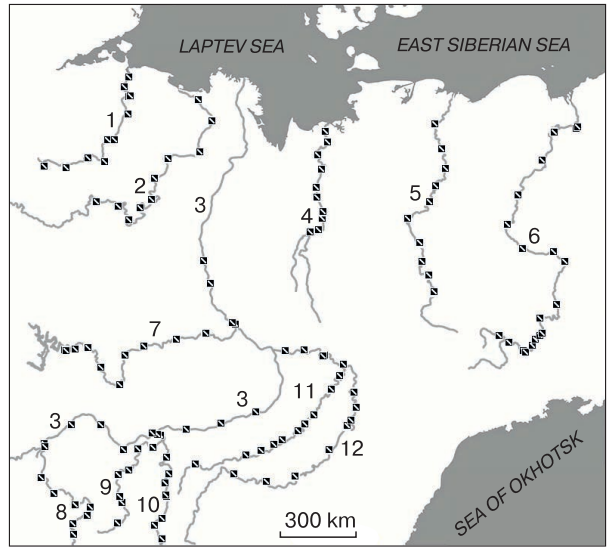

Fig. 1. Schematic map of the studied region and observation points (squares).

Rivers: 1 – Anabar, 2 – Olenek, 3 – Lena, 4 – Yana, 5 – Indigirka, 6 – Kolyma, 7 – Vilyui, 8 – Vitim, 9 – Chara, 10 – Olekma, 11 – Amga, 12 – Aldan.

RESULTS

The content of suspended substances in water from the Aldan, Olenek, and Kolyma rivers does not exceed 10 mg/dm^3 (hereinafter, average values for the entire river are provided). For the Yana, Anabar, and Indigirka rivers, it varies in the range from 25 to 65 mg/dm^3, for the Vilyui, Chara, Olekma, Lena, Vitim, and Amga rivers, it is 14–18 mg/dm^3. According to the hydrogen index, river waters are non-aggressive. The values of pH indicate a shift in the reaction to the neutral side (7.14–7.47) for the Aldan, Vilyui, Yana, and Kolyma rivers. The waters of the Chara, Olekma, Lena, Vitim, Amga, Anabar, Olenek, and Indigirka rivers are slightly alkaline (7.57–8.44).

Most rivers are characterized by an average oxygen content of 8.90–10.80 mg/dm^3 at 93–99% saturation. The waters of the Aldan, Yana, and Amga rivers are slightly oversaturated with oxygen; on average, the degree of saturation is 102–118% with an oxygen concentration of 9.90–11.50 mg/dm^3. In the Anabar River, the degree of saturation is characterized by lower values: 7.43 mg/dm^3 at 69% saturation, which also indicates a favorable oxygen regime. No cases of oxygen deficiency were recorded. The carbon dioxide content is low and varies within relatively narrow limits from 1 to 6 mg/dm^3.

According to the classification of O.A. Alekin, the waters of most of the studied rivers are fresh and low-mineralized (43.4 to 113.8 mg/L); in terms of hardness, they are very soft (from 0.49 to 1.28 meq/L). The exceptions are the Amga and Olenek rivers. Water of the Amga River is moderately mineralized (279.3 mg/L) and moderately hard (3.39 meq/L), and water of the Olenek River is also moderately mineralized (249.3 mg/L) and soft (2.84 meq/L).

All rivers are characterized by relatively low concentrations of major ions. The calcium content does not exceed 45 mg/dm^3, magnesium – 20 mg/dm^3, sodium – 10 mg/dm^3, potassium – 2 mg/dm^3, bicarbonates – 200 mg/dm^3, sulfates – 50 mg/dm^3, chlorides – 15 mg/dm^3. According to the classification of O.A. Alekin, waters of most of the rivers (Aldan, Vilyui, Lena, Vitim, Amga, Anabar, Olenek, and Kolyma) belong to the bicarbonate class, calcium group, type II–III. Waters of Chary, Olekma, Yana, and Indigirka rivers belong to the sulfate class, calcium group, type II–III.

The studied rivers are characterized by relatively high COD values and increased concentrations of ammonium and total iron. The average concentration of ammonium ions varies across rivers from 200 to 1095 μg/dm^3 (MPCpw 500 μg/dm^3); the color index varies from 7° to 57° (maximum permissible level 20°); total iron concentration varies from 0.04 to 0.98 mg/dm^3 (MPCpw 0.10 mg/dm^3); COD, from 11 to 58 mg/dm^3 (MPCpw 15 mg/dm^3).

The content of inorganic compounds is low: nitrites 11 μg/dm^3, phosphates 55 μg/dm^3, total phosphorus 150 μg/dm^3, nitrates 650 μg/dm^3, silicon 3 mg/dm^3. The concentration of phenols does not exceed 5 μg/dm^3; petroleum products, 45 μg/dm^3; surfactants, 157 μg/dm^3. The BOD_5 value is low – 1.50 mg/dm^3.

The studied rivers are characterized by a low excess of the MPC for COD (1.0–3.9 MPC), water color (1.0–2.9 MPC), and ammonium ions (1.0–2.2 MPC). An exception was noted for the total iron content. The detected total iron concentrations exceeded the MPCpw by 5–10 times in water of the Lena, Vitim, Indigirka, and Yana rivers and by 1.9–4.0 times in water of the Chara, Aldan, Vilyui, Olekma, Lena, Anabar, and Kolyma rivers.

The search for relationships between pairs of variables characterizing the physicochemical parameters of river water (28 variables, hereinafter referred to as the HYDROCHEMISTRY set) and the STL in the area of river basins (3 variables, hereinafter referred to as the STL set) was performed by the method of canonical correlations. As is known, the number of calculated canonical correlation coefficients corresponds to the minimum number of variables in one of the two analyzed sets. In our study, it equals to 3. For the most informative (first) solution, the canonical correlation R between STL characteristics and parameters of chemical composition of river water adjusted for the number of observations is 0.75. Thus, variables of the STL set and the HYDROCHEMISTRY set are strongly correlated. The significance level of the first canonical correlation has a value of $p < 0.0001$, therefore the obtained result is suitable for analysis. In applied research, four criteria (Table 1) are widely acceptable. They represent test statistics on the basis of which the researcher can make a conclusion on the null hypothesis. In addition, Table 1 shows the F-value (Fisher's test) and the Pr indicator (>F), which means the probability of the absence of correlation between the sets of variables. The Fisher test for each test statistic varies (Table 1), but Pr (>F) for each test is less than 0.05, so we reject the null hypothesis and conclude that the two sets of variables under study (STL and HYDROCHEMISTRY) are really correlated.

For a more detailed comparative analysis, normalized canonical coefficients, i.e., z-transformed variables with zero mean and one standard deviation were considered. The correlation coefficients between the variables of both sets (STL and HYDROCHEMISTRY) and the three canonical axes were calculated. Maximum correlations were found between the first canonical axes – most informative and interesting for further analysis. Table 2 shows the correlation coefficients between the STL variables and the canonical STL1 axis, ranked in descending order of their absolute values. These coefficients are standardized and dimensionless, so they are suitable for comparison with one another. The maximum weight in

Table 1. **Multivariate statistics of canonical correlation of variables in the STL (3 variables) and HYDROCHEMISTRY (28 variables) sets**

Statistic	Value	F value	Pr (>F)
Wilks' lambda	0.17	7.81	<0.0001
Pillai's trace	1.26	7.05	<0.0001
Lawley-Hotelling trace	2.65	8.56	<0.0001
Roy's largest root	1.55	15.20	<0.0001

Note: F is Fisher's test; Pr is probability value for Fisher's test.

Table 2. **Normalized canonical coefficients for the STL1 axis**

Variable: STL thickness, m	Weight of variable
Maximum	0.94
Minimum	0.15
Average	–0.04

the studied canonical axis is marked as the "maximum STL thickness". Other STL variables have insignificant weights.

Among the physicochemical characteristics of water, the most important ones are the hardness, total content of salts, and ionic composition (concentrations of calcium, bicarbonate, magnesium, and sulfate ions) (Table 3).

Thus, these components of the salt composition of water are closely related to the STL thickness. Moreover, the greater the depth of seasonal thawing, the higher the salt content in river water.

The data set was discriminated along the two obtained canonical axes for the rivers under study. In the scatterplot diagram (Fig. 2), the vertical axis collectively reflects a subset of hydrochemical variables, and the horizontal axis reflects the STL variables. Each point in Fig. 2 is a single observation (sampling point). The method of canonical correlations used in this study makes it possible to discriminate data between groups of observations. The authors discriminated data for the twelve rivers. In order to read the results of the analysis from a given scatterplot, it is necessary to evaluate the location of the observation points in the two canonical axes. The ordinate axis in the diagram corresponds to the canonical axis HYDROCHEMISTRY1, in which variables such as hardness and total salts have maximum weights. The X-axis corresponds to the canonical STL1 axis, where the variable "maximum STL thickness" shows the greatest weight. By assessing in which quarter of the diagram each point of observation is located, and where most of them are grouped, it is possible to determine the conditions that characterize the river in terms of maximum STL thickness, hardness, and degree of mineralization of water. Along the corresponding axis of the diagram, these parameters increase.

Table 3. **Normalized canonical coefficients for the HYDROCHEMISTRY1 axis**

Variable	Weight of variable
Hardness, meq/L	196.90
Ca^{2+}, mg/L	143.62
Total salts, mg/L	142.07
HCO^{3-}, mg/L	104.48
Mg^{2+}, mg/L	88.68
SO_4^{2-}, mg/L	27.94
Cl^{-}, mg/L	7.09
Na^{+}, mg/L	5.05
Phenols, μg/L	1.09
K^{+}, mg/L	–0.75
Si, mg/L	0.38
NH_4, mg/L	–0.36
CO_2, mg/L	0.29
AS, mg/L	0.22
COD, mg/L	0.22
BOD_5, mg/L	0.17
Oxygen saturation, %	–0.16
PO_4, μg/L	0.12
Water color, degrees	–0.12
Water transparency, m	–0.11
pH, units.	–0.10
NO_3, mg/L	–0.10
Fe_{tot}, mg/L	–0.10
O_2, mg/L	0.09
NO_2, μg/L	0.09
Suspended solids, mg/L	–0.04
P_{tot}, μg/L	–0.04
Oil products, mg/L	0.03

The results of observations along the studied rivers in these two axes clearly illustrate the fact that the Arctic rivers flowing into the Arctic Ocean such as the Olenek, Indigirka, and Yana rivers flow through territories with a low STL thickness (Fig. 2). The rivers in the central part of the region (Amga, Olekma, Aldan, and Vilyui) are located in the area with a thick STL. Rivers that cross significant distances in the meridional direction (Kolyma, Lena), as well as southern rivers (Vitim and Chara), the upper reaches of which are located in mountainous regions, in their different sections flow in the areas with different thickness of the STL. For the Anabar River, the sampling points were divided along the STL1 axis into two groups. Some of them characterize the areas with a thin STL, and some are shifted along the abscissa axis to the left of mark 0. This suggests that some of the sampling points on this river belong to the areas with a thicker STL. It is also evident that the rivers with the highest concentrations of salt components are located in the central part of the studied region (Amga, Olekma, Vilyui, and Aldan rivers).

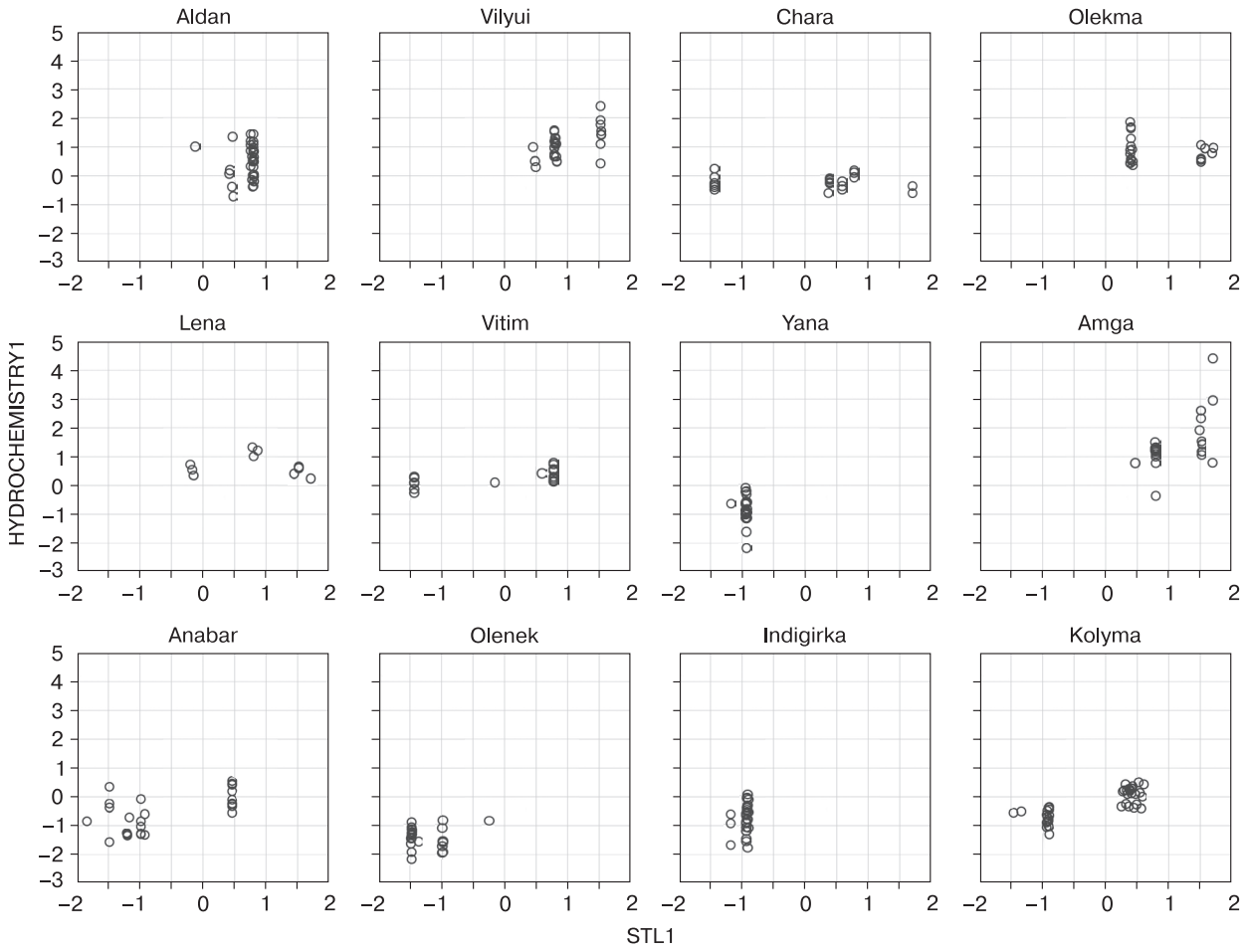

Fig. 2. Scatterplot of observations categorized by the studied rivers in the canonical axes HYDROCHEMISTRY1 (28 variables) and STL1 (3 variables).

DISCUSSION

For the studied large rivers of East Siberia, a favorable oxygen regime is typical. Most of the rivers are characterized by the low salt content. It is known that groundwater plays a significant role in the feeding of the Amga River compared to other rivers in the region [*Savvinov et al., 2000*]. This may explain the increased water hardness in this river. Relatively high COD and color values and increased concentrations of total iron and ammonium ions are characteristic of many reservoirs and watercourses in the region and are caused by natural factors [*Kirillov et al., 1979; Venglinsky et al., 1987*]. This phenomenon is associated with the entry of substances of natural origin into surface waters as a result of leaching from ferromanganese, copper pyrite, and other ores, as well as a result of the decomposition of bottom sediments [*Zenin, Belousova, 1988*].

The results of the canonical correlation indicate the relationship between the STL thickness and the concentration of a number of components of the salt composition of river water, namely hardness, sum of salts, calcium ions, bicarbonates, magnesium, and sulfate ions. The STL is characterized by low values in the north of the region and in the mountainous areas in the south. In the central part of the region, the STL is generally deeper [*Beer et al., 2013*]. A comparison between the patterns of spatial distribution of STL in the catchments of East Siberian rivers and the analyzed characteristics of the physical and chemical composition of river water made it possible to identify the following pattern: the deeper the base of STL of permafrost-affected soils in the drainage area, the higher the concentration of salt components.

The highest concentration of the six listed salt components was observed for four rivers in the central part of the region (Amga, Olekma, Vilyui, and Aldan rivers) flowing through the territory with the deepest STL. On the contrary, the majority of Arctic rivers confined to the catchments with thin STL are characterized by low concentrations of salt components.

This pattern can be explained using elements of the conceptual model of the STL influence on the chemical composition of surface water developed by R. MacLean [*MacLean et al., 1999*]. In spring, surface runoff is limited by the upper soil layers regardless of the presence of permafrost or seasonal frost. However, later, closer to the summer low-water period, such a factor as the STL thickness greatly influences the depth of penetration of runoff water flows into the soil. The conceptual model in question is based on the well-known fact that the upper soil horizon is characterized by accumulation of organic matter, and the underlying layer is mineral. A shallow STL keeps runoff flows close to the surface preventing them from penetration into the mineral soil horizons. A deep STL leads to a reduction in the time of contact of infiltrating surface water with the upper soil horizon and provides suprapermafrost runoff through underlying horizons rich in mineral substances [*Frey, McClelland, 2009*]. This difference in surface runoff pathways affects the chemical composition of water due to exchange reactions between soil and water [*Colombo et al., 2018*]. Thus, the STL thickness influences the natural process of transfer of soluble substances from soils to rivers with surface runoff.

A comparative study conducted on watercourses in the Western Siberia also showed that permafrost prevents the saturation of river water with mineral components. Thus, it was found that the total content of inorganic dissolved substances defined as the sum of eight components (Ca^{2+}, K^{+}, Mg^{2+}, Na^{+}, Si, Cl^{-}, HCO_3^{-}, SO_4^{2-}) averages 289 mg/L for rivers with catchments without permafrost and 48 mg/L for rivers located in the permafrost zone [*Frey et al., 2007*]. The authors associate this difference in the total mineralization of water with the hydrological features of the catchments, which depend on the presence of permafrost. According to researchers, permafrost forms a barrier that prevents the infiltration of surface runoff into deep mineral horizons, and also limits the influx of mineral-enriched sub-permafrost groundwater into surface water [*Woo, Winter, 1993; Michel, van Everdingen, 1994; Woo et al., 2000*].

This hypothesis is confirmed in other studies. Using the example of Alaskan watersheds with isolated permafrost, a higher content of bicarbonates, sulfates, as well as calcium, magnesium, potassium, and sodium ions was established in rivers flowing in areas of watersheds devoid of permafrost in comparison with adjacent areas of the permafrost zone [*Stottlemyer, 2001; Petrone et al., 2006, 2007; Keller et al., 2007*]. A significant decrease in the concentration of Ca^{2+} and Mg^{2+} ions was shown for taiga streams in Alaska influenced by permafrost distribution, which limits runoff within the upper soil horizon [*MacLean et al., 1999*].

Studies conducted in the watersheds of Central Siberia indicate that the concentration of calcium, sodium, magnesium, and potassium ions in river water increases significantly in the summer compared to the spring. Researchers attribute this to the fact that the mineral horizons become part of the STL in the summer, so that runoff flows penetrate into them, and these horizons become the source of mineral ions entering runoff flows and, finally, river water [*Parham et al., 2013*].

Comparative geochemical studies of the modern STL and the top of permafrost show that the upper permafrost layer is richer in minerals in relation to the overlying STL, which is due to a gradual removal of dissolved substances from the STL [*Kokelj, Burn, 2005*]. This indirectly confirms the validity of the above-mentioned conceptual model.

CONCLUSIONS

The catchments of East Siberia are characterized by the widespread distribution of continuous, discontinuous, and sporadic permafrost. The STL thickness in permafrost-affected soils greatly varies within the region. This is a factor that controls the natural transfer of soluble substances from soils to rivers with surface and soil runoff. The authors found that the studied rivers of the region are characterized by a favorable oxygen regime, relatively high COD and color values, increased concentrations of total iron and ammonium ions, and a low salt content.

The chemical composition of river water is formed in a complex natural system under operation of many factors, including the lithological composition of the soils in river catchments and the rocks of river beds, under-channel taliks with pressure waters, relief features controlling the speed of river flows and, hence, the time of interaction between river water and underlying sediments, etc.

In this study, we considered the influence of the STL thickness on the chemical composition of river water in permafrost landscapes of East Siberia. It was found that the STL thickness in the catchments is correlated with some hydrochemical characteristics of river water, such as hardness, the sum of salts, and concentrations of calcium, magnesium, bicarbonate, and sulfate ions. In the catchments with a thicker STL, the concentration of these salt components in river water is higher in comparison with rivers flowing in areas with a shallower STL. Rivers in the central part of the region (Amga, Olekma, Vilyui, and Aldan) flowing through the catchments with a thick STL are characterized by the highest concentrations of the salt components. The revealed pattern is consistent with the main provisions of the conceptual model of the STL influence on the chemical composition of river waters.

In recent decades, an increase in the STL thickness in permafrost-affected soils has been observed throughout the entire permafrost area in the northern hemisphere. Further increase in the STL thickness in

the 21st century is predicted. In this regard, our results are important for assessing possible changes in the chemical composition of river water in the Arctic regions in the future and the entry rate of dissolved substances into the Arctic Ocean.

Acknowledgments. *This study was carried out within the framework of the state assignment of the Ministry of Science and Higher Education of the Russian Federation, project nos. FWRS-2021-0026, EGISU R&D AAAA-A21-121012190036-6 and FWRS 0297-2021-0023, EGISU R&D AAAA-A21-121012190038-0, as well as the Ministry of Natural Resources and Environment of the Russian Federation, project no. 1-22-81-4.*

References

Afifi A.A., Azen S.P., 1982. *Statistical Analysis: A Computer-Oriented Approach*. Moscow, Mir, 1982, 488 p. (Russian translation).

Alekin O.A., 1953. *Fundamentals of Hydrochemistry*. Leningrad, Gidrometeoizdat, 250 p. (in Russian).

Alekin O.A., 1970. *Fundamentals of Hydrochemistry*. Leningrad, Gidrometeoizdat, 1970, 443 p. (in Russian).

Beer C., Fedorov A.N., Torgovkin Y., 2013. Permafrost temperature and active-layer thickness of Yakutia with 0.5° spatial resolution for model evaluation. *Earth Syst. Sci. Data* **5** (2), 305–310. doi: 10.5194/essd-5-305-2013.

Colombo N., Salerno F., Gruber S. et al., 2018. Review: Impacts of permafrost degradation on inorganic chemistry of surface fresh water. *Glob. Planet. Change* **162**, 69–83. doi: 10.1016/j.gloplacha.2017.11.017.

Desyatkin R.V., Okoneshnikova M.V., Desyatkin A.R., 2009. *Soils of Yakutia*. Yakutsk, Bichik Publ. House, 4 p. (in Russian).

Frey K.E., McClelland J.W., 2009. Impacts of permafrost degradation on arctic river biogeochemistry. *Hydrol. Process.* **23** (1), 169–182. doi: 10.1002/hyp.7196.

Frey K.E., Siegel D.I., Smith L.C., 2007. Geochemistry of West Siberian streams and their potential response to permafrost degradation. *Water Resour. Res.* **43**, W03406. doi: 10.1029/2006WR004902.

Gabyshev V.A., Gabysheva O.I., 2018. *Phytoplankton of the Largest Rivers of Yakutia and Adjacent Territories of Eastern Siberia*. Novosibirsk, SibAK Publ., 416 p. (in Russian).

Keller K., Blum J.D., Kling G.W., 2007. Geochemistry of soils and streams on surfaces of varying ages in arctic Alaska. *Arct. Antarct. Alp. Res.* **39** (1), 84–98. doi: 10.1657/1523-0430(2007)39[84:GOSASO]2.0.CO;2.

Kirillov F.N., Kirillov A.F., Labutina T.M., 1979. *Biology of the Vilyui Reservoir*. Novosibirsk, Nauka, 272 p. (in Russian).

Kokelj S.V., Burn C.R., 2005. Geochemistry of the active layer and near-surface permafrost, Mackenzie Ddelta region, Northwest Territories, Canada. *Can. J. Earth Sci.* **42**, 37–48. doi: OI:10.1139/e04-089.

MacLean R., Oswood M.W., Irons J.G., McDowell W.H., 1999. The effect of permafrost on stream biogeochemistry: A case study of two streams in the Alaskan (USA) taiga. *Biogeochemistry* **47** (3), 239–267. doi: 10.1007/BF00992909.

Matveev I.A. et al. (eds.), 1989. *Atlas of Agriculture of the Yakut ASSR*. Moscow, GUGK USSR, 116 p. (in Russian).

Michel F.A., van Everdingen R.O., 1994. Changes in hydrogeologic regimes in permafrost regions due to climatic-change. *Permafr. Periglac. Process.* **5**, 191–195. doi: 10.1002/ppp.3430050308.

National Atlas of Russia, Vol. 2. Nature. Ecology, 2001. Map of seasonal freezing and thawing of soils (scale 1:30 M). Moscow, Roskartografiya, p. 240–242.

Parham L.M., Prokushkin A.S., Pokrovsky O.S. et al., 2013. Permafrost and fire as regulators of stream chemistry in basins of the Central Siberian Plateau. *Biogeochemistry* **116**, 55–68. doi: 10.1007/s10533-013-9922-5.

Petrone K.C., Hinzman L.D., Shibata H. et al., 2007. The influence of fire and permafrost on sub-arctic stream chemistry during storms. *Hydrol. Process.* **21** (4), 423–434. doi: 10.1002/hyp.6247.

Petrone K.C., Jones J.B., Hinzman L.D., Boone R.D., 2006. Seasonal export of carbon, nitrogen, and major solutes from Alaskan catchments with discontinuous permafrost. *J. Geophys. Res.* **111**, G02020. doi: 10.1029/2005JG000055.

Savvinov D.D., Savvinov G.N., Prokopiev N.P. et al., 2000. *Applied Ecology of the Amga River*. Yakutsk, Publ. House of YaSC SB RAS, 168 p. (in Russian).

Semenov A.D., 1977. *Manual on the Chemical Analysis of Land Surface Waters*. Leningrad, Gidrometeoizdat, 540 p. (in Russian).

Shepelev V.V., 2009. *Permafrost of the Republic of Sakha (Yakutia):* A Comprehensive Atlas. Yakutsk, Izd. Yakutsk Aerogeod. Predpriyatie, p. 30–31 (in Russian).

Smith L.C., Sheng Y., MacDonald G.M., Hinzman L.D., 2005. Disappearing arctic lakes. *Science* **308** (5727), 1429. doi: 10.1126/science.1108142.

Stendel M., Christensen J.H., 2002. Impact of global warming on permafrost conditions in a coupled GCM. *Geophys. Res. Lett.* **29** (13), 1632. doi: 10.1029/2001GL014345.

Stottlemyer R., 2001. Biogeochemistry of a treeline watershed, northwestern Alaska. *J. Environ. Qual.* **30** (6), 1990–1998. doi: 10.2134/jeq2001.1990.

Venglinsky D.L., Labutina T.M., Ogay R.I. et al., 1987. *Specific Features of the Ecology of Hydrobionts in the Lower Lena River*. Yakutsk, Izd. YaF SO AN SSSR, 184 p. (in Russian).

Woo M-K., Marsh P., Pomeroy J.W., 2000. Snow, frozen soils and permafrost hydrology in Canada, 1995–1998. *Hydrol. Process.* **14** (9), 1591–1611. doi: 10.1002/1099-1085(20000630)14:9<1591::AID-HYP78>3.0.CO;2-W.

Woo M-K., Winter T.C., 1993. The role of permafrost and seasonal frost in the hydrology of northern wetlands in North America. *J. Hydrol.* **141**, 5–31. doi: 10.1016/0022-1694(93)90043-9.

Zenin A.A., Belousova N.V., 1988. *Hydrochemical Dictionary*. Leningrad, Gidrometeoizdat, 239 p. (in Russian).

Zhang T., Barry R.G., Knowles K. et al., 1999. Statistics and characteristics of permafrost and ground ice distribution in the Northern Hemisphere. *Polar Geogr.* **23** (2), 132–154. doi: 10.1080/10889379909377670.

Received April 14, 2022
Revised October 17, 2022
Accepted January 24, 2023

Translated by E.S. Shelekhova

EARTH'S CRYOSPHERE
SCIENTIFIC JOURNAL

Earth's Cryosphere, 2023, vol. XXVII, No. 2, pp. 21–26

PERMAFROST ENGINEERING

EXPERIMENTAL STUDY OF DEFLECTIONS AND BREAKING LOAD ON ICE REINFORCED WITH LONGITUDINAL ROD ELEMENTS FROM POLYPROPYLENE AND FIBERGLASS

V.L. Zemlyak[1,*], A.S. Vasilyev[1], V.M. Kozin[2], D.S. Zhukov[1]

[1] *Sholem-Aleichem Priamursky State University, Shirokaya St. 70A, Birobidzhan, 679015 Russia*
[2] *Institute of Machining and Metallurgy, Far Eastern Branch of the Russian Academy of Sciences, Metallurgov St. 1, Komsomolsk-na-Amure, 681005 Russia*

**Corresponding author; e-mail: vellkom@list.ru*

To date, the issue of using ice-based composite materials for engineering construction under harsh weather conditions remains poorly understood. Application of ice as a construction material is favored by its ease of use and low manufacturing cost. In turn, ice can be reinforced with various additional materials that change its physical and mechanical properties as part of an ice-based composite material. The results of an experimental study of the behavior of reinforced ice beams under pure bending are discussed. For reinforcement, longitudinal rods made of fiberglass and polypropylene with different physical and mechanical characteristics were used. The results of the study were compared with previous experiments on loading ice beams reinforced with steel armature. It is concluded that the proposed materials can be efficiently used to improve the mechanical characteristics of the ice. There is a positive effect of polypropylene on the deformability of the samples, as well as their bearing capacity. Schematic diagrams of deformation of ice beams when reinforced with steel and fiberglass armature and with polypropylene rods are presented. Prospects for the use of fiberglass and polypropylene rods in the ice-based composite materials are discussed.

Keywords: *ice beam, reinforcement, pure bending, carrying capacity, experimental research.*

Recommended citation: Zemlyak V.L., Vasilyev A.S., Kozin V.M., Zhukov D.S., 2023. Experimental study of deflections and breaking load on ice reinforced with longitudinal rod elements from polypropylene and fiberglass. *Earth's Cryosphere* XXVII (2), 21–26.

INTRODUCTION

In terms of the length of inland waterways, Russia ranks second in the world after China. In vast areas of the Far North, Siberia, and the Far East, where transport infrastructure is virtually absent, the main means of transportation and cargo delivery are river vessels. However, today, cargo transportation by inland waterways in Russia accounts for less than 1% of the total transport operations. Among the many reasons for the decrease in cargo turnover, the limited possibility of navigation in winter occupies an important place. In this regard, the issue of using the ice cover as ice crossings, winter roads, and cargo-carrying platforms is becoming increasingly relevant.

Examples of the successful use of ice for the engineering construction have been known since the beginning of the 20th century [*Nagrodsky, 1935; Lorch, 1977*]. With the intensive development of the Arctic basin, the task of designing and constructing ice aerodromes also arose, which required a deep understanding of the physical and mechanical properties and structure of the ice cover. In that time, K.F. Voitkovsky investigated the mechanical properties of ice [*Voitkovsky, 1960*]. J.T. Wilson, based on experimental data, developed a theoretical model of the behavior of the ice cover under the influence of single and paired load movements [*Wilson, 1955*]. The dependences of the stress-strain state of the ice on the speed of movement and other characteristics of various vehicles were experimentally studied [*Squire et al., 1988; Takizawa, 1988*]. Methods for calculating the ice cover rivers and reservoirs for the purpose of setting up temporary construction sites, access roads, and crossings were developed [*Bychkovsky, Guryanov, 2005*]. However, the increase in the mass of transported cargo and the complex behavior of the ice cover under static and dynamic loads necessitate the development of new approaches to the use of ice as a composite material of increased strength with specified physical and mechanical properties.

It was demonstrated that the ice strengthening at the microlevel can be achieved via adding fine particles (fibers, fine fibers, and some water-soluble compounds) to the ice cover [*Vasiliev et al., 2015; Cherepanin et al., 2018; Buznik et al., 2019*]. Fillers in the

form of polymers of various chemical compositions and morphologies can be used as reinforcement elements [*Buznik et al., 2017*].

Traditional methods of increasing the bearing capacity of the ice cover consist of the additional freezing of ice from below or from above, strengthening the ice with wooden track flooring, etc. Experience in practical implementation of these methods shows that the physical and mechanical properties of ice strongly depend on external factors at the time of freezing and may not always correspond to the required operational characteristics. Geosynthetic materials can also be used as reinforcement [*Sirotyuk et al., 2016*]; the greatest effect is achieved when using fiberglass meshes [*Yakimenko, Sirotyuk, 2015*]. Earlier, the authors obtained the results of an experimental and numerical study of the stress-deformed state of ice samples enhanced with longitudinal and transverse reinforcing elements made of steel and various modern composite materials [*Kozin et al., 2019a*]. The efficiency of using different reinforcement schemes to increase the bearing capacity of ice was evaluated. The bearing capacity of the samples with a high degree of rigidity increased significantly (up to 400%). However, the use of steel reinforcement has a number of technological and environmental limitations, and the efficiency and duration of operation of the ice crossing also depends on the elastic-plastic properties of ice caused by the introduction of elements with elastic properties into it.

The aim of this work was an experimental study of destructive an deflecting loads on ice samples reinforced with different number of elastic elements located in the zones of tension and compression under load.

PREPARATION FOR THE EXPERIMENTAL STUDIES

Tests of ice samples are carried out by three methods: by destruction of ice beams lying freely on supports, by destruction of ice consoles, and by destruction of a round ice plate lying freely on an annular support loaded in the center [*Stepanyuk, 2001*].

Within the framework of this study, the optimum method turned out to be the destruction of ice beams lying freely on two supports. The scheme of the test bench is shown in Fig. 1 [*Kozin et al., 2019b*].

The study was carried out according to the recommendations of the Committee on Ice Research and Engineering of the International Association of Hydro-Environmental Engineering and Research (IAHR) [*Test methods..., 2021*].

The length of the ice beams was 2000 mm, width and height 200 mm. As a reinforcing material, longitudinally spaced rods made of fiberglass composite reinforcement (FCR) and polypropylene rods with tubular cross-section (PRTS) placed in a specially made hermetically sealed formwork, which was filled with water and exposed to negative temperatures were used. The number of elements located in the zones of stretching and compression to ensure spatial rigidity and the integrity of the frame was 2–3 pieces for the FCR beams and 1–3 pieces for the PPTS beams. The rods were located at the same distance from one another and the neutral axis. An example of the PRTS reinforcement scheme is presented in Fig. 2.

As the PRTS rods in the ice samples had a significant diameter of 32 mm, it was decided to conduct tests for the beams reinforced with only two elements. For each reinforcement scheme, three ice samples were prepared, which were frozen under natural con-

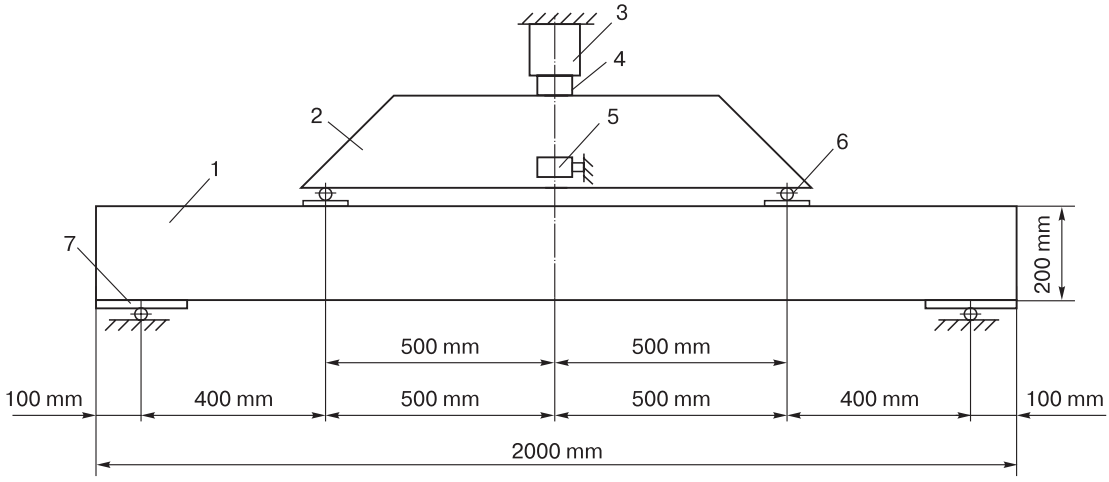

Fig. 1. Experimental installation scheme:

1 – ice beam; 2 – distribution beam; 3 – hydraulic cylinder; 4 – SH-20 weight terminal; 5 – LAS-Z vertical displacement sensor; 6 – hinge supports of the distribution beam; 7 – hinge supports of the ice beam [*Zemlyak et al., 2019*].

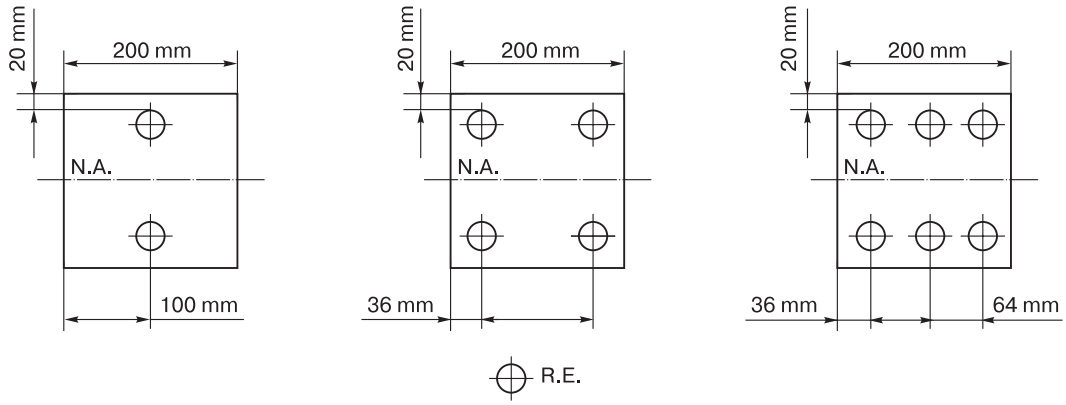

Fig. 2. Schemes of ice reinforcement with propylene rods of tubular section.

N.A. – neutral axis. R.E. – reinforcing element with the gravity center designation.

ditions at temperatures from –30 to –15°C for 7 days. The thickness of the protective layer of ice from the lateral plane of the beam to the nearest surface of the reinforcing element was 20 mm. Loading was carried out until the integrity of the sample was lost and pronounced through cracks appeared. The loading rate for all experiments was constant and equal to 135 kPa/s.

A GP2Y0E03 digital infrared vertical displacement sensor and an LPA-22t weight load cell with an SH-20 weighing terminal were used as measuring equipment. The destruction of samples was recorded by a high-speed high-resolution video camera VLXT-50M.I.

The experiments were carried out from December 2020 to February 2021 at ambient temperature from –20 to –15°C.

To assess the nature of the work of ice samples, the experimental data were compared with the results of loading of nonreinforced ice beams of similar size and beams reinforced with A400 metal armature with the same number of longitudinal connections (Fig. 3) [*Zemlyak et al., 2019*].

The mechanical characteristics of reinforcing materials are given in Table 1.

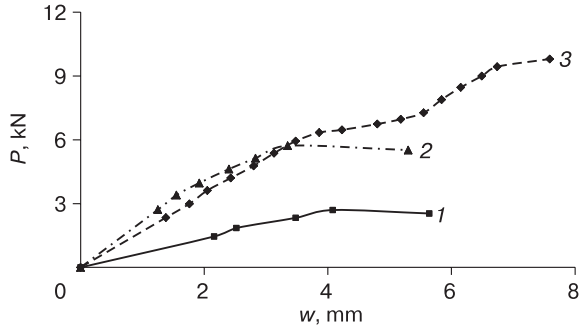

Fig. 3. Experimental load–deflection dependences for previously tested samples:

1 – nonreinforced sample; *2* – A400-4-6; *3* – A400-6-6.

Table 1. **Mechanical characteristics of reinforcing materials**

Parameter	A400	FCR	PRTS
Tensile strength limit σ_{bt}, MPa	365	168	50
Compressive strength limit σ_{bc}, MPa	365	63	50
Initial modulus of elasticity E, MPa	$20 \cdot 10^4$	$50 \cdot 10^3$	$1.5 \cdot 10^3$

MAIN RESULTS OF MODEL EXPERIMENTS

Figures 4 and 5 demonstrate a comparison of the averaged load–deflection dependencies obtained by processing the results of at least three experiments for nonreinforced ice samples and samples reinforced with FSR and PRTS with different amounts of reinforcing elements in the zones of tension and compression. In the names of FCR, PRTS, and A400, the first digit is the total number of rods in the section, the second digit is the diameter of the reinforcing element.

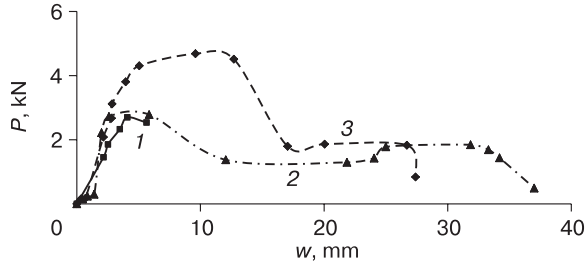

Fig. 4. Experimental load–deflection dependences for samples with fiberglass composite reinforcement:

1 – nonreinforced ice; *2* – FCR-4-10; *3* – FCR-6-10.

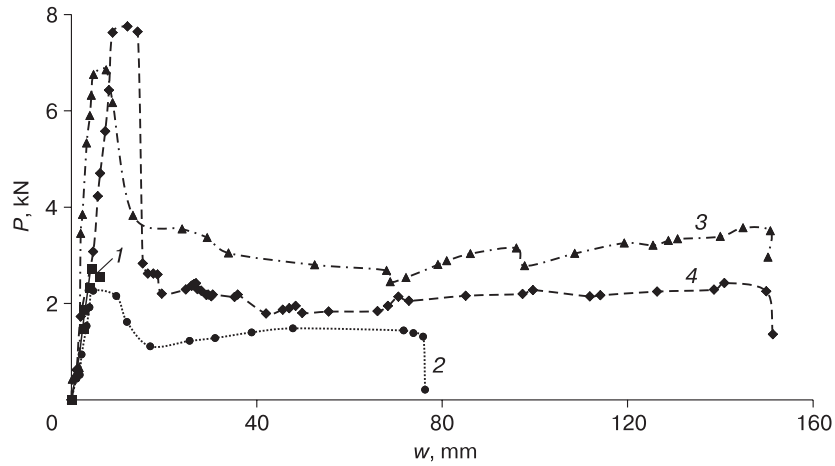

Fig. 5. Experimental load–deflection dependences for samples reinforced with polypropylene rods of tubular section (SPTS):

1 – non-reinforced ice; *2* – PRTS-2-32; *3* – PRTS-4-32; *4* – PRTS-6-32.

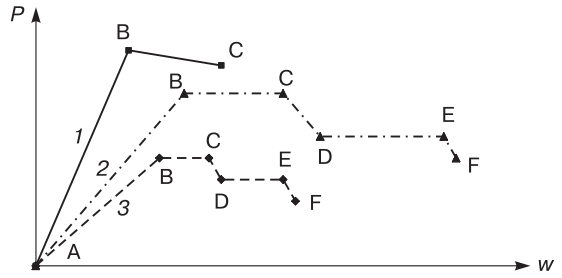

Fig. 6. Schematization of load–deflection diagrams for samples reinforced with various elements:

1 – A400; *2* – PRTS; *3* – FCR.

Figure 6 demonstrates the schematization of load–deflection diagrams when reinforcing samples with rod elements with different physical and mechanical properties.

Visualization of the destruction of an ice beam on the example of the PRTS-4-32 sample is shown in Fig. 7. The AB section is an elastic part of the diagram, where the relationship between stresses and deformations is linear and obeys Hooke's Law. The BC section is the deformability area, where the samples withstood the maximum destructive load P_{max} (Fig. 7*a*). In this section, the redistribution of forces between the material of the ice matrix and the rein-

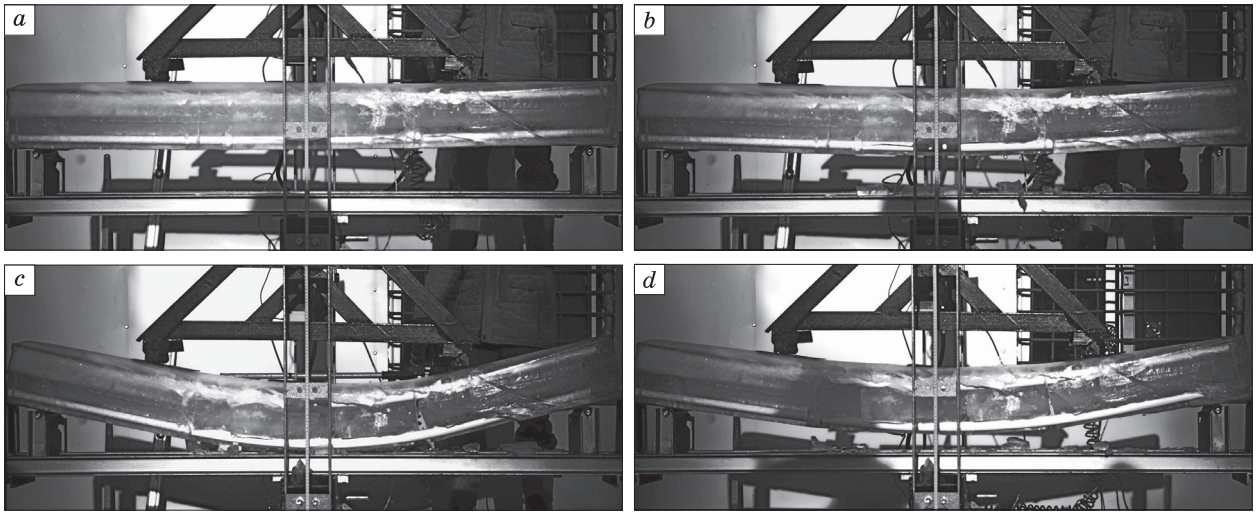

Fig. 7. Visualization of the process of destruction of the PRTS-4-32 sample according to the loading sections of the load–deflection diagram (see Fig. 6).

a – section BC; *b* – section CD; *c* – section DE; *d* – sample after removing the load.

forcing elements with the formation of the first cracks took place. It should be noted that for samples reinforced with A400 armature, the BC section displays the descending branch. For further analysis, we shall use the samples reinforced with PRTS and FCR. A decrease in the values of the load, the redistribution of the forces in the samples, and the most active formation of cracks was observed within the CD section; the destruction of ice took place in the tensile zone of the maximum bending moment (Fig. 7*b*). In the DE section, the main part of the load was taken by reinforcing elements, and plastic deformations accompanied by stress relaxation were observed in the ice, During loading, main through cracks were formed, but the reinforcing frames, despite significant deformations, continued to maintain the integrity of the ice beams (Fig. 7*c*). The greatest bearing capacity was shown by the samples PRTS-4-32 and PRTS-6-32, for which the maximum deflection value w_{max} was ~150 mm. Note that after removing the load, the samples partially returned to their original state, which indicates the efficiency of the elastic elements (Fig. 7*d*).

The main results of the model experiments are presented in Table 2.

Table 2. **Main results of model experiments**

Sample	w, mm	w_{max}, mm	P_{max}, kN
PRTS-2-32	5.06	75.9	2.24
PRTS-4-32	7.50	150	6.85
PRTS-6-32	12.1	150	7.75
FCR-4-10	2.60	27.90	2.72
FCR-6-10	5.54	36.93	4.31
No reinforcement	4.08	5.64	2.70
A400-4-6	3.35	5.30	5.72
A400-6-6	7.59	7.59	9.81

Note: In the names of FCR, PRTS, and A400, the first digit is the total number of rods in the cross section, the second digit is the diameter of the reinforcing element. w is the deflection when the maximum bearing capacity of ice samples is indicated; w_{max} is the maximum deflection of the sample after the complete or partial destruction of the ice matrix material and the redistribution of forces between the reinforcing material rods and ice; P_{max} is the maximum destructive load.

DISCUSSION

The tests demonstrated that the deformability of FCR-4-10 and FCR-6-10 samples was significantly higher than that of nonreinforced beams. Nonreinforced beams with comparable initial rigidity turned out to be significantly more brittle in comparison with beams reinforced with fiberglass armature, in particular FCR-6-10. For reinforced beams, after the P_{max} was reached, there was an insignificant area, where deformations continued to grow under a load of less than half of the maximum values (Fig. 4).

It can be seen in Fig. 5 that PRTS-2-32 samples did not have an obvious advantage in comparison with nonreinforced beams in initial rigidity and ultimate destructive load, but they showed significantly higher plasticity, even in comparison with the samples FCR-6-10. Samples PRTS-4-32 and PRTS-6-32 were subjected to significant bending during the experiments; they came into contact with the steel frame and rested against it upon a deflection of ~ 150 mm, which indicates the presence of a reserve of plasticity in such composite materials.

Comparison of the experimental results with the results of loading tests of the samples reinforced with A400 rods showed that the presence of steel reinforcement with a small diameter of cross section gives the structure the greatest rigidity; samples reinforced with A400-6-6 withstood the load P_{max} = 9.8 kN. However, the beams reinforced with steel armature were significantly inferior to FCR- and, especially, PRTS-reinforced ice beams in deformability and w_{max} value. It should also be noted that P_{max} for PRTS-4-32 and PRTS-6-32 were 6.85 and 7.75 kN, which greatly exceeded the P_{max} values for samples FCR-4-10 and FCR-6-10.

CONCLUSIONS

The model experiments have demonstrated good prospects of using surface reinforcement methods to increase the bearing capacity of the ice cover. When reinforcing elements exhibiting elastic properties are introduced into ice, the resulting load-deflection diagrams are more complex than when reinforcing ice with rigid elements in the form of metal armature.

The use of FCR and PRTS elements leads to a significant increase in the ultimate destructive load compared to nonreinforced samples. With the same number of rods, the use of PRTS ensures better indicators of deformability and ultimate destructive load in comparison with FCR.

At the initial stage of loading, PRTS samples are able to withstand a significant load, which drops sharply after the formation and opening of the main through cracks. Further ice hardening occurs in the compression zone, as a result of which the strength increases while maintaining the integrity provided by the reinforcing frame, and the load-bearing capacity of the beam also increases. Despite the large margin of deformability of the obtained composite materials, the diameter of the deflection bowl can be significant (which excludes the destruction of ice due to bending), and compression forces and reinforcing elements maintain the integrity of the ice providing an increased bearing capacity of the ice crossing.

The obtained experimental data on the strength of reinforced ice samples (reinforced ice beams) can

be used in the future when conducting numerical experiments on loading a reinforced ice plate (ice crossing) with a moving load (vehicle). Numerical modeling will make it possible to replace the extremely complex and labor-consuming field tests and determine the optimum solutions for the reinforcement of long crossings and winter roads, the length of which can be hundreds of meters.

References

Bychkovsky N.N., Guryanov Yu.A., 2005. *Ice Construction Sites, Roads, and Ice Crossings*. Saratov, Saratov State Technical University, 180 p. (in Russian).

Buznik V.M., Golushko S.K., Amelina E.V. et al., 2019. Determining the law of ice deformation. *J. Physics: Conf. Ser.* Art. 012010.

Buznik V.M., Landik D.N., Erasov V.S. et al., 2017. Physical and mechanical properties of composite materials on the basis of an ice matrix. *Inorganic Materials: Appl. Res.* **8** (4), 618–625.

Cherepanin R.N., Nuzhnyi G.A., Buznik V.M. et al., 2018. Physicomechanical properties of glacial composite materials reinforced by rusar-s fibers. *Inorganic Materials: Appl. Res.* **9** (1), 114–120.

Kozin V.M., Vasilyev A.S., Zemlyak V.L., Ipatov K.I., 2019a. Bearing capacity of reinforced ice beams exposed to simple bending. *Earth's Cryosphere* XXIII (5), 57–61.

Kozin V.M., Vasilev A.S., Zemlyak V.L., Ipatov K.I., 2019b. Investigation of the limit state of ice cover under conditions of pure bending when using reinforcing elements. *Vestn. Tomsk Gos. Univ. Mathematics and Mechanics*, 61, 61–69.

Lorch W., 1977. *Snow Travel and Transport. The Story of Snow Mobility in Pictures*. Macclesfield, England, The Gawsworth Ser., 243 p.

Nagrodsky L.V., 1935. *Railway Crossings*. Moscow, Transzheldorizdat, 120 p. (in Russian).

Sirotyuk V.V., Yakimenko O.V., Levashov G.M., Zakharenko A.A., 2016. Reinforcement of ice cover with geosynthetic materials. *Earth's Cryosphere* XX (3), 79–86.

Stepanyuk I.A., 2001. *Sea Ice Testing and Modeling Technologies*. St. Petersburg, Gidrometeoizdat, 77 p. (in Russian).

Squire V.A., Robinson W.H., Langhorne P.J., Haskell T.G., 1988. Vehicles and aircraft on floating ice. *Nature* 333, 159–161.

Takizawa T., 1988. Response of a floating sea ice sheet to a steadily moving load. *J. Geophys. Res.* 93, 5100–5112.

Test Methods for Model Ice Properties. International Towing Tank Conference (ITTC) – Recommended Procedures and Guidelines, 7.5-02.04-02, 2021, 19 p.

Vasiliev N.K., Pronk A.D.C., Shatalina I.N. et al., 2015. A review on the development of reinforced ice for use as a building material in cold regions. *Cold Regions Sci. Technol.* 115, 56–63.

Voitkovsky K.F., 1960. *Mechanical Properties of Ice*. Moscow, Izd. Akad. Nauk SSSR, 99 p. (in Russian).

Wilson J.T., 1955. *Coupling between moving loads and flexural waves in floating ice sheets*. US Army SIPRE Rep. 34, 28 p.

Yakimenko O.V., Sirotyuk V.V., 2015. *Strengthening of Ice Crossings by Geosynthetic Materials*. Omsk, SibADI, 168 p. (in Russian).

Zemlyak V.L., Kozin V.M., Vasilyev A.S., Ipatov K.I., 2019. Experimental and numerical study of the effect of reinforcement on the bearing capacity of ice crossings. *Soil Mechanics Foundation Engin.* 1, 14–19.

Received May 12, 2022
Revised December 9, 2022
Accepted January 30, 2023

Translated by S.B. Sokolov

Earth's Cryosphere, 2023, vol. XXVII, No. 2, pp. 27–38

PREVENTING THE NEGATIVE IMPACT OF FLOODING ON THE TEMPERATURE REGIME OF THE FROZEN BASE OF ROAD EMBANKMENTS

J.B. Gorelik[1,*], I.V. Zemerov[1], A.K. Khabitov[2]

[1] *Earth Cryosphere Institute, Tyumen Scientific Center, Siberian Branch of the Russian Academy of Sciences, Malygina St. 86, Tyumen, 625000 Russia*
[2] *Giprotyumenneftegaz, Respublika St. 62, Tyumen, 625000 Russia*

**Corresponding author; e-mail: gorelik@ikz.ru*

The article presents the initial assumptions of the predictive model of changes in the temperature regime of the frozen soil massif in the case of surface flooding. Heat exchange of the soil surface with the atmosphere through a shallow (up to 1 m) water cover is described using an effective heat exchange coefficient, which takes into account the intensity of mixing of the water layer in the summer. The results of calculation of two parameters of the new thermal condition of the frozen massif (temperature at a depth of zero annual amplitude and the maximum depth of seasonal thawing) appearing as a result of flooding are presented. In addition, the rate of transformation to the new condition is considered. Significant warming of the frozen base occurs in the case of intense mixing of the water layer during the summer season. If the mixing process does not take place in the water reservoir of a shallow depth, its cooling effect is possible. In deeper reservoirs, the warming effect is possible, but it is weaker than that under mixing conditions. This analysis has been performed for the least studied element of the "roadway embankment – reservoir – frozen soil" technical system in order to control the correctness of the calculation procedure in a more complex case for a two-dimensional process. The results of numerical modeling of the temperature field in the frozen base of the roadway in contact with a shallow water basin are presented. It is demonstrated that the frozen base warms up essentially, if the water layer is mixed intensively (by wind) in summer time. The initial temperature state may be preserved during the whole period of road exploitation, if the summer mixing of water is blocked by fairly simple technical measures that are proposed in this paper.

Keywords: *frozen ground, seasonal thawing, depth of seasonal thaw penetration, depth of zero annual amplitude of temperatures, surface water reservoir, roadbed.*

Recommended citation: Gorelik J.B., Zemerov I.V., Khabitov A.K., 2023. Preventing the negative impact of flooding on the temperature regime of the frozen base of road embankments. *Earth's Cryosphere* XXVII (2), 27–38.

INTRODUCTION

During road construction in permafrost areas, the formation of shallow (up to 1-m-deep) water bodies is often observed. These water bodies remain in contact with the slopes of road embankment for a long time and have an uncontrolled thermal effect on its frozen base [*Vorontsov et al., 2014; Grebenets, Isakov, 2016; Kondratiev, 2016; Dydyshko, 2017*]. Their occurrence may be associated with a change in natural factors or with flaws in the design of drainage and culvert constructions along the embankment. The main technical measures to eliminate the negative impact of flooding include special drainage solutions and repair and restoration works on existing structures, or the construction of new ones. Meanwhile, the efficiency of these works is low and requires additional measures to strengthen the foundation [*Andrinov, 2011; Litovko, 2011*]. As a result, this method of eliminating the negative impact of watering turns out to be ineffective and labor-intensive.

Today, in fact, the issues of assessing and forecasting the impact of such water bodies on the temperature regime of the frozen foundation of embankment structures, the practical significance of which for ensuring embankment stability is very important, remain unresolved. The purpose of this work is to create an adequate method for predicting the consequences of the influence of a shallow reservoir on the temperature regime of the frozen base of an embankment, to establish on this basis the most important factors that determine the intensity of the negative impact, and to evaluate possible proposals for its elimination.

INITIAL ASSUMPTIONS OF THE PROPOSED FORECASTING MODEL

The forecast of changes in the temperature regime of frozen soils under any violation of the conditions of heat exchange with the environment should answer two main questions: (a) what will be the values of the parameters of the new stable state of soils after the impact of disturbing factors and (b) what is the characteristic time to reach a new stable state of soils.

Individual elements of the embankment and the embankment as a whole can have both cooling and warming effects on the base [*Ashpiz et al., 2008; Ashpiz, Khrustalev, 2013; Zhang et al., 2018*]. The influence of the reservoir on the frozen ground is also complex and is not known in advance. For the correct statement of the mathematical problem of calculating the temperature regime of the frozen base of the roadway embankment (this type of embankment is considered below as an example) in contact with a water body, it is advisable, first of all, to find out the nature of the separate (i.e., independent of the embankment)

influence of the water reservoir on the underlying frozen ground. A certain step in solving this part of the problem was made in [*Gorelik, Zemerov, 2020*].

Determination of a new thermal state of soils in the event of water cover

In the complete formulation of the problem of the influence of a reservoir, the most important is the boundary condition that describes the heat exchange of the upper surface of the soil massif with the atmosphere through the water cover, and additional relations to it. It is usually written as a boundary condition of the 3rd kind. However, it should be noted that the exact recording of this relationship involves the division of the heat flux into radiative and convective components with specified methods for their determination, which significantly complicates the calculation procedure and is often impossible in practice because of the complexity of actinometric measurements with due account for the action of local factors of a particular terrain [*Pavlov, 1965*]. As a rule, the radiation component is not taken into account for solving practical problems, and the boundary condition has the form

$$\alpha\left(t_a - t\right) = -\lambda\left(dt/dz\right)_{z=0}. \qquad (1)$$

This condition must be supplemented by the following relations:

$$\alpha_{ss} = \left(\alpha_s^{-1} + \frac{h}{\lambda_{ef}}\right)^{-1}; \qquad (2)$$

$$\alpha_{ww} = \left(\alpha_w^{-1} + \frac{h}{\lambda_i}\right)^{-1}; \qquad (3)$$

$$\int_0^{\tau_h} t_a(\tau)\, d\tau = \frac{h\kappa_v}{\alpha_s}; \qquad (4)$$

$$\int_0^{\tau_i} t_a(\tau)\, d\tau = -\left[\kappa_v h\left(h + \frac{2\lambda_i}{\alpha_w}\right)\right] \Big/ 2\lambda_i. \qquad (5)$$

Table 1. **Mean monthly air temperatures for the area of the Urengoy weather station**

Month	Mean air temperature, °C	Month	Mean air temperature, °C
January	–26.4	July	15.4
February	–26.4	August	11.3
March	–19.2	September	5.2
April	–10.3	October	–6.3
May	–2.6	November	–18.2
June	8.4	December	–24.0

Here t, $t_a(\tau)$ are the soil surface temperature and the time-dependent air temperature τ in the annual cycle; α is the heat exchange coefficient at the upper boundary of the massif with the atmosphere, the dependence of which on the season is piecewise constant; α_s, α_w are the time-averaged summer and winter heat transfer coefficients determined without taking into account the influence of the reservoir (i.e., in the state before its appearance); α_{ss} is the summer heat transfer coefficient after the formation of a reservoir determined from the thickness of the water layer h and its effective thermal conductivity coefficient λ_{ef}, which takes into account the nature of water mixing (the range of its possible change: $\lambda_w \leqslant \lambda_{ef} \leqslant \infty$, where $\lambda_w = 0.5$ W/ (m·°C) is the thermal conductivity of water); α_{ww} is the winter heat transfer coefficient after the formation of a reservoir, which is determined similarly to the summer coefficient through the thermal conductivity of ice ($\lambda_i = 2.2$ W/(m·°C)). Soil thermal conductivity coefficient λ in Eq. (1) also takes piecewise constant (seasonal) values: λ_u in the thawed state and λ_f in the frozen state. Equations (4) and (5) determine the time of melting of the ice layer τ_h with the onset of summer and the time of freezing of the water layer τ_i with the onset of winter (taking into account the prerequisites formulated in [*Gorelik, Zemerov, 2020*]); κ_v is the volumetric heat of the water–ice phase transition. In the examples considered below, the air temperature $t_a(\tau)$ is taken from the Urengoy weather station (Table 1).

The mean annual temperatures at the bottom of the seasonally thawed layer (t_m) and at the depth of zero annual amplitudes (t_0) are determined by averaging the time-dependent temperatures $t_m(\tau)$ and $t_0(\tau)$ at the corresponding levels according to the relations

$$t_m = \frac{1}{\tau_0}\int_0^{\tau_0} t_m(\tau)d\tau, \quad t_0 = \frac{1}{\tau_0}\int_0^{\tau_0} t_0(\tau)d\tau \qquad (6)$$

(the depth of zero annual amplitudes z_0 is assumed to be 12 m; τ_0 is a year).

In the procedure for calculating the temperature field of the soil during periods of thawing and freezing of the water layer (the duration of which is a certain part of the summer and winter seasons), the temperature at the contact of water with the bottom of the reservoir is assumed to be 0°C [*Gorelik, Zemerov, 2020*]. Thus, in the presence of a reservoir on the surface of a frozen soil massif, the processes of seasonal freezing–thawing in its upper layers and the temperature dynamics below the base of the seasonally thawed layer beyond the time intervals of freezing and thawing of the reservoir itself in the general formulation of the mathematical problem are described by relations (1)–(3) for the corresponding seasons. During the periods of freezing or thawing of the water layer at the upper boundary of the soil (coinciding

with the surface of the bottom of the reservoir), the boundary condition of the 1st kind (with a temperature of 0°C on its surface) is used. Note that under steady-state conditions of heat transfer, the temperatures t_m and t_0 coincide [*Carslaw, Jaeger, 1964; Dostovalov, Kudryavtsev, 1967; Tikhonov, Samarsky, 1972*].

In all the examples of calculations given below, the following characteristics of soils and initial conditions are assumed (index u refers to thawed soil, and index f, to frozen soil): heat capacity (J/(m^3·°C): $C_u = 2.86 \cdot 10^6$, $C_f = 2.20 \cdot 10^6$; thermal conductivity of the soil (W/(m·°C)): $\lambda_u = 1.76$, $\lambda_f = 2.10$; thermal conductivity of water and ice $\lambda_w = 0.5$, $\lambda_i = 2.2$; bulk density of the skeleton $\gamma_s = 1500$ kg/m^3, thermal diffusivity $\mu_f = 9.55 \cdot 10^{-7}$ m^2/s, weight water content $w = 0.2$, initial temperature at the depth of zero annual amplitudes in the undisturbed soil massif $t_0 = -2.0$°C.

Equations (2)–(5) explicitly single out the contribution of only the water cover to the heat exchange with the soil surface. However, it must be remembered that even for undisturbed conditions, coefficient α in its seasonal components α_s and α_w implicitly depends on a significant number of influencing factors of a physical-geographical, climatic, and geological nature. It is difficult to establish the influence of the totality of these factors in the problem under consideration, and it is often impossible to single out the prevailing influence of their minimum number. To solve this problem, the work [*Gorelik, Pazderin, 2017*] proposes a method for determining coefficients α_s and α_w on the basis of empirical data obtained during engineering surveys, which contain actual information on the maximum depth of seasonal thawing (ξ_m) and temperature at the depth of zero annual amplitudes (t_0) (it is better to use monitoring data and calculated long-term average values). The coefficients determined by this method implicitly take into account the action of the entire group of influencing factors and ensure the invariance of the values of ξ_m and t_0 (in the area outside the contour of the structure) throughout the entire life of the structure (usually at least 30 years) provided that external conditions are constant. At the same time, to predict the effect of a structure on frozen soils, the thermal effect of the structure itself is considered separately in an explicit form (just as it was done for a reservoir).

For the above characteristics of soils and air temperature, the values of the coefficients for the undisturbed soil mass (W/(m^2·°C)) were obtained in this way: $\alpha_s = 17.5$, $\alpha_w = 1.02$. As seen from Fig. 1, these values ensure the constancy of the maximum depth of seasonal thawing $\xi_m = 1.7$ m (determined by the break point of temperature on the corresponding curves) and $t_0 = -2$°C for 30 years of cyclically recurring seasonal temperature fluctuations. It is important that this state of the soil, when using numerical methods, is also taken as the initial condition in the problems of finding the temperature field in the soil for surface disturbances of any nature. With this method of setting the coefficients α_s, α_w and the initial condition consistent with them, the systematic error of calculations associated with the "unreasonable influence" of the soil mass outside the zone of surface disturbances on the calculation results is eliminated.

Note that in some works, the constancy of the temperature t_0 for the entire life of the structure is ensured by a special selection of the dynamics of the snow cover depth during this period. In our opinion, this approach has a significant drawback, because it requires an additional prediction of the temperature at the base of the soil massif, which has no factual justification. Its inconsistency is seen from the absence of a trend in climate change during the period under consideration. In this case, there are no reasons for changing the average long-term values of any of the climatic parameters (in particular, snow accumulation), and they should be taken constant over time. At the same time, it is practically impossible to select seasonal heat transfer coefficients (based, for example, on the known relationships between wind speed and data from local weather stations) that ensure the constancy of temperature t_0 for a given period. This can lead to significant errors in the quantitative prediction of

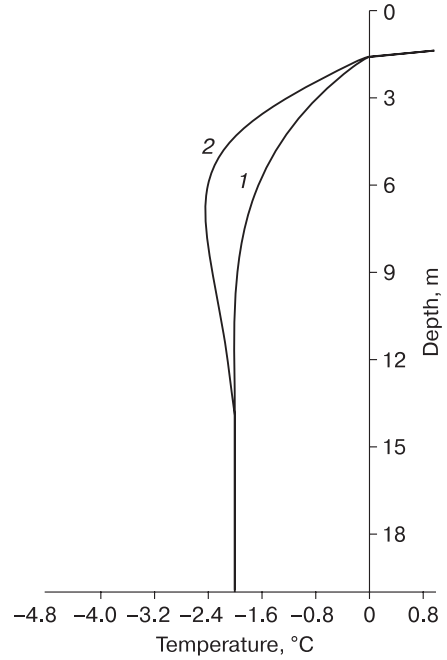

Fig. 1. Calculated temperature distribution over the depth of the soil mass under conditions of natural heat exchange during the first year (*1*) and the final calculation year (*2*) at $\alpha_s = 17.5$ W/(m^2·°C), $\alpha_w = 1.02$ W/(m^2·°C).

1 – July 1, 2000–July 1, 2001; *2* – July 1, 2031–July 1, 2032.

the thermal impact of structures on the frozen basement. The approach proposed by the authors is based only on actual data (long-term average values of ξ_m and t_0, which implicitly reflect the action of the entire set of influencing factors, including snow cover); thus, it is free from the indicated drawback. A modification of this approach can be applied to predict the temperature in the soil massif also in the case of some trend of climate change [*Gorelik, Zemerov, 2022*].

Using Eqs. (1)–(6), the dependences of the new steady-state temperature at a depth of zero annual amplitudes t_0 on the depth of the reservoir were obtained for two limiting cases related to mixing of the water layer (Fig. 2) [*Gorelik, Zemerov, 2020*]. Two independent methods – analytical (curves *1′*, *2′*) and numerical (curves *1*, *2*) – were applied. If necessary, additional calculations can be carried out for intermediate values of the coefficient λ_{ef}. If a sufficiently reliable method of preventing mixing is used, then the need for such calculations is eliminated.

Important features of the behavior of the new steady-state temperature t_0 are closely related to two characteristics of the water layer – its depth and the intensity of mixing in summer. With intensive mixing (due to wind action and natural convective motion), the soil temperature increases monotonically with increasing depth of the reservoir (Fig. 2, curves *1*, *1′*). If conditions arise in summer that prevent mixing of the water layer, then there is a range of depths at which the water layer has a cooling effect on the underlying soils (Fig. 2, curves *2*, *2′*). When analyzing the graphs (Fig. 2), it should be kept in mind that the point ($h = 0$, $t_0 = -2$°C) characterizes the state of frozen soil in the absence of a reservoir, it is the same for both pairs of curves *1*, *1′* and *2*, *2′*. Therefore, both pairs have this common starting point on the charts. The extraordinary behavior of temperature in the absence of mixing is due to the multidirectional influence of the depth of the reservoir on the time of freezing of bottom sediments and on the duration of the cooling pulse in winter. The magnitude of seasonal thawing monotonically decreases with increasing depth of the reservoir, which, at shallow depths, leads to a shorter time of water freezing in winter and increases the duration of the cooling impact on the soil. Starting from a certain depth, the duration of freezing of the water layer (in the first approximation, proportional to the square of its depth) begins to have a decisive influence, which leads to a reduction in the duration of the cooling pulse and an increase in soil temperature [*Gorelik, Zemerov, 2020*]. At the same time, it can be seen that in the depth range where the soil is heated in the absence of mixing ($h > 0.5$ m), the soil temperature remains significantly lower than in the case of water mixing.

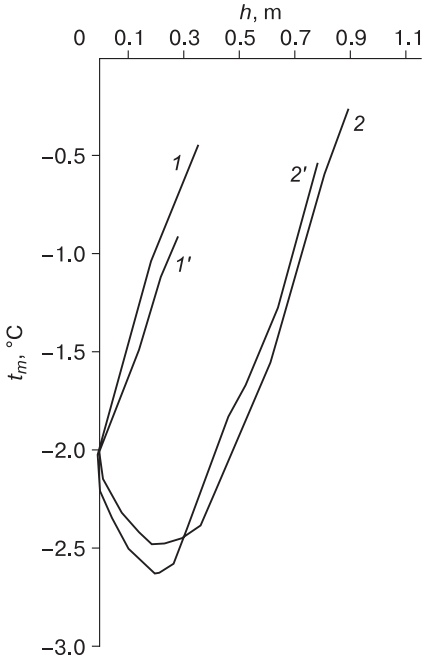

Fig. 2. Dependence of the mean annual temperature at the depth of zero annual amplitudes under the reservoir (t_m) on its depth h in the mode of steady oscillations:

1, *1′* – with full mixing ($\lambda_{ef} \to \infty$); *2*, *2′* – in the absence of mixing ($\lambda_{ef} = \lambda_w$); *1*, *2* – calculation by numerical method; *1′*, *2′* – calculation by analytical method.

Conditions that prevent mixing may occur due to natural causes (for example, when a reservoir is overgrown or silted and enriched with organomineral matter brought in by wind or by flows from adjacent slopes). This explains the well-known facts of the attenuation of thermokarst during the overgrowing of thermokarst lakes at the initial stage, which leads to a reduction in the heat flux into the ice-rich frozen base, or the cooling effect of mires (with a significant proportion of the organomineral component) on the temperature regime of the underlying soils [*Dostovalov, Kudryavtsev, 1967; Kudryavtsev, 1978; Feldman, 1984; Shur, 1988*]. It is also possible to prevent the mixing of a shallow reservoir in the summer season by purely technical means [*Method..., 2021*]. For this, the following methods are used: (a) artificial sowing of marsh grasses (as opposed to sowing of field grasses on slopes of the embankment to strengthen them); (b) adding of organomineral substances (peat, peat–soil mixtures) in the required amount; (c) installation of lightweight mesh (or cellular) structures (for example, in the form of mats made of thin plastic threads or natural fibers). If necessary, mats can be attached to the bottom of the reservoir with anchor pins. It is possible to use various combinations of these methods.

The main requirements for the material filling the reservoir are a sufficiently high moisture capacity (ensuring considerable heat consumption during summer thawing) and the formation of a rigid or viscous structure in the water, which prevents water

mixing under the influence of wind and natural convection.

The foregoing allows us to highlight the following main points: the most significant factors that determine the thermal effect of a reservoir on the underlying frozen soils are the depth of the reservoir and the intensity of mixing of the water layer in the summer season. It is possible to reduce the negative impact of water reservoirs via eliminating or minimizing the possibility of mixing of the water layer in the summer season. To determine the new thermal state of soils during watering of the surface, Eqs. (1)–(6) should be used for the mathematical description of heat exchange between the frozen soil and the atmosphere through the water layer (for preliminary analysis, the calculation results presented in Fig. 2 can be used).

Relaxation time to a new state

The time of transition τ_f of the soil temperature t_0 to a new stable state corresponding to a new value of t_m upon the appearance of water reservoir is determined by an approximate method using the formula [*Gorelik, Zemerov, 2020*]:

$$\tau_f = \frac{z_0^2}{12\mu_f\left(1-\sqrt{1-n}\right)^2},\ \Delta t = t_0 - t_m,\ \delta t = t_f - t_m,$$

$$n = \left|\delta t/\Delta t\right|. \qquad (7)$$

Due to the fact that the relaxation time from temperature t_0 to t_m is, generally speaking, infinite [*Carslaw, Jaeger, 1964; Tikhonov, Samarsky, 1972*], an auxiliary (intermediate) temperature t_f is introduced; t_f is sufficient to achieve engineering goals, but some-

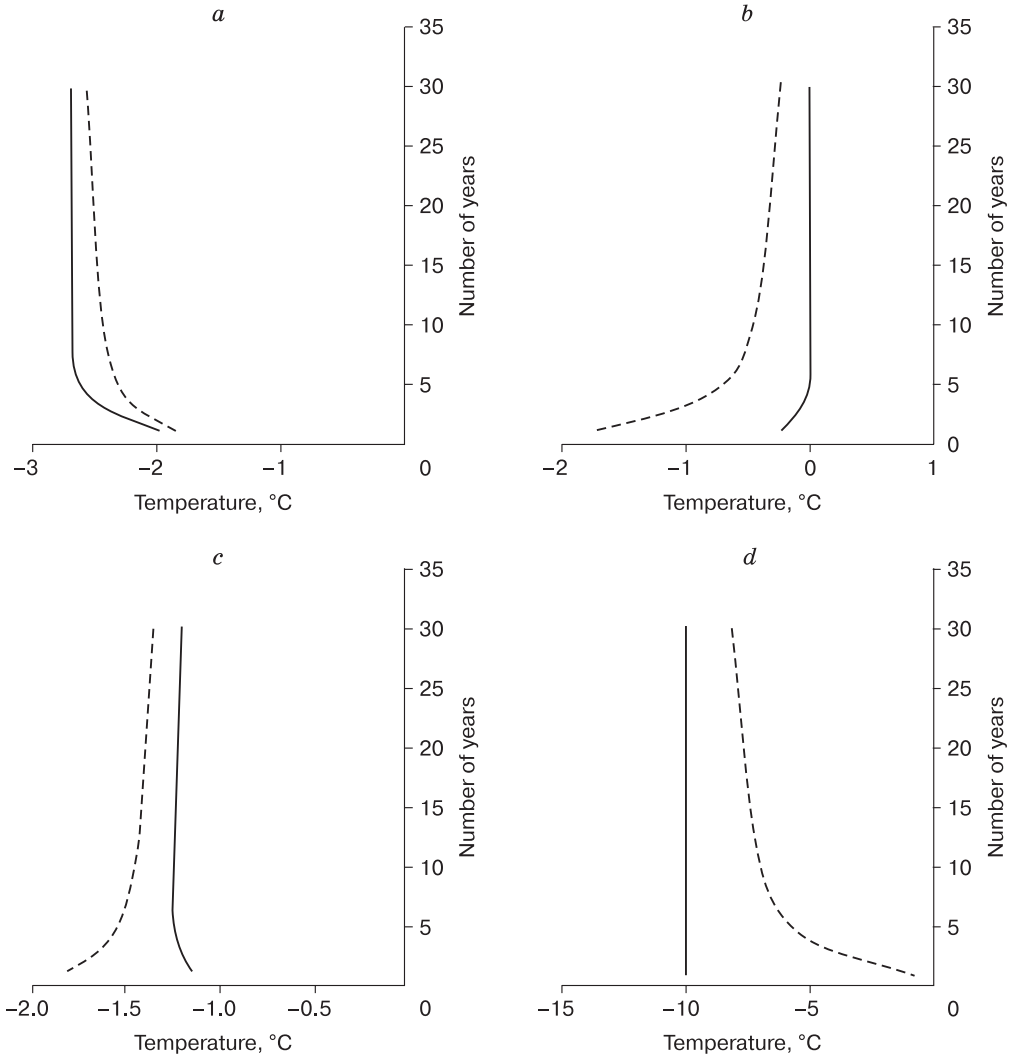

Fig. 3. Variation of the mean annual temperature at the base of the seasonally thawed layer (solid line) and at the depth of zero annual amplitudes (dashed line):

(*a*, *b*) h = 0.3 m without (*a*) and with (*b*) water layer mixing in summer; (*c*) h = 0.6 m without water layer mixing in summer; (*d*) when applying special technical measures ensuring a low mean annual temperature at the base of the seasonally thawed layer.

what differs from t_m. It follows from Eq. (7) that at $t_f = t_m$, we get $n = 0$, and the time τ_f goes to infinity. The temperature t_f is reached in a finite time τ_f, which is a function of this temperature. Previously, this formula was also used to estimate the relaxation time for special surface methods of base cooling [*Gorelik, Khabitov, 2021; Gorelik et al., 2021*].

At the time of publication of the work [*Gorelik, Zemerov, 2020*], the authors were not able to compare the results of calculations using Eq. (7) with the results of calculations by numerical methods. Such a comparison is given below for some important cases (Fig. 3). Figure 3*a* presents the results of calculations by numerical methods of the change in temperature over time at the bottom of the seasonally thawed layer and at a depth of zero amplitudes, when a reservoir with a depth $h = 0.3$ m appears on the surface of the soil without the possibility of mixing the water layer ($t_0 = -2$°C, $t_m = -2.6$°C). It can be seen that the temperature at depth z_0 reaches the value $t_f = -2.3$°C after $\tau_f = 5$ yr; at $t_f = -2.4$°C, $\tau_f = 10$ yr. The values of τ_f obtained from Eq. (7) for these cases are 3.2 and 8.2 yr, respectively. For the case of layer mixing at $h = 0.3$ m, the results of numerical calculations are shown in Fig. 3*b* ($t_0 = -2$°C, $t_m = -0$°C). Soil warming up to (for example) $t_f = -0.5$°C takes place over time $\tau_f = 10$ yr; according to Eq. (7), we get $\tau_f = 15$ yr. The dynamics of both temperatures at $h = 0.6$ m without mixing (but at which the warming process also occurs, see Fig. 2) is shown in Fig. 2*c* ($t_0 = -2$°C, $t_m = -1.24$°C). In this case, the relaxation time to the value $t_f = -1.5$°C is equal to $\tau_f = 7.5$ yr; according to Eq. (7), $\tau_f = 7.8$ yr.

In the case when, with the help of special technical means, the temperature at the bottom of the seasonally thawed layer is kept very low (Fig. 3*d*, $t_0 = -2$°C, $t_m = -10$°C), the temperature decrease by one degree at the depth z_0 ($t_f = -3$°C) is achieved very quickly (in about one year), which is confirmed by calculations both by the numerical method and by Eq. (7). The graphs can also be used to control the correctness of the computational procedure: the dashed curve should asymptotically approach the solid line as $\tau_f \to \infty$; in case of disturbances on the ground surface of a cooling nature, the solid curve should lie to the left of the dashed curve, and vice versa. In general, it can be argued that despite the lack of accuracy, Eq. (7) can be used for preliminary estimates. Its advantage lies in the simplicity of calculations, and the procedure for its derivation allows us to understand the physics of the ongoing processes. At the same time, numerical methods are more accurate and allow one to take into account the dependence of external factors on coordinates and time; also, they make it possible to obtain much more complete information about the spatial characteristics of the temperature field and its dynamics in cases, where the dimension of the computational domain exceeds unity. In studies of the dynamics of the temperature field under surface disturbances, both methods are useful and complement one another.

Meanwhile, during each year, there is a change in temperature at each of the two levels considered, which has the character of almost periodic changes during a 30-yr time cycle. Thus, the temperature behavior at the bottom of the seasonally thawed layer during the 1st, 5th, 15th, and 30th years after the formation of the reservoir is shown in Fig. 4*a*; at a depth of zero annual amplitudes, in Fig. 4*b*. The mean annual temperatures at these depths calculated according to Eq. (6) are shown as corresponding points on the curves (Fig. 4*b*). Note that with a noticeable

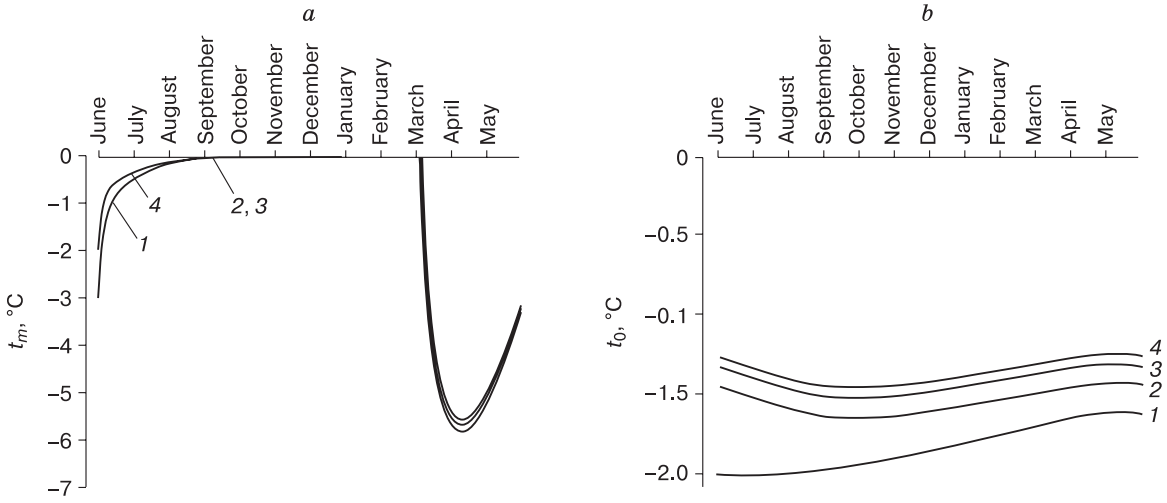

Fig. 4. Temperature change at the bottom of the seasonally thawed layer t_m (*a*) and at a depth of zero annual amplitudes t_0 (*b*) during the calculated years:

1 – 1st year; 2 – 5th year; 3 – 15th year; 4 – 30th year.

quantitative change in temperature at a depth of z_0, its behavior at the bottom of the active layer, after a short initial period, remains practically unchanged over a 30-yy-long period, which is reflected in the almost constant value of the mean annual temperature (Fig. 3*a*). That is, at the level ξ_m, a stable value of the new temperature is reached very quickly (the relaxation time does not exceed five years). A slight increase in this temperature (within 0.1°C over 30 yr) shown in Fig. 3*c* is most likely due to the insufficient accuracy of the calculations and will be analyzed in further studies. In this case, the value of ξ_m changes slightly: ξ_m = 0.59 m at τ = 1 yr, ξ_m = 0.57 m at τ = 30 yr.

At the level ξ_m, the differences in the temperature dynamics during each year are blurred, but they are noticeable in the mean annual values, which is reflected in the behavior of the initial segment of the solid curves in Fig. 3. It follows from the position of the curves in Fig. 3 that the mean annual temperature at base of the active layer is the main reason for the temperature change at the depth of zero annual amplitudes, which was previously noted in a number of works [*Porkhaev, 1970; Kudryavtsev, 1978; Feldman, 1984; Gorelik, Zemerov, 2020, 2022*]. The vagueness of changes in the mean annual temperature at the base of the active layer can contribute to the development of adequate criteria for determining the accuracy of temperature measurements within the active layer during monitoring studies.

The analysis of curves shown in Figs. 3–5 is very useful from the point of view of quantitative assessment of the influence of various types of surface disturbances or the application of special technical measures on the temperature regime of the frozen soil massif. For example, it follows from it that the efficiency of open ventilated underground or suspended structures can be significantly increased by periodical compaction of the snow cover in the winter season. An increase in snow density strongly increases thermal conductivity of the snow [*Feldman, 1977; Smorygin, 1988*], which leads to a noticeable decrease in its warming effect on soils in the winter season. A similar effect can be achieved by maintaining snow cover for most of the summer period (which can be achieved through the seasonal application of thermal insulation coatings). Although the possibility of implementing these measures in the form of any acceptable technologies is currently not achievable, they can be applied in extreme conditions using fairly simple technical means. It is also interesting that permafrost islands can be formed in this way inside massifs of thawed soil in areas with rather moderate depths of seasonal freezing provided that the initial temperature t_0 does not significantly exceed 0°C. In addition, an analysis of the results of calculation of the temperature dynamics of frozen soils will be useful for predicting their thermal response to climate change [*Gorelik, Zemerov, 2022*].

TEMPERATURE CALCULATIONS AT THE BASE OF EMBANKMENT IN THE PRESENCE OF A WATER RESERVOIR

This paper describes the problem statement and the results of calculating the temperature field in the frozen base of a road embankment during its service life (30 yr) in the presence of a shallow water reservoir near one of the slopes. The purpose of the calculations is to evaluate the efficiency of technical measures to eliminate the mixing of the water layer in summer to stabilize the frozen state of the embankment base.

Characteristics of design conditions

Figure 5 shows a diagram of the computational domain, which includes a cross section of a roadbed embankment laid on permafrost and in contact with a shallow water body. It is assumed that there is no water filtration through the body of the embankment, and in all parts of the soil massif (including the body of the embankment and base soils) heat transfer occurs only by conduction. Convective heat transfer is

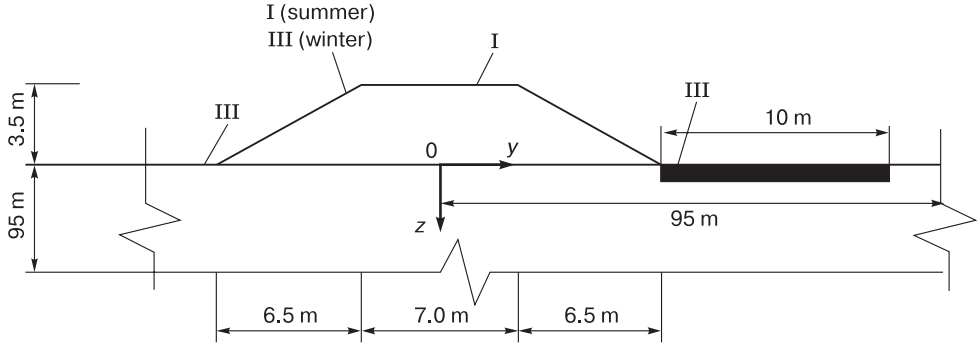

Fig. 5. Geometric parameters of the computational domain and the type of boundary conditions at the elements limiting it.

I, III – boundary conditions of the 1st and 3rd kind, correspondingly. Explanations are in text.

present only within the reservoir and is taken into account through the coefficient of effective thermal conductivity of the water layer. The problem statement includes: a non-stationary heat equation written in enthalpy form [*Gorelik et al., 2021*], a set of boundary conditions over the entire surface of the allocated computational domain, and initial temperature condition for its internal points.

The calculation of the dynamics of the temperature field in a soil mass that is inhomogeneous in properties is carried out taking into account the change in the phase state in the seasonally thawed layer. The boundaries of the computational domain from the top are formed by a combination of the outer boundary of the embankment, the bottom of the reservoir, and the horizontal surface of the natural massif (Fig. 5). The upper boundary of the water layer coincides with the level of the horizontal surface of the base soils (excavation of arbitrary genesis). The coordinate system is located in a horizontal plane coinciding with the surface of the base, its center coincides with the center of symmetry of the cross section of the embankment. The *Oz* axis is directed vertically downwards, the *Ox* and *Oy* axes lie in the horizontal plane and are directed along the longitudinal and transverse axes of the embankment, respectively. The dimensions of the computational domain along each of the axes are determined by the radius of the thermal influence [*Gorelik, Pazderin, 2017*]; when calculating for a 30-yr period, this radius is 95 m. Thus, the boundaries of the computational domain should be 95 m away from the boundaries of the embankment contour in the plan and at the same distance vertically deep into the array. At these boundaries, the zero value of the heat flux is set. The heat exchange of the upper boundary of the soil with the air (under natural conditions – outside the structure and reservoir) through the ground covers is taken into account by the boundary condition of the 3rd kind with different heat transfer coefficients in summer and winter. These coefficients ensure that the temperature remains unchanged at the depth of zero amplitudes ($t_0 = -2.0$°C) during the entire period under consideration (30 yr): $\alpha_s = 17.5$ W/(m^2·°C); $\alpha_w = 1.02$ W/(m^2·°C). The heat exchange of the surface of the carriageway of the embankment with the air is taken into account by the boundary condition of the 1st kind with a temperature equal to the air tempera-

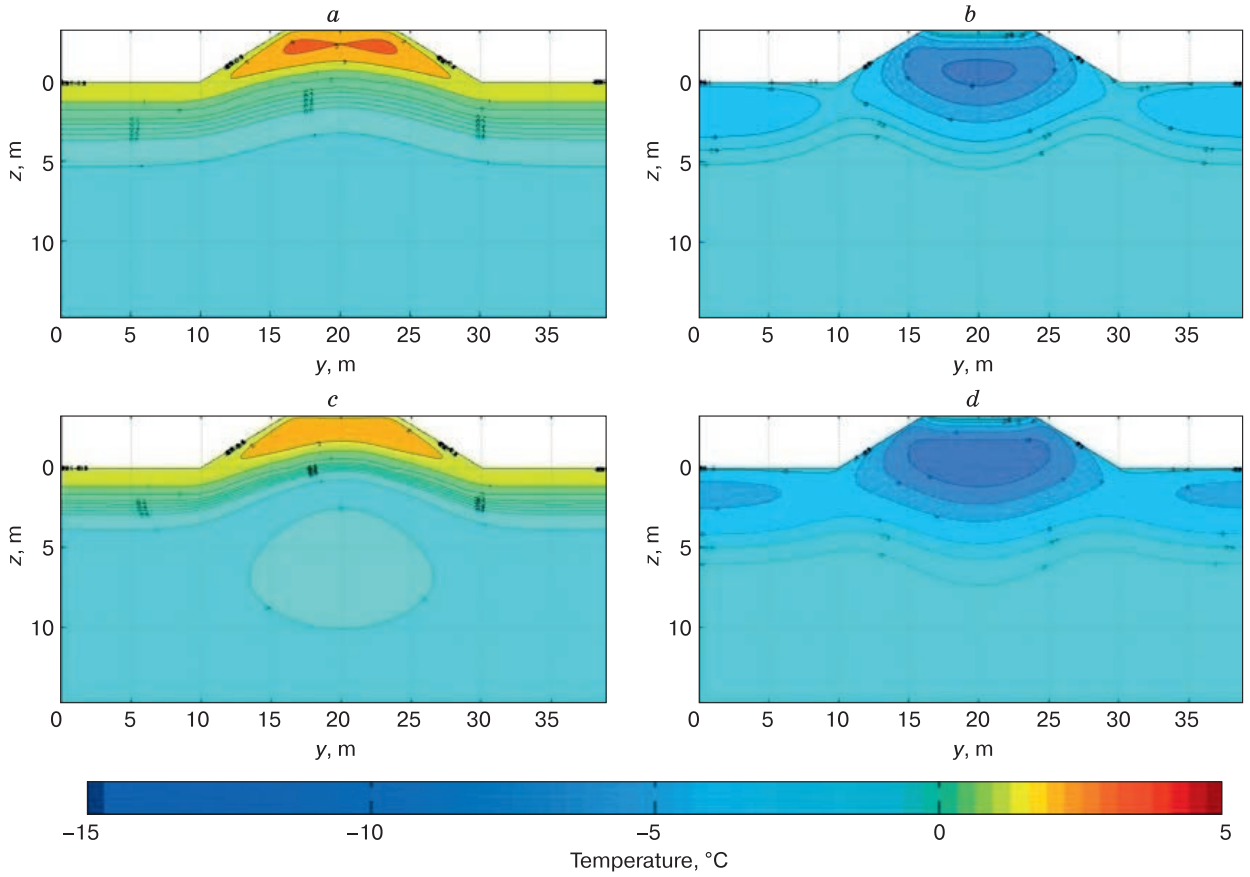

Fig. 6. Temperature field at the base of the embankment in the absence of watering.

a, *b* – the first year of operation: *a* – Oct. 1, 2000; *b* – June 1, 2001; *c*, *d* – the thirtieth year of operation: *c* – Oct. 1, 2030; *d* – June 1, 2031. At the lowest part of the figure is a scale for matching color and temperature.

ture (assuming the presence of a hard coating and regular snow removal in winter). The heat exchange of the upper boundary of the embankment slopes with the air in summer is determined by the boundary condition of the 1st kind at a temperature equal to the air temperature (taking into account the absence of moisture accumulation conditions), and in winter – by the 3rd kind boundary condition with a winter heat transfer coefficient, which is half as much as under natural conditions (α_w = 0.55 W/(m^2·°C)), taking into account additional snow accumulation due to clearing of the roadway and wind deposits.

The thermophysical characteristics of soils are piecewise constant, different for thawed and frozen states. For foundation soils, they are taken as described above. For the embankment material (sand), the characteristics are as follows: volumetric heat capacity (J/(m^3·°C)): $C_u = 2.26 \cdot 10^6$, $C_f = 2.10 \cdot 10^6$; thermal conductivity coefficients (W/(m·°C)): λ_u = 2.1, λ_f = 2.14; volumetric heat capacity of phase transition $\kappa_v = 3.34 \cdot 10^7$ J/m^3. The initial soil temperature at the depth of zero amplitudes is t_0 = –2°C.

The geometrical parameters of the cross section of the embankment are taken as follows (the section has a trapezoidal shape): the height of the embankment is 3.5 m; width of the main platform (top of the embankment) is 7 m; width at the base is 20 m (Fig. 5).

The depth of the reservoir adjacent to the slope in the example is h = 0.6 m. The heat exchange of the surface of the soil base (bottom of the reservoir) with the air through the water layer is described by Eqs. (1)–(6), taking into account the above, relative to the temperature of the bottom of the reservoir during periods of freeze-up and ice cover melting. When describing convective heat transfer in the form (1), the heat transfer coefficient between moving media (or the equivalent effective thermal conductivity of the water layer λ_{ef}) increases without limit with increasing mixing intensity [*Mikheev, Mikheeva, 1973*]. The limiting values for intensive mixing of these coefficients can be taken to be infinitely large. Calculations show that the calculation results practically cease to depend on λ_{ef} if its value exceeds 200 W/(m·°C). For

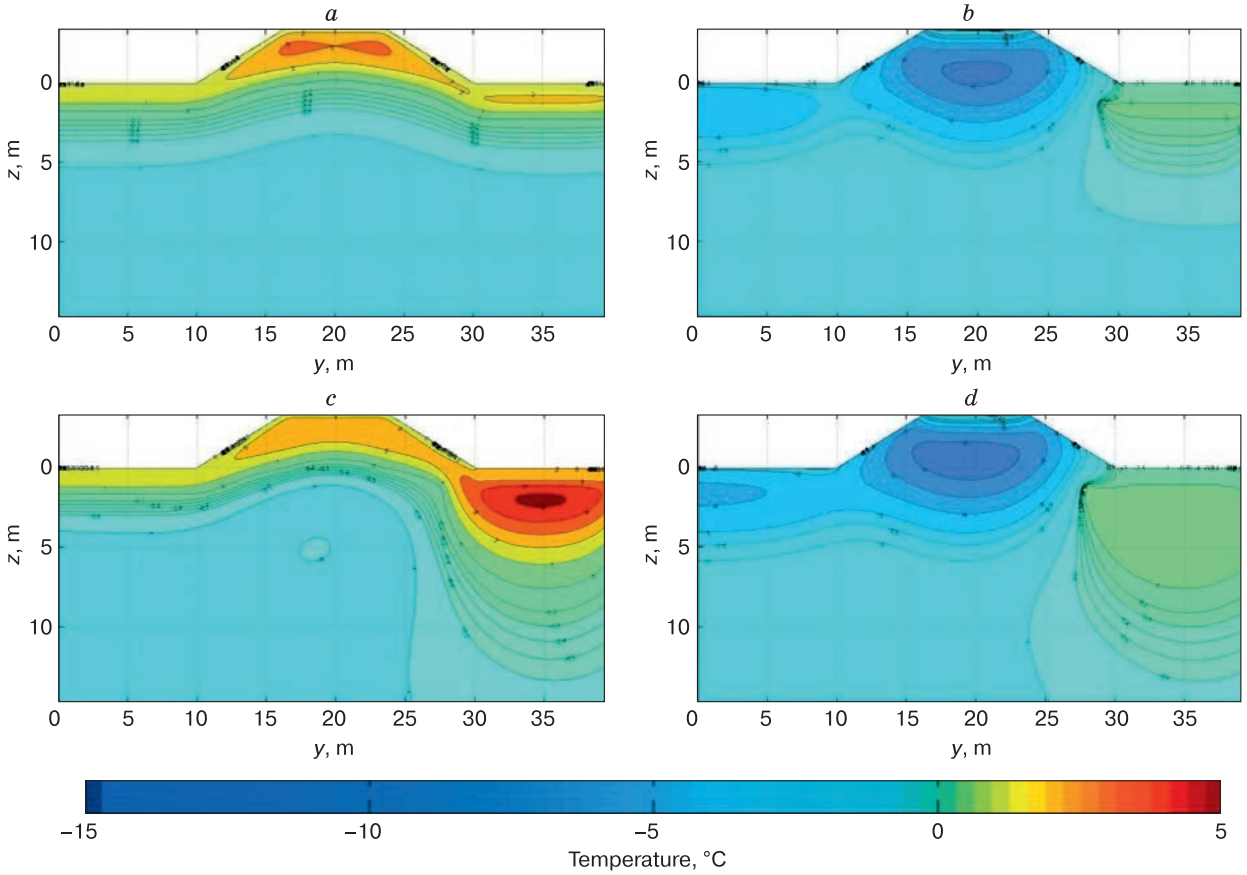

Fig. 7. Temperature field at the base of the embankment in the presence of a reservoir on the right side in the case of strong mixing.

a, *b* – the first year of operation: *a* – Oct. 1, 2000; *b* – June 1, 2001; *c*, *d* – the fifteenth year of operation: *c* – Oct. 1, 2015; *d* – June 1, 2016.

this reason (and also to maintain sufficient generality of the algorithm used), when considering the case of intense mixing in the summer, the effective thermal conductivity of the water layer is taken to be λ_{ef} = 300 W/(m·°C). Under the condition of absence of mixing λ_{ef} = 0.5 W/(m·°C) (conductive thermal conductivity of water). When a water body freezes in winter, the thermal conductivity of its frozen part is identical to the thermal conductivity of ice (2.2 W/(m·°C)), and mixing in the liquid phase of water is negligibly small, so the thermal conductivity of this part is assumed to be equal to the conductive thermal conductivity of water [*Gorelik, Zemerov, 2020*]. The melting of the ice cover with the beginning of the summer season occurs in a floating state [*Feldman, 1977; Pavlov, 2008; Gorelik, Zemerov, 2020*], and during this period the same assumptions regarding the values of the thermal conductivity coefficients of ice and water remain valid as during the freeze-up period.

The problem is solved numerically. The applied calculation procedure has been repeatedly tested on various problems and described earlier [*Gorelik, Khabitov, 2021; Gorelik et al., 2021*]. For verification calculations, we also used the Frost-3D computer program (academic version, License agreement of the Earth Cryosphere Institute, Tyumen Scientific Centre SB RAS with LLC "NTC Simmakers" no. D 8/20-01), as well as a version of the Q-Frost training program modified by the authors of this work.

Results of Temperature Dynamics Calculation

In the absence of a water reservoir, the embankment has a weak cooling effect on the base (Fig. 6). Figure 7 shows the calculation results in the presence of water body (shown in the right part of the figure) with its intensive mixing in the summer. The results are given at the end of the summer and winter periods in the first and fifteenth year of operation of the roadway. Compared to Fig. 6, the calculation results show a significant warming of the foundation soils on the 15th year of operation of the structure from the side of the slope of the embankment in contact with the reservoir. On the 30th year, these disturbances manifest themselves even more significantly.

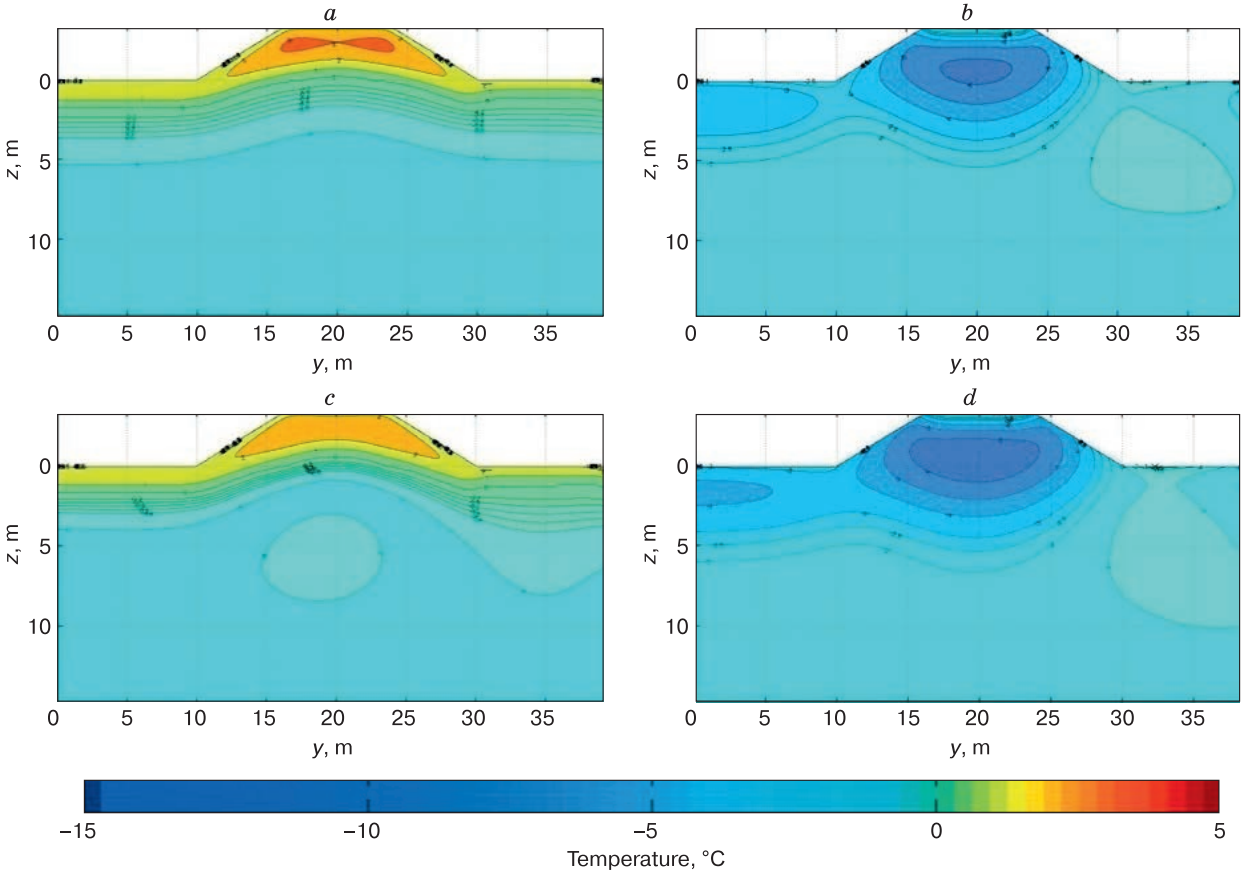

Fig. 8. Temperature field at the base of the embankment in the presence of a reservoir on the right side in the absence of mixing.

a, *b* – the first year of operation: *a* – Oct. 1, 2000; *b* – June 1, 2001; *c*, *d* – the thirtieth year of operation: *c* – Oct. 1, 2030; *d* – June 1, 2031.

In the absence of water mixing in summer, there are practically no disturbances in the 30th year of operation at the end of both the summer and winter seasons (Fig. 8).

CONCLUSIONS

The results of mathematical modeling of the formation of a temperature field in a frozen basement under a shallow water reservoir, as well as under an embankment of the roadway in the presence of inundation of one of its slopes, allow us to draw the following conclusions.

1. The general thermal interaction of the frozen base with the roadbed embankment and the water layer in contact with it is complex, and in order to ensure the correctness of the numerical modeling procedure for this process, it is advisable to first analyze the thermal effect of the reservoir on the base (as the least studied element of the overall system) with the selection of the most important factors that determine this interaction. It has been established that such factors in the problem under consideration are the depth of the reservoir and the nature of the mixing of the water layer in the summer season (Fig. 2).

2. An important preliminary assessment of the new stable thermal state of frozen soils and the relaxation time to it in the event of the appearance of a shallow reservoir on the surface of the massif is provided by an analysis of the temperature dynamics at the bottom of the seasonally thawed layer and at a depth of zero annual amplitudes of temperature, as well as their behavior during the expected period of operation of the structure. The proposed analysis method can be generalized to almost any type of changes in surface conditions of natural or artificial origin and can be useful in evaluating the efficiency of various technical measures aimed at improving the thermal state of soils during the construction and operation of structures.

3. Intensive mixing of water in a shallow reservoir occurs due to wind action and the influence of natural convection in the summer. With intensive mixing of the water layer in contact with the slope of the embankment, a significant warming of the base soils occurs. This warming occurs long before the completion of the life of the structure and can lead to partial (and uneven) thawing of the soil.

4. Prevention of the summer mixing of the water layer by any means leads stabilizes the initial temperature state at the base of the road, so that it can be maintained throughout the entire period of operation.

Acknowledgements. *This study was carried out within the framework of state assignment of the Earth Cryosphere Institute, theme no. 121041600047-2.*

References

Andrianov A.I., 2011. Railway on permafrost. In: *Proc. Int. Conf. on Engineering Geocryology*. Tyumen, NPO Fundamentstroiarkos, p. 77–79 (in Russian).

Ashpiz E.S., Khrustalev L.N., 2013. Prevention of permafrost thawing in roadbeds. *Dorogi* 25, 32–34.

Ashpiz E.S., Khrustalev L.N., Emelyanova L.V., Vedernikova M.A., 2008. Using of synthetic thermal insulators for conservation of frozen soil conditions in the base of railway embankment. *Kriosfera Zemli* XII (2), 84–89.

Carslaw H., Jaeger J., 1964. *Conduction of Heat in Solids*. Moscow, Nauka, 487 p. (translation from English).

Dostovalov B.N., Kudryavtsev V.A., 1967. *General Geocryology*. Moscow, Izd. Mosk. Gos. Univ., 403 p. (in Russian).

Dydyshko P.I., 2017. Deformations of railway subgrade upon permafrost and stabilization measures. *Earth's Cryosphere* XXI (4), 36–47.

Feldman G.M., 1977. *Forecasting of Temperature Regime for Grounds and Evolution of Cryogenic Processes*. Novosibirsk, Nauka, 102 p. (in Russian).

Feldman G.M., 1984. *Thermokarst and Permafrost*. Novosibirsk, Nauka, 262 p. (in Russian).

Gorelik J.B., Khabitov A.K., 2021. Affectivity of surface cooling of frozen ground in connection with mechanism of temperature shift formation. *Earth's Cryosphere* XXV (2), 22–34.

Gorelik J.B., Khabitov A.K., Zemerov I.V., 2021. Efficiency of surface cooling of frozen soil foundation using a forced refrigerant circulation unit. *Earth's Cryosphere* XXV (4), 30–39.

Gorelik J.B., Pazderin D.S., 2017. Correctness of formulation and solution of thermotechnical problems of forecasting temperature field dynamics in the ground base of structures on permafrost. *Earth's Cryosphere* XXI (3), 45–54.

Gorelik J.B., Zemerov I.V., 2020. Influence of the surface water reservoir to the thermal regime of frozen ground. *Byull. TGU (Tyumen State University Bulletin. Physical and Mathematical Modeling. Oil, Gas, Energy)* **6** (1), 10–40.

Gorelik J.B., Zemerov I.V., 2022. Prognosis method of temperature response of permafrost to climate warming. In: *Proc. 6th Conf. Russian Geocryologists*. Moscow, Izd. Mosk. Gos. Univ., p. 529–535 (in Russian).

Grebenets V.I., Isakov B.A., 2016. Deformation and stabilization of motor and rail roads within the Norilsk–Talnakh transportation corridor. *Earth's Cryosphere* XX (2), 62–68.

Kondratiev C.V., 2016. Deformations of the Amur Highway (Chita–Khabarovsk) in Areas with Ice-Rich Permafrost. Extended Abstract of Cand. Sci. Diss. Irkutsk, 22 p. (in Russian).

Kudryavtsev V.A. (ed.), 1978. *General Geocryology*. Moscow, Izd. Mosk. Gos. Univ., 464 p. (in Russian).

Litovko A.V., 2011. Geocryological conditions of the ice complex and their action on the Berkakit–Tommot–Yakutsk railway. In: *Proc. Int. Conf. Engineering Geocryology*. Tyumen, NPO "Fundamentstroiarkos", p. 386–390 (in Russian).

Method of protection of frozen roadbeds against negative influence of contact with water basin, 2021. Gorelik J.B., Zemerov I.V.: Patent RF No. 2753329/Aug. 13, 2021. (in Russian).

Mikheev M.A., Mikheeva I.M., 1973. *The Fundamentals of Heat Transfer*. Moscow, Energiya, 320 p. (in Russian).

Pavlov A.V., 1965. *Heat Exchange of Freezing and Thawing Soils with the Atmosphere*. Moscow, Nauka, 254 p. (in Russian).

Pavlov A.V., 2008. *Monitoring of Permafrost*. Novosibirsk, Acad. Publ. Geo, 230 p. (in Russian).

Porkhaev V.G., 1970. *Thermal Interaction of Buildings with Permafrost*. Moscow, Nauka, 208 p. (in Russian).

Shur Yu.L., 1988. *Upper Layer of Frozen Ground and Thermokarst*. Novosibirsk, Nauka, 213 p. (in Russian).

Smorygin G.I., 1988. *Theory and Methods of Production of Artificial Ice*. Novosibirsk, Nauka, 284 p. (in Russian).

Tikhonov A.N., Samarsky A.A., 1972. *Methods of Mathematical Physics*. Moscow, Nauka, 736 p. (in Russian).

Vorontsov V.V., Kraev A.N., Igoshin M.E., 2014. Stabilization of the car road critical deformations in permafrost. *Vestnik SibADI* **6** (40), 67–72.

Zhang A.A., Ashpiz E.S., Khrustalev L.N., Shesternev D.M., 2018. A new way for thermal stabilization of permafrost under rail way embankment. *Earth's Cryosphere* XXII (3), 59–62.

Received July 25, 2022
Revised December 2, 2022
Accepted February 16, 2023

Translated by A.V. Muravyev

EARTH'S CRYOSPHERE
SCIENTIFIC JOURNAL

Earth's Cryosphere, 2023, vol. XXVII, No. 2, pp. 39–46

SNOW COVER AND GLACIERS

SPATIAL AND TEMPORAL DIFFERENTIATION OF SNOW COVER PARAMETERS IN THE TAIGA ZONE OF THE NORTHEAST OF EUROPEAN RUSSIA

M.I. Vasilevich*, V.M. Shchanov

Institute of Biology, FRC Komi Science Center, Ural Branch of the Russian Academy of Sciences, Kommunisticheskaya St. 28, Syktyvkar, 167982 Russia

**Corresponding author; e-mail: mvasilevich@ib.komisc.ru*

Data on the snow cover in the middle and southern taiga subzones of the northeast of European Russia (Komi Republic) are analyzed. Field surveys were carried out in the second half of March in 2005–2007 and 2014–2015 on open flat spaces and in the intercrown spaces of forest stands. The studies were conducted at the same monitoring points, which allowed for a correct analysis of spatial and temporal differences. By route observations, measurements of the snow depth and snow density were carried out, and the values of snow water equivalent were calculated. The obtained data were compared with the results of measurements at the stations of the federal meteorological service. Schematic maps of the spatial distribution of snow cover parameters were constructed. The influence of the landscape on snow accumulation was shown: snow depth increased in intercrown spaces of forest stands; in open areas, snow compaction with a decrease in snow depth took place. The wide territorial distribution of measurement points made it possible to estimate the longitudinal effect on the snow cover parameters as related to the corresponding features of the relief. The maximum snow accumulation was observed along the Ural Mountains in the eastern part of the study area, where intense moisture condensation and precipitation take place. Snow depth and snow water equivalent in the foothills increased to the east. At the same time, the zone of increased snow density was noted in the western part of the Komi Republic. The obtained field data are consistent with long-term observations by other authors, as well as with the results of measurements at the network of weather stations.

Keywords: *snow cover, snow depth, snow density, snow water equivalent, taiga zone, northeast of European Russia.*

Recommended citation: Vasilevich M.I., Shchanov V.M., 2023. Spatial and temporal differentiation of snow cover parameters in the taiga zone of the northeast of European Russia. *Earth's Cryosphere* XXVII (2), 39–46.

INTRODUCTION

Snow cover in northern regions is an important landscape-forming factor controlling many environmental processes, as well as economic activity of humans. Among parameters of the snow cover, the most important ones are the thickness (depth), density, and snow water equivalent (SWE) influencing the thermal regime of soils [*Osokin et al., 2013a; Shmakin et al., 2013; Osokin, Sosnovskiy, 2016a,b; Komarov et al., 2019*]. Snow accumulation largely controls spring runoff, soil moisture, and the risk of dangerous hydrological processes [*Gray, Male, 1981*]. Hydrological regime of most Russian rivers depends on the snow forming and melting processes. Snowmelt contributes to 60–70% of the total annual runoff and up to 90% in some areas [*P'yankov, Shikhov, 2016*]. Changes in the snow accumulation in the permafrost zone resulting from the anthropogenic impact are of utmost importance [*Osokin et al., 2013b*]. Global warming observed over the past decades triggers the changes in all environmental systems. Climatic changes and its consequences are uneven in space in time. Modern climatic changes largely affect snow accumulation and the snow cover parameters [*Sosnovskiy et al., 2018a; Ashabokov et al., 2019*]. This concerns the main characteristics of the snow cover: the mean ten-day snow depth, the dates of the onset and end of the stable snow cover, etc. In recent decades, the area covered by snow in the Northern Hemisphere has decreased significantly compared to the middle of the 20th century [*Osokin, Sosnovskiy, 2014*].

In populated areas, the technogenic redistribution and compaction of snow lead to changes in the soil temperature regime and in the depth of seasonal freezing and thawing. Spatial variability in the snow thickness within a small area is high due to natural factors and technogenic impact, while the air temperature at this scale does not change significantly. One of the main snow cover characteristics is snow density, which affects both the thermal conductivity of snow and its thickness. It is known that the thermal insulation properties of snow, which determine the thermophysical state of soils, depend on the snow thickness and density [*Osokin et al., 1999; Gel'fan, Moreydo, 2014*]. For example, an increase in the snow

density from 200 to 300 g/dm^3 decreases the snow thickness by 1.5 times and increases the thermal conductivity coefficient by 1.9 times. As a result, thermal resistance is decreased by 2.8 times. In the case of a small thermal resistance of snow, a layer of frozen soil (pereletok) may form as part of the seasonally frozen layer, which remains frozen throughout one or several summers and then thaws [*Osokin et al., 2013b*]. Therefore, snow cover acts as a protecting layer for the surface in areas with the negative annual air temperatures [*Formozov, 1990; Sosnovskiy et al., 2018a*].

In Russia, snow depth is measured once a day at stations of the federal meteorological service using a stationary snow probe. Snow cover depth is measured during snow surveys along transects. The values of snow depth obtained by these methods can differ by more than 15% (up to 40%) [*Osokin, Sosnovskiy, 2014*].

Numerous measurements show that SWE by the beginning of snow melting is higher in forests than in forest-free areas. Snow accumulation in forest is controlled by many factors – species composition, stand density, canopy levels, age, canopy density, and weather conditions during snow accumulation period [*Faria et al., 2000; Osokin, Sosnovskiy, 2014; Komarov, 2021*]. On the basis of these data, the snow accumulation coefficient in forests (Cf) – the ratio between snow stocks in forest and forest-free areas – was determined for forests with different taxation characteristics. There is no strict zonal pattern of Cf. In 75% of cases, Cf values are within 1.3–2.0, which allows using the average value of 1.6 for estimating snow accumulation in forest [*Mishon, 2007*].

One of the important snow characteristics is SWE. Information about SWE is required, for example, for forecasting spring floods. Especially relevant is the spatial monitoring of SWE required for the assessment of regional climate-forming factors. Nowadays, two directions of studying soil cover are being actively developed: remote sensing data interpretation and numerical weather modelling with built-in cyclic data assimilation systems. In both cases, there is a decline in accuracy of SWE estimations compared to snow surveys along transects. Throughout validation with ground truth data is required while using the snow storage estimates from satellite monitoring [*Churyulin et al., 2018*].

Snow survey data are necessary for the verification of climate models and remote sensing data, whose spatial resolution for snow cover estimates is hundreds of meters in best cases. Combined field and satellite observations and GIS-based modeling are the main approaches to increase the accuracy of SWE estimates within large catchments [*Marshall, Koh, 2008; Harder et al., 2016; P'yankov, Shikhov, 2016; Komarov, 2021*].

In this paper, data of ecochemical monitoring of snow cover in the taiga areas of the northeast of European Russia (Komi Republic). Usually, these data include information in the snow cover depth and other characteristics.

The aim of this work is to assess the spatial dynamics of snow cover parameters on the basis of snow surveys in the taiga zone of the northeast of the European part of Russia (Komi Republic) and to compared these data with data obtained by the Hydrometeorological Service stations over the study period.

MATERIALS AND METHODS

Field studies were out in the taiga area of the Komi Republic (KR) in the winter periods of 2005–2007 and 2014–2015. Snow cover sampling was performed at the same points, which allows comparison across years (Fig. 1).

Sampling and measurement points for snow parameters were located on flat open spaces or within large intercrown spaces (glades) in the forests, because the main aim of the monitoring was to reduce the impact of vegetation on the chemical composition of the snow. Studies were mainly concentrated in southern and middle taiga subzones. It should be noted that monitoring points covered all areas of snow accumulation [*Atlas..., 1997*], which made it possible to perform an objective analysis of the data.

The period with stable snow cover period in taiga lasts 175–200 days a year. The average date for the establishment of stable snow cover is November 1; snow melting begins in the tenths–twenties of March. Precipitation of the winter period varies in the range of 170–350 mm depending on the location. The cold season lasts approximately five months.

For the analysis, we used data from the All-Russia Research Institute of Hydrometeorological Information – World Data Center (http://www.meteo.ru). The results of both stationary snow depth measurements and areal snow surveys along transects were taken into account.

Snow cover characteristics in the tenths–twenties of March over the study periods in 2005–2007 and 2014–2015 are shown in Table 1. These are data from the Ust'-Vym' weather station in the center of the taiga zone of the KR, in fairly open area; this a key station in the region. In our study, we compared data obtained at weather stations with data of snow surveys performed within 5-km buffer zones from the stations; long-term meteorological records obtained in the KR were also taken into account [*Atlas..., 1997*].

Field studies were performed in the middle and late March, in the period of maximum snow accumulation and the very beginning of snow melting. Snow was sampled for quantitative chemical analyses according to GD 52.04.186-89 [*Veres, 1991*].

We measured snow depth using cylindrical snow samplers with a centimeter scale printed on the outer side. For each sampling point, the final value was obtained by averaging 5–10 measurements within the

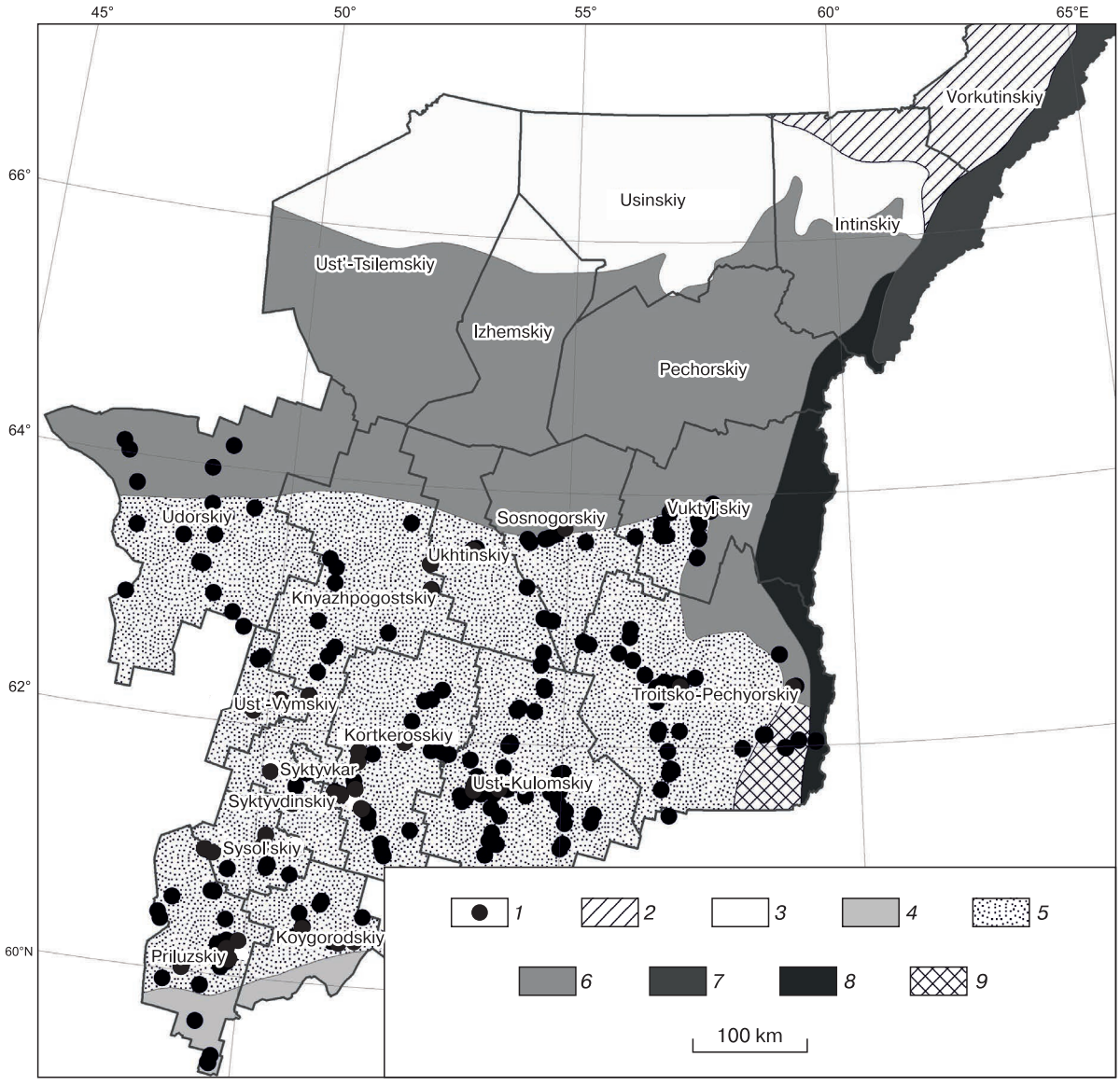

Fig. 1. Map of sampling points (*1*) of snow cover parameters.

Geo-botanical zoning: *2* – shrub-tundra subzone, *3* – forest-tundra, *4* – southern taiga subzone, *5* – middle taiga subzone, *6* – northern taiga subzone, *7* – woodlands and mountainpus tundra of the Urals, *8* – mountainous northern taiga, *9* – mountainous middle taiga.

plot of 10 × 10 m in area. Normally, snow cores were taken from the entire thickness of the snow cover, except for the lowermost 1–2 cm with inclusions of soils and vegetation. The location of sampling points could be corrected, it the initially chosen point was covered by shrubs (this could lower the accuracy of measurements). Each snow core sample was weighted. The obtained data were used to calculate snow density (ρ) and SWE (*W*) using equations:

$$\rho = m/V = m/(Sh_{av}),$$

$$W = \rho h_{av} \cdot 10,$$

where ρ is snow density, g/cm^3; *m* is snow sample weight, g; *S* is snow core area (23.7 cm^2); h_{av} is the average snow depth within each sampling point (n = 5–20), cm; 10 is the scale factor.

Mean arithmetic values and standard deviations were calculated. Statistical processing of data was performed using Statistica 6 software. Maps of soil cover characteristics were created using ArcGIS 9.3.1 software as grid raster data. Spatial interpolation of data was based on the Inverse Distance Weighting method included in the Spatial Analyst toolbox of ArcGIS.

Table 1. **Parameters of snow cover recorded at Ust'-Vym' station**

Period	Snow depth, cm	Snow density, g/cm^3	Snow water equivalent, mm
2004–2005	72	0.26	187
2005–2006	58	0.22	189
2006–2007	52	0.23	209
2013–2014	49	0.30	218
2014–2015	51	0.29	151

RESULTS

Sampling points were confined to road network, which more or less evenly covers taiga areas of the KR. All taiga subzones were surveyed. Statistical data on snow cover parameters for administrative districts are presented in Table 2. The analysis of these data indicates snow accumulation by the end of the snow season has an uneven pattern: snow depth and SWE tend to increase from the southwest (Koigorodskiy, Priluzskiy, Sysol'skiy districts) to the northeast (Vuktyl'skiy and Troitsko-Pecherskiy districts) of the KR. The highest variability of snow cover parameters is observed in the Troitsko-Pecherskiy district in the southeast of the KR, which is associated with topographic heterogeneity and altitudinal zonation [*Atlas..., 1997*]. The highest snow density values are observed in the western districts (Udorskiy and Ust'-Vymskiy). In general, the distribution of the main physical characteristics of the snow cover obtained in our study corresponds to long-term records at weather stations of the KR [*Atlas..., 1997*].

In Russia, a trend for an increase in maximum snow reserves was established for a period from 1976 to 2015 according to snow surveys along transects in forest-free areas [*Popova et al., 2018*]. According to these surveys, average SWE in Russia increased by 2.12 mm over 10 years [*Report..., 2016*]. Our study suggests that the average values of snow parameters differ depending on the year of study. The minimum depth of snow cover was observed in March 2007. However, this was accompanied by the high snow density values. In general, our data attest to certain differences in snow accumulations between 2005–2007 and 2014–2015. After averaging snow parameters for the same monitoring points with equal ratio of open areas and forest glades, snow accumulation in 2013–2015 exceeds that in 2004–2007 (Table 3).

The average depth of snow cover in 2005–2007 was 68.4 ± 11.8 cm; in 2014–2015, it increased to 78.6 ± 9.4 cm. The same tendency was observed for SWE. Most likely, this reflects a general tendency for an increase in the amount of winter precipitation in European Russia [*Popova et al., 2018*]. Herewith, snow density values remain at the same level varying between 0.14 and 0.46 g/cm^3 with the average value of 0.25 ± 0.04 g/cm^3.

Table 2. **Averaged parameters of snow cover during 2005–2007 and 2014–2015**

Districts	Snow depth, cm	Snow density, g/cm^3	Snow water equivalent, mm
Koygorodskiy	63 ± 11 48 – 82	0.23 ± 0.06 0.18 – 0.37	141 ± 34 94 – 208
Priluzskiy	70 ± 11 55 – 94	0.25 ± 0.07 0.17 – 0.46	173 ± 45 106 – 311
Sysol'skiy	66 ± 15 55 – 107	0.27 ± 0.07 0.18 – 0.38	176 ± 67 98 – 330
Syktyvkar	61 ± 13 50 – 79	0.27 ± 0.09 0.21 – 0.39	158 ± 34 113 – 196
Syktyvdinskiy	62 ± 10 51 – 80	0.24 ± 0.03 0.18 – 0.27	145 ± 18 104 – 166
Ust'-Kulomskiy	74 ± 12 35 – 105	0.23 ± 0.03 0.18 – 0.40	172 ± 35 72 – 274
Kortkerosskiy	68 ± 10 46 – 88	0.25 ± 0.05 0.19 – 0.41	167 ± 29 97 – 227
Ust'-Vymskiy	62 ± 8 51 – 76	0.29 ± 0.07 0.20 – 0.36	176 ± 33 120 – 227
Troitsko-Pechyorskiy	98 ± 20 34 – 135	0.24 ± 0.04 0.14 – 0.39	237 ± 55 102 – 352
Sosnogorskiy	77 ± 15 44 – 100	0.22 ± 0.03 0.17 – 0.28	166 ± 31 121 – 243
Ukhta	72 ± 14 44 – 95	0.23 ± 0.04 0.16 – 0.29	161 ± 35 111 – 208
Knyazhpogostskiy	63 ± 15 27 – 93	0.27 ± 0.07 0.18 – 0.39	164 ± 40 71 – 219
Vuktyl'skiy	92 ± 12 71 – 115	0.25 ± 0.03 0.16 – 0.29	229 ± 46 132 – 296
Udorskiy	59 ± 8 45 – 71	0.31 ± 0.06 0.20 – 0.46	177 ± 32 101 – 227

Note: Numerator – average value and standard deviation for the district; denominator – sample range.

Table 3. **Average parameters of snow cover and standard deviation**

Period	Snow depth, cm	Snow density, g/cm^3	Snow water equivalent, mm
2004–2005	80.0 ± 7.9	0.20 ± 0.02	157 ± 20
2005–2006	65.5 ± 10.2	0.29 ± 0.02	179 ± 28
2006–2007	64.5 ± 11.0	0.24 ± 0.03	158 ± 35
Average	*68.4 ± 11.8*	*0.25 ± 0.02*	*166 ± 31*
2013–2014	75.7 ± 8.6	0.24 ± 0.01	181 ± 24
2014–2015	81.6 ± 9.9	0.25 ± 0.01	207 ± 26
Average	*78.6 ± 9.4*	*0.25 ± 0.01*	*194 ± 26*

DISCUSSION

The obtained data were compared with the results of long-term monitoring of snow cover. Statistical analysis of snow parameters showed that our monitoring data are highly correlated with snow cover parameters from the Atlas of Climate and Hydrology [*Atlas..., 1997*], which includes long-term observation data for 1960–1991 at 52 weather stations of the KR (Table 4).

In the atlas, all data are presented in the form of electronic maps, which allowed a comparison with the results of snow surveys along transects. Thus, the highest value of the correlation coefficient was noted for snow cover depths obtained by us and presented in the atlas (Fig. 2). Figure 2*A* shows a tendency for increasing snow cover depth from west to east of the KR, where precipitation is intensified under the influence of the Ural Mountains; this tendency is also clearly seen in the long-term pattern of snow distribution in the KR (Fig. 2*B*).

Our study confirms the longitudinal effect on the snow accumulation, which is determined by the longitudinal differences in topography and altitudinal zonation. Long-term studies indicate that average snow cover depths increase from west to east and decrease in the north (in the tundra zone) and in the southwest (in the southern taiga) [*Atlas..., 1997*]. Exponential dependence of the snow cover depth on longitude is shown in Fig. 3. The effect of more intense precipitation in the Cis-Urals while moving towards the mountain ranges as compared with central and western districts of the KR is manifested not only in winter but also throughout the year as a whole.

Table 4. **Correlation matrix for snow cover parameters ($r_{5\%}$ = 0.11, n = 387)**

Parameter	1	2	3	4	5	6	7
1	1.000	–0.271	0.759	0.528	0.697	0.736	0.681
2		1.000	0.401	–0.136	–0.012	–0.026	–0.078
3			1.000	0.410	0.653	0.677	0.587
4				1.000	0.546	0.529	**0.645**
5					1.000	0.958	0.848
6						1.000	**0.853**
7							1.000

Note: 1 – snow depth, cm (a real snow survey); 2 – snow density, g/cm^3 (a real snow survey); 3 – snow water equivalent, mm (a real snow survey); 4 – elevation of the monitoring point, m (topographic map); 5 – snow water equivalent, mm [*Atlas..., 1997*]; 6 – snow depth, cm [*Atlas..., 1997*]; 7 – total winter precipitation, mm [*Atlas..., 1997*].

While moving up into the mountains, snow cover depth increases up to the upper tree line because of more abundant precipitation in the mountains [*Kitaev et al., 2007*]. Snow cover depth is correlated with elevation (r = 0.65). According to literature data, SWE and snow depth are higher in forests than in forest-free areas. This relationship depends on the species composition of forest stands. Thus, birch forests retain approximately 5% more winter precipitation, and snow retention under spruce forests is 25–50% higher than that in open spaces [*Hydrological role..., 1989*].

As our studies were carried out not only in areas unoccupied by forest vegetation, we tried to estimate

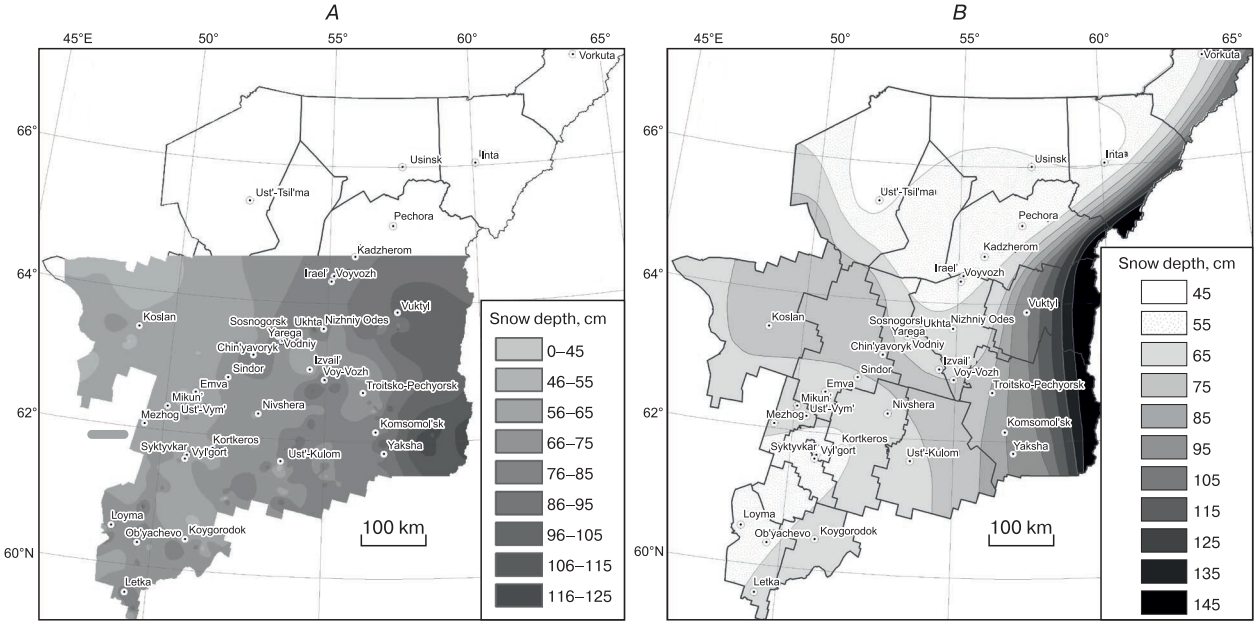

Fig. 2. Maps of snow depth distribution in the Komi Republic obtained from (*A*) field measurements and (*B*) long-term records at weather stations.

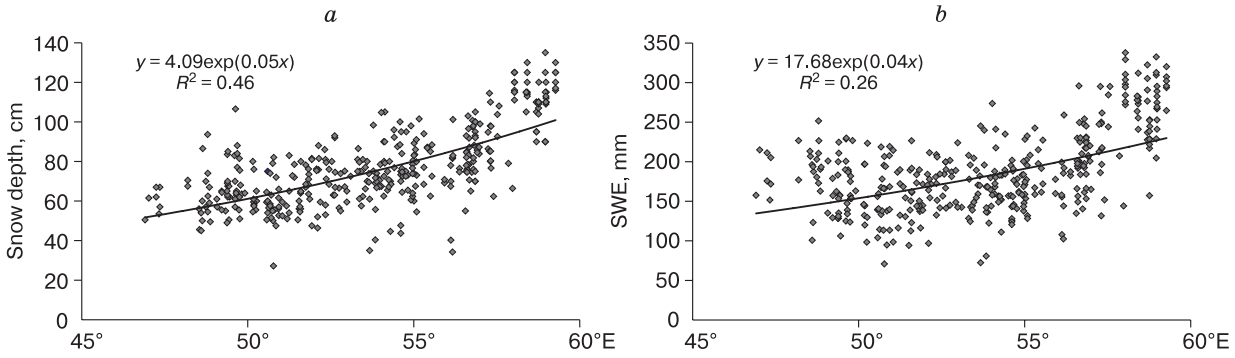

Fig. 3. Exponential dependences between (*a*) snow depth and (*b*) snow water equivalent and longitude in taiga of the Komi Republic for the periods of 2005–2007 and 2014–2015.

the differences in snow accumulation between the forest-free areas and in the inter-crown spaces of the forest. The proportion of measurement and sampling points in open areas and in large intercrown spaces (glades) within forests was 60% and 40%, respectively. The analysis demonstrated that the influence of forest on the snow depth is stronger (84%) than the factor of snow compaction and blowing in open spaces (64%). In general, the influence of forest vegetation on of snow parameters was reliably observed in 72% of cases.

Snow density is also higher in forest, which was documented before [*Hydrological role..., 1989; Formozov, 1990*]. However, our studies indicate that snow density in open areas and within forest glades is 0.25 and 0.24 g/cm^3, respectively, i.e., it is 4% higher in open areas. Further, average SWE in forests is 4–5% higher than in open areas. Given these values, the coefficient of snow accumulation in forests (Cf = 1.05) reflects a certain influence of forest stands on snow accumulation within glades due to the absence of the blowing effect and snow compaction in comparison with open areas. Low Cf values for the northeast of the European part of Russia was also mentioned in other studies [*Sosnovskiy et al., 2018b*].

Snow density map in the taiga zone of the KR shows a tendency for an increase in this parameter along the western border of the region (Fig. 4). This is confirmed by a negative correlation between snow density and longitude ($r = -0.22$, $r_{5\%} = 0.11$, $n = 387$) shown on Fig. 5. Ranking of snow density values by longitudes with a step of 3° demonstrates a decrease in average slow density from 0.28 g/cm^3 (<50°E) to 0.23–0.24 g/cm^3 (>56°E).

The analysis of the literature confirms the obtained trends in the distribution of snow density values. Thus, a zone of increasing snow density and, hence, decreasing thermal resistance of snow during soil freezing of snow extends towards the European northwest [*Osokin, Sosnovskiy, 2014, 2016b*]. The formation of this zone can be explained by temperature conditions in the spring: in the southwestern part of

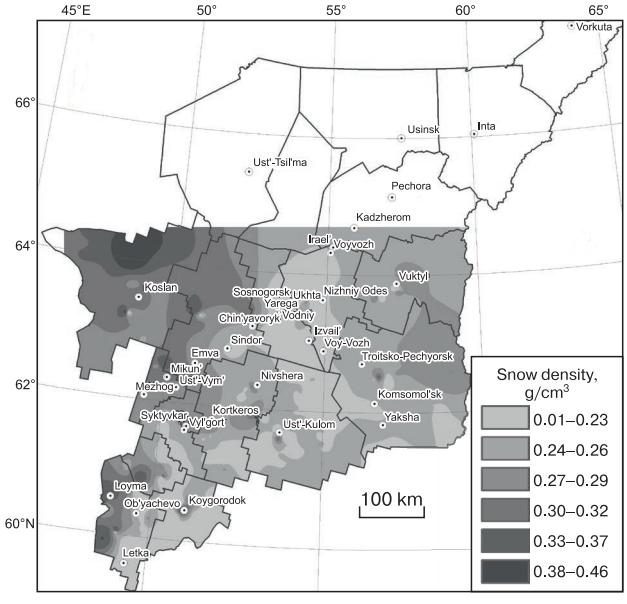

Fig. 4. Snow density distribution map.

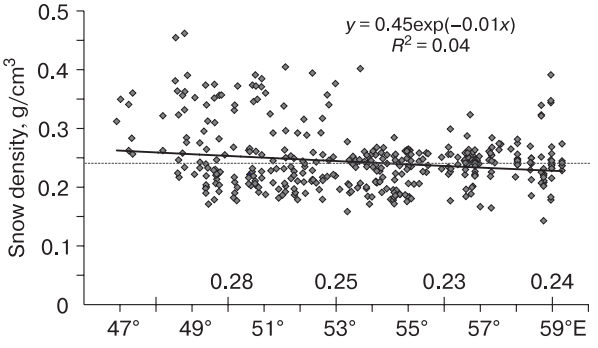

Fig. 5. Scatterplot of snow density and longitude.

X-axis represents ranked average values.

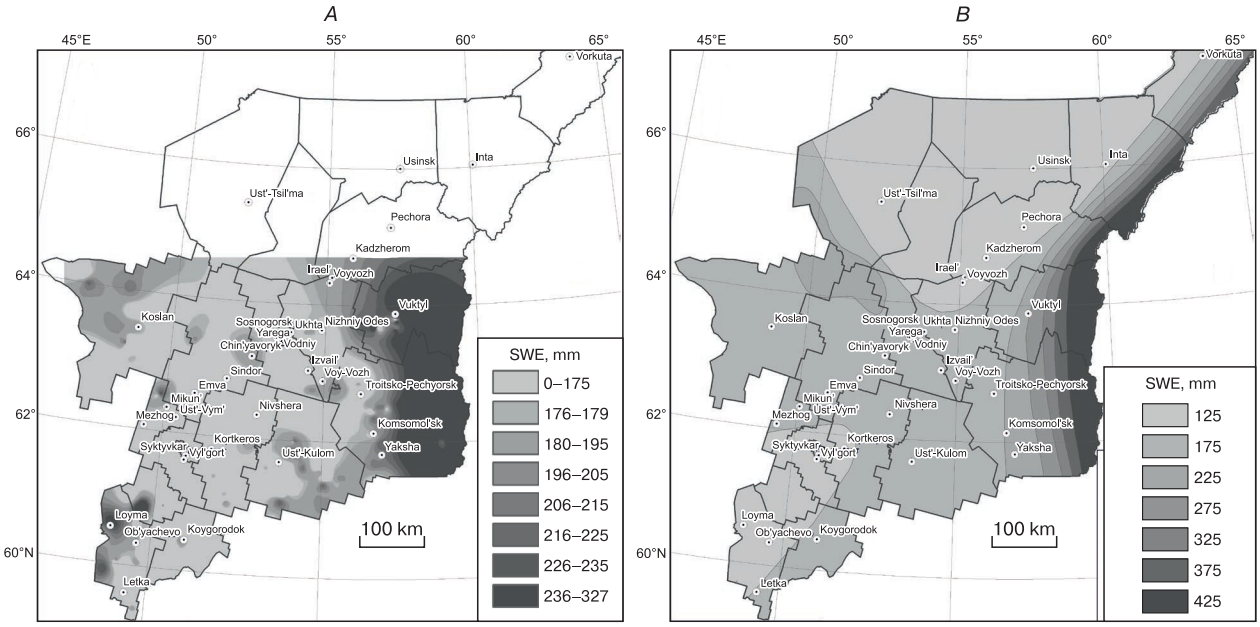

Fig. 6. Snow water equivalent according to (*A*) field survey data and (*B*) long-term records at weather stations.

the taiga zone, snow tracking and melting processes leading to snow compaction begin earlier than in the northern and eastern parts.

With an increase in the average snow cover depth, SWE also increases. However, the rates of these processes are different. Our maps show a clear tendency for the rise in SWE along the Ural Mountains in the east of the region (Fig. 6). Maximal values reach 350 mm, while the average is 190 mm. An increase in snow depth within the mountainous forest zone occurs exceptionally due to higher precipitation in the mountains [*Kitaev et al., 2007*].

To assess the correctness of the obtained data, we have compared our results of snow depth measurements with data recorded of obtained at weather stations (within 5-km buffer zones) located in Syktyvkar, Ust'-Vym', Troitsko-Pechyorsk, and Irael'. A comparison of 21 measurements indicates that the deviation of our data from data obtained at weather stations averages 10%. The maximum difference between snow depth values measured at weather stations and during our survey reaches 28% and is mainly conditioned by the influence of open areas on snow compaction and lowering of its thickness.

CONCLUSION

An assessment of spatial and temporal differences in snow cover parameters was performed for the territory of the middle and southern taiga subzones in the northeast of the European part of Russia (Komi Republic). Snow depth and density measurements along field survey routes made it possible to calculate snow water equivalent and to compare our data with the results of long-term monitoring of snow parameters at weather stations of Roshydromet. Maps of the spatial distribution of snow cover parameters were constructed.

Field data obtained in 2014–2015 suggest an increase in snow accumulation compared to the previous surveys in 2005–2007. Our data confirm the influence of landscape conditions on snow accumulation: snow depth and snow density are higher within intercrown spaces and small glades in the forest than in open areas. The influence of relief conditions on snow accumulation is clearly shown, especially along the Ural Mountains along the eastern border of the region, where intensive precipitation occurs. This leads to an increase in the average snow depth and snow water equivalent. At the same time, a zone of increasing snow density is noted along the western border of the region.

The obtained results are consistent with both long-term observations at weather stations and with earlier revealed tendencies. The difference between the data obtained at weather stations and during field route surveys is quite allowable. Thus, the results of this study show the correctness of the applied measurement and sampling methods for the purposes aimed, first of all, at assessing the supply of substances from the atmosphere to a given territory in winter, which is extremely important for substantiating geochemical patterns.

References

Ashabokov B.A., Tashilova A.A., Kesheva L.A., 2019. Changes in snow cover characteristics in the south of the European territory of Russia as a response to global warming. *Tr. Glavn. Geofizich. Observatorii im. A.I. Voeikova* 592, 141–158.

Atlas of Climate and Hydrology of the Komi Republic, 1997. Moscow, Drofa, DiK, 16 p. (in Russian).

Churyulin E.V., Kopejkin V.V., Rozinkina I.A. et al., 2018. Analysis of snow cover characteristics based on satellite and model data for various catchments in the European territory of the Russian Federation. *Gidrometeorol. Issled. Prognozy* **368** (2), 120–143.

Faria D.A., Pomeroy J.W., Essery R.L.H., 2000. Effect of covariance between ablation and snow water equivalent on depletion of snow-covered area in a forest. *Hydrol. Process.* **14** (15), 2683–2695.

Formozov A.N., 1990. *Snow Cover in the Life of Mammals and Birds*. Moscow, Izd. Mosk. Gos. Univ., 286 p. (in Russian).

Gel'fan A.N., Moreydo V.M., 2014. Dynamic-stochastic modeling of snow cover formation on the European territory of Russia. *Led i Sneg* 126 (2), 44–52.

Gray D.M., Male D.H. (eds.), 1981. *Handbook of Snow*. Pergamon Press, Canada. Translated under the title Snow: A Reference Guide. Leningrad, Gidrometeoizdat, 1986, 751 p. (in Russian).

Harder P., Schirmer M., Pomeroy J., Helgason W., 2016. Accuracy of snow depth estimation in mountain and prairie environments by an unmanned aerial vehicle. *The Cryosphere* **10** (6), 2559–2571. doi: 10.5194/tc-10-2559-2016.

Hydrological Role of Forest Geosystems, 1989. Novosibirsk, Nauka, 167 p. (in Russian).

Kitaev L.M., Volodicheva N.A., Oleynikov A.D., 2007. Long-term dynamics of snowfall in the north-west of the Russian Plain. *Materialy Glyatsiolog. Issled.* 102, 65–72.

Komarov A.Yu., 2021. Influence of vegetation and microrelief on the stratigraphy of snow cover in the Moscow region. *Byull. Mosk. Gos. Univ., Ser. 5: Geogr.* 6, 77–88.

Komarov A.Yu., Seliverstov Y.G., Grebennikov P.B., Sokratov S.A., 2019. Spatial variability of snow water equivalent – the case study from the research site in Khibiny Mountains. *J. Hydrol. Hydromech.* **67** (1), 110–112.

Marshall H.P., Koh G., 2008. FMCW radars for snow research. *Cold Reg. Sci. Technol.* **52** (2), 118–131.

Mishon V.M., 2007. Theoretical and Methodological Foundations for the Assessment of Surface Water Resources in Areas of Insufficient and Unstable Moistening in the European Part of Russia. Doctor. Sci. (Geogr.) Diss. Voronezh, 65 p. (in Russian).

Osokin N.I., Samoilov R.S., Sosnovskiy A.V. et al., 1999. On estimation the influence of snow cover characteristics variability on soils freezing. *Kriosfera Zemli* III (1), 3–10.

Osokin N.I., Sosnovskiy A.V., 2014. Spatial and temporal variability in the depth and density of snow cover in the territory of Russia. *Led i Sneg* **54** (4), 72–80.

Osokin N.I., Sosnovskiy A.V., 2016a. Thermal resistance of snow as a control of permafrost stability. *Earth's Cryosphere* XX (3), 96–101.

Osokin N.I., Sosnovskiy A.V., 2016b. Spatial distribution of thermal resistance of snow cover on the territory of Russia and its influence on freezing and thawing of soils. *Led i Sneg* **56** (1), 52–60.

Osokin N.I., Sosnovskiy A.V., Chernov R.A., 2013a. Influence of snow cover stratigraphy on its thermal resistance. *Led i Sneg* **53** (3), 63–70.

Osokin N.I., Sosnovskiy A.V., Nakalov P.R., Nenashev S.V., 2013b. Thermal resistance of snow cover and its effect on soil freezing. *Led i Sneg* 1 (121), 93–103.

P'yankov S.V., Shikhov A.N., 2016. Modeling of the spatial distribution of snow reserves in a large catchment area using satellite information. *Sovrem. Probl. Distants. Zondirov. Zemli iz Kosmosa* **13** (4), 29–41.

Popova V.V., Shiryaeva A.V., Morozova P.A., 2018. Changes in the snow depth characteristics in the territory of Russia in 1950–2013: the regional features and connection with the global warming. *Earth's Cryosphere* XXII (4), 58–67.

Report on Peculiarities of the Climate in the Territory of the Russian Federation for 2015, 2016. Moscow, Rosgidromet, 68 p. (in Russian).

Shmakin A.B., Osokin N.I., Sosnovskiy A.V. et al., 2013. The effect of snow cover on freezing and thawing of the soil in Western Svalbard. *Led i Sneg* **53** (4), 52–59.

Sosnovskiy A.V., Osokin N.I., Chernyakov G.A., 2018a. Dynamics of snow reserves on the plain territory of Russia in the forest and in the field under climatic changes. *Led i Sneg* **58** (2), 183–190.

Sosnovskiy A.V., Osokin N.I., Chernyakov G.A., 2018b. Impact of climate change on snow depth in forest and field areas in the first decade of the 21st century. *Earth's Cryosphere* XXII (2), 80–87.

Veres I.L. (ed.), 1991. *Guidelines for Air Pollution Control*. Leningrad, Gidrometeoizdat, 683 p. (in Russian).

Received April 21, 2022
Revised October 22, 2022
Accepted March 4, 2023

Translated by Yu.A. Dvornikov

EARTH'S CRYOSPHERE
SCIENTIFIC JOURNAL

Earth's Cryosphere, 2023, vol. XXVII, No. 2, pp. 47–55

METHODS OF CRYOSPHERIC RESEARCH

COMPARATIVE ANALYSIS OF AREA DISTRIBUTIONS FOR THERMOKARST LAKES WITHIN DIFFERENT TYPES OF THE SURFACE OF THERMOKARST PLAINS WITH FLUVIAL EROSION

A.S. Victorov*, V.N. Karpalova, T.V. Orlov

Sergeev Institute of Environmental Geoscience, Russian Academy of Sciences, Ulansky per. 13, str. 2, Moscow, Russia 101000

**Corresponding author; e-mail: dist@geoenv.ru*

Thermokarst plains with fluvial erosion include two genetically different types of surface: slightly undulating watersheds with primary termokarst lakes and lowered surfaces of khasyreys (drained thermokarst lakes) with secondary lakes. The research deals with a comparative analysis of statistical distributions of the areas of thermokarst lakes and secondary lakes. Using statistical criteria and remote sensing data for eight key sites in different natural conditions, such as Yamal and Tazovsky peninsulas, the Kolyma Lowland, and the Penzhina River valley, we determined statistically significant differences in the area distributions of thermokarst lakes within different genetic types of the surface. Statistical analysis shows that the areas of thermokarst lakes correspond to an integral-exponential distribution. This allows us to conclude that a dynamic equilibrium is established within each type of the surface in the course of the initiation, growth, and drainage of thermokarst lakes. Though the parameters of thermokarst lakes differ significantly, we find a correlation between the distribution parameters of lake areas within the main surface of thermokarst plains with fluvial erosion and the surface of khasyreys with secondary lakes.

Keywords*: thermokarst plains with fluvial erosion, mathematical morphology of landscape, khasyrey, alas, thermokarst lakes.*

Recommended citation: Victorov A.S., Karpalova V.N., Orlov T.V., 2023. Comparative analysis of area distributions for thermokarst lakes within different types of the surface of thermokarst plains with fluvial erosion. *Earth's Cryosphere* XXVII (2), 47–55.

INTRODUCTION

A significant number of studies are devoted to the development of thermokarst lakes on plains in the permafrost zone. Within the Permafrost Region Pond and Lake Database (PeRL) project, information is collected about the boundaries of thermokarst lakes obtained from high-resolution satellite images. Studies of thermokarst lakes based on the analysis of satellite images from different times are also being developed [*Olefeldt et al., 2016*].

Vast and numerous research dedicated to the morphological study and inventory of lakes in general is currently being conducted. Thus, in [*Verpoorter et al., 2014*] approximately 1.7 million lakes larger than 0.002 km^2 were analyzed throughout the world, and the dependence of their quantity, surface area, and perimeter on latitude and elevation a.s.l. was described. In other works [*Cael, Seekell, 2016*] size distribution and boundary fractality (based on the relationship of perimeter to surface area) were studied for a large number of lakes throughout the world and compared to the distribution of lakes in Sweden. About 70 sites in Western Siberia were analyzed with respect to lake size distribution [*Polishchuk et al., 2018*]. Other authors performed analogous studies also. In particular, an analysis of shoreline sinuosity and lake area was made; it was concluded that the sinuosity of a shoreline decreases as lake area increases [*Muratov et al., 2021*]. It should be noted that many authors [*Verpoorter et al., 2014; Cael, Seekell, 2016; Polishchuk et al., 2018*] use either cartographic inventory methods or automated analysis of satellite images and do not separate lakes based on genesis and type. Consequently, lakes of different types are mixed in such works, which is important for a complete inventory of the number and areas of lakes, but limits possibility for the analysis of processes typical for the studied objects in light of their polygenetic nature.

Similar study is being conducted by Chinese researchers for the Tibetan Plateau [*Wei et al., 2021*]. They analyze thermokarst lakes in mountain conditions. It should be emphasized that the authors do not make conclusions about the law of lake surface area distribution, possibly because of a large number of analyzed lakes existing under different conditions.

Local and regional research of the state and dynamics of thermokarst lakes is also being conducted. A study of lakes in the Kolyma Lowland demonstrated their increase by 4.5% during 1999–2018 [*Vereme-*

eva et al., 2021]. For Yukon plains, a decrease in the area of lakes from the 1970s to the 1990s was identified along with an increase in their number [*Lantz, Turner, 2015*]. The number of thermokarst lakes in the studied territory increased by 10% over the span of 60 years, while the overall lake area and the number of large lakes decreased [*Jones et al., 2011*]. A decrease in the number of lakes in the Siberian part of the Arctic was reported in [*Smith et al., 2005*]. In the area of Eight Mile Lake (Canada), new primary thermokarst landforms appeared in about 12% of local landscapes [*Belshe et al., 2013*]. At the same time, upon analysis of remote sensing data for Yukon plains, the presence of multidirectional tendencies in changing lake sizes was identified: a 14% increase by 1994 and a 10% decrease during 1999–2002 compared to 1984 [*Chen et al., 2014*].

Changes in the morphological pattern of permafrost landscapes have been considered in relatively few works [*Kravtsova, Bystrova, 2009; Morgenstern et al., 2011; Polishchuk V., Polishchuk Yu., 2013; Grosse et al., 2016; Polishchuk et al., 2018*]. Furthermore, thermokarst plains and thermokarst plains with fluvial erosion have not been properly separated. Under thermokarst plains with fluvial erosion the present article implies vast surfaces with thermokarst depressions and a well-developed erosional network, which separates them from thermokarst plains with lakes, where the erosional network is significantly less developed. Fully or partly, drained thermokarst basins are known as khasyreys in Western Siberian and as alases in Yakutia.

Finally, a series of studies have attempted to create a mathematical model for the morphological pattern of thermokarst plains with fluvial erosion [*Victorov, 2005, 2006; Victorov et al., 2016*]. However, the proposed model has certain disadvantages, to which attention was brought during discussions at conferences, including by V.E. Tumskoy. These disadvantages were associated, first of all, with the assumption that the progression is the same for the processes of initiation, growth, and drainage of thermokarst lakes forming on the main watershed surface and lakes forming on the surface of thermokarst depressions.

Thus, studies of thermokarst lakes aimed at identifying patterns in their development, including qualitative ones, usually insufficiently considered the peculiarities of lake development; lakes of thermokarst plains with and without a pronounced erosional network were often considered together, without making distinction between them. Meanwhile, the development of such lakes apparently occurs under different conditions and follows different patterns. Without knowledge about these patterns, it is difficult to continue studies of the development of thermokarst in permafrost landscapes and to conduct a retrospective analysis.

The goal of the present article is to present the results of a comparative analysis of statistical distributions of thermokarst lake areas within different genetic types of surfaces of thermokarst plains with and without fluvial erosion. An attempt is made to find general patterns typical for the corresponding type of surfaces at sites located in different physical-geographical, geological, and geocryological conditions.

METHOD FOR COMPARATIVE ANALYSIS OF AREA DISTRIBUTIONS OF THERMOKARST LAKES

Thermokarst plains with fluvial erosion represent undulating or slightly hilly surfaces with tundra or forest-tundra vegetation, with inclusions of thermokarst lakes and thermokarst depressions and the development of stream channels. Lakes and ther-

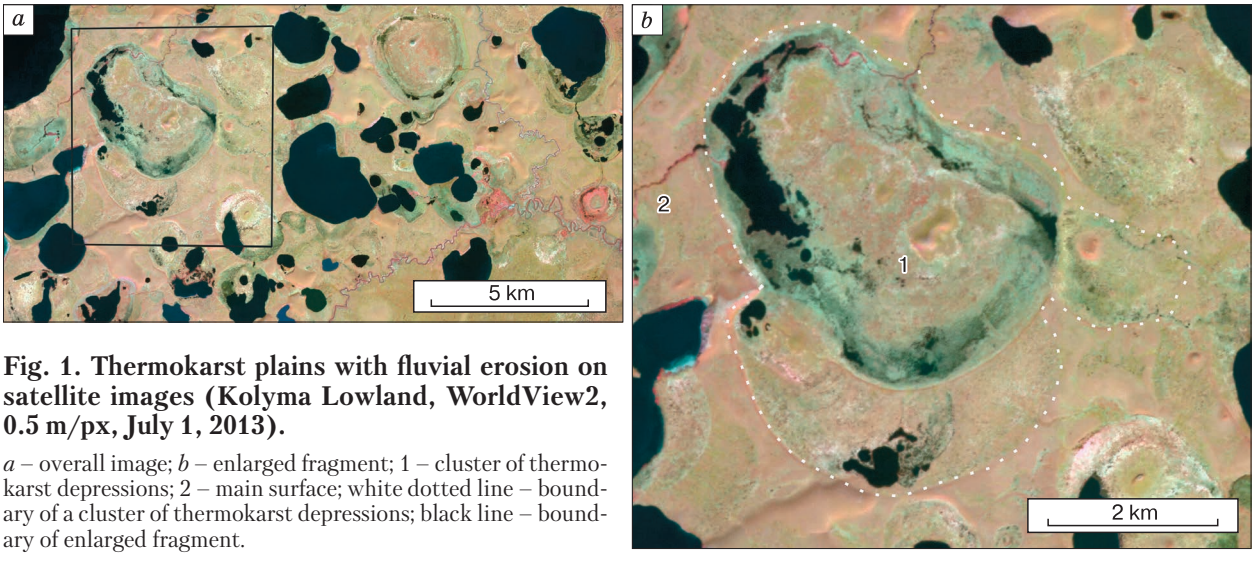

Fig. 1. Thermokarst plains with fluvial erosion on satellite images (Kolyma Lowland, WorldView2, 0.5 m/px, July 1, 2013).

a – overall image; *b* – enlarged fragment; 1 – cluster of thermokarst depressions; 2 – main surface; white dotted line – boundary of a cluster of thermokarst depressions; black line – boundary of enlarged fragment.

mokarst depressions usually have rounded shapes and are irregularly distributed throughout the plain (Fig. 1*a*). A relatively elevated surface with the development of lakes is nominally called the main surface; this is the background element of topography and represents the first element of analysis in the present study (Fig. 1*b*).

Thermokarst depressions frequently merge together forming clusters; the lakes forming within them are largely secondary lakes that developed due to thermokarst process after the formation of the initial thermokarst depressions. We delineated these lakes based on clear, sharp outlines, often a rounded shape, and a discrepancy between the center of the lake and the center of the thermokarst depression. Contrarily, residual lakes in thermokarst depressions are characterized by blurred irregular outlines and vague boundaries. The aforementioned surface of thermokarst depressions, which are often joined (Fig. 1*b*), and the secondary lakes located in them are the second object of analysis (residual lakes are not considered).

Figure 2 shows satellite images of lakes on the main surface and secondary lakes on the surface of thermokarst depressions.

The study areas are located in different physico-geographical and geocryological conditions (Fig. 3) [*Geocryological Map..., 1991; State Geological Map..., 2000, 2015, 2016*].

The first group of sites is located on the territory of the Yamal and Tazovsky peninsulas with characteristic elevations of 20–70 m asl. The areas are predominantly composed of marine-alluvial and marine sediments of the Late Pleistocene–Holocene and Late Pleistocene ages. The upper part of the section is composed of fine- and medium-grained sand with inclusions of fine and medium gravel and with interlayers of loam, loamy sand, and clay; less often, loamy sand and loamy layers are present. This is the area of continuous permafrost with the mean annual temperature from –3 to –9°C is typical.

The second group of sites is found in the Kolyma Lowland with typical elevations of 20–70 m asl.

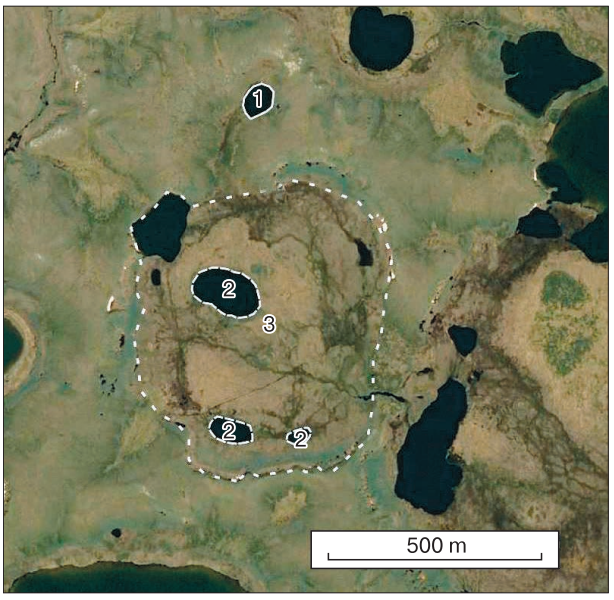

Fig. 2. Example of lakes seen on satellite image (Yamal Peninsula, image SPOT 7, 1.5 m/px, July 18, 2017).

1 – lakes on the main surface; 2 – secondary lakes on the surface of thermokarst depressions; 3 – white dotted line – boundary of thermokarst depression.

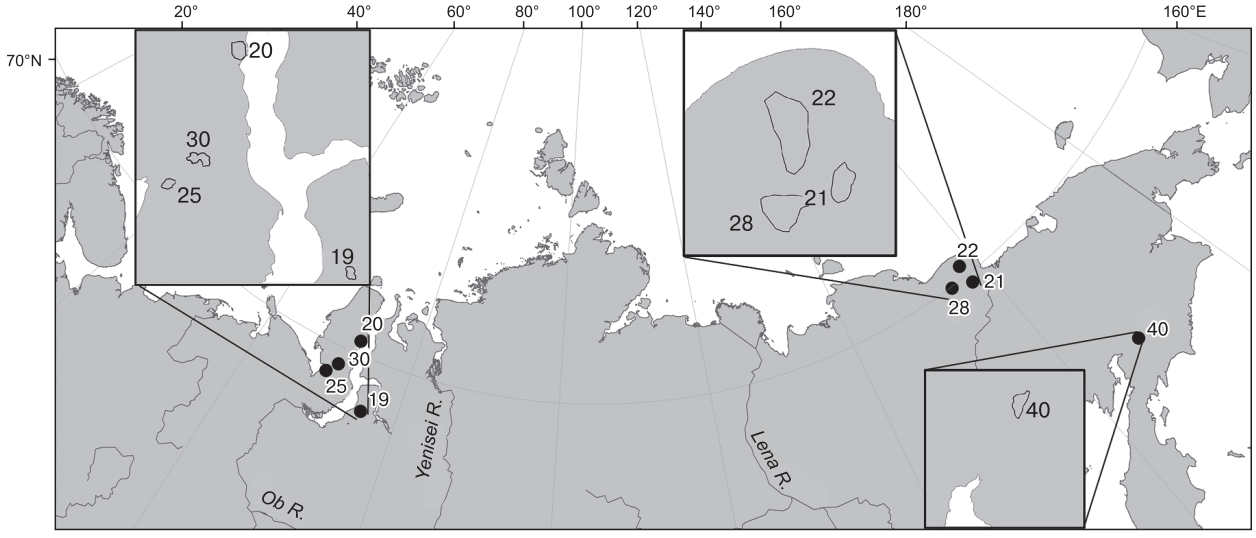

Fig. 3. Location of key sites.

Numbers – site numbers; black circles – site location; grey lines – boundaries of sites on the enlarged parts.

Loesslike lacustrine–alluvial sediments of the Late Pleistocene are overlain by lacustrine–bog sediments of the Early Holocene in thermokarst depressions. Lacustrine–alluvial sediments are silty and contain interlayers and lenses of peat. This is the area of continuous permafrost with the mean annual temperature from –7 to –11°C. The upper parts of the section are mainly composed of ice-rich sandy silt loams with massive cryostructure and large ice wedges.

The third group includes one site in the area of the Penzhina Bay (Parapolsky Dol) with typical elevations of 70–230 m asl. This territory is mainly composed of glaciofluvial sediments of the Middle Pleistocene: medium and fine gravels, sand, and boulders. Continuous permafrost has the mean annual temperature from –1 to –3°C.

The methodology of research included the following stages:

– selection of key sites within thermokarst plains with fluvial erosion and obtaining satellite images;

– development of a mathematical model of the morphological pattern of thermokarst plains with fluvial erosion, taking into consideration the existence of two types of conditions for the development of thermokarst lakes: on the main surface of thermokarst plains and on the surface of thermokarst depressions;

– delineation of lakes and calculation of their area;

– selection of samples of thermokarst lakes formed on the main surface of thermokarst plains and in the already existing thermokarst depressions[1];

– comparison of empirical distributions of these types of lakes for each site using Smirnov's criterion;

– comparison of empirical distributions and theoretical distributions obtained using the model with calculation of distribution parameters;

– comparison of the values of lake area distribution parameters for thermokarst lakes of type 1 (on the main surface of thermokarst terrain) and type 2 (lakes in thermokarst depressions) and analysis of the relationships between them;

– comprehensive comparison and analysis of the obtained data.

Key sites were selected based on the homogeneity of physico-geographical and geocryological conditions, as well as morphological homogeneity. Satellite images taken in June–September 2013–2019 with a resolution of 0.5–1.5 m (WorldView-2, SPOT 6,7) were mainly used; for key site 22, Sentinel-2 images with a resolution of 10 m were used.

The formation of samples of the areas of thermokarst lakes of the first and second type for each site implied interpretation of satellite images, delineation of the lakes, and determination of their areas using modules of QGIS software. Delineation (vectorization) of the lakes (water area) was carried out manually by an operator. As indicated above, the lakes were separated into two types: type 1, isolated lakes on the main surface of thermokarst plain; type 2, lakes in the existing thermokarst depressions that often formed clusters.

The next stage implied the comparison of empirical distributions of lake areas for the two samples for each site. To estimate the significance of the differences, Smirnov's criterion was applied, as this criterion does not necessitate knowledge about the type of distribution.

Then, we compared the empirical and theoretical integral-exponential distributions using Pearson's goodness-of-fit criterion. The necessary condition for using this criterion – the number of values in each separated class of the sample should no less than 5, and the sample itself should include no less than 50 values – was met. Sample sizes varied from 87 to 350. Next, the values of the area distribution parameter for lakes of type 1 was compared with that for lakes of type 2. In particular, the correlation coefficients for parameter values were determined for all the sites.

During the final stage, analysis of the entire data set was performed.

RESULTS

The mathematical model of the morphological pattern of thermokarst plains with fluvial erosion [*Victorov, 2005, 2006*] was applied in this study with certain adaptation of basic assumptions for the considered conditions:

(1) The formation of initial thermokarst depressions (lake foci) on the main surface and on the surface of the already existing thermokarst depressions during non-intersecting periods of time (Δt) and in non-intersecting areas (Δs) are independent random events; the probability of the formation of depressions p_k (where k is the number of depressions) depends only on the length of the time period and on the size of the site[2]:

$$p_1 = \lambda_i \Delta s \Delta t + o(\Delta s \Delta t), \quad i = 1, 2,$$

$$p_k = o(\Delta s \Delta t), \quad k = 2, 3...,$$

where λ_1 and λ_2 are the parameter values for the main surface and for the surface of thermokarst depressions, respectively.

(2) The formation of primary lakes does not occur on the surface of existing thermokarst lakes.

[1] For brevity, the former lakes are called type 1 lakes and the latter are called type 2 lakes.

[2] For small areas and short time periods, the probability of formation of one thermokarst depression is much greater than the probability of formation of several depressions.

(3) The radius of the formed thermokarst lake as a function of time is a random process; the change in the radius occurs independently of other lakes, and the rate of its growth is proportional to the density of heat losses through the lateral surface of the lake basin.

(4) During the growth process, a lake can transform into a thermokarst depression when drained through the erosional network; the probability of this process does not depend on other lakes; meanwhile, the growth of drained lakes stops.

(5) The formation of the sources of stream channels on non-intersecting areas is a random event with an average density of sources γ_1 and γ_2 for the main surface and for the surface of thermokarst depressions, respectively; the probability of the presence of such a source at the key site depends only on its size[3].

In the basic version of the model, the density of lake generation and the distribution density of the sources of stream channels were assumed to be close both for the main surface and for the surface of thermokarst depressions, i.e., the entire key area was assumed to be relatively homogenous in terms of the indicated parameters [*Victorov, 2005; Victorov et al., 2016*]. It was shown that in a wide range of physico-geographical and geocryological conditions, given a significant time of development, the territory comes to a state of dynamic equilibrium [*Victorov, 2005, 2006*]. In this case, the initiation and growth of thermokarst lakes is compensated by their drainage and transformation into thermokarst depressions. The analysis of this basic version of the model indicates that the state of dynamic equilibrium is characterized by a specific type of distribution of the areas of thermokarst lakes, which was conventionally called the integral-exponential distribution [*Victorov et al., 2016, 2021*].

In the studied situation, upon analysis of the errors of the created model, it is easy to see that for each individual surface (the main surface and the surface of thermokarst depressions and their clusters), essentially, the conditions of the base model are met, i.e., each type of the surface types is relatively uniform in terms of the density of generation of lakes and sources of stream channels. In this case, using the base model, it can be concluded that, over a significant time, each type of the surface may come to a state of dynamic equilibrium. Consequently, the distribution of lake areas will be close to the integral-exponential distribution, with its own parameter values for each type of the surface:

$$f_1(x,\infty) = -\frac{1}{x\mathrm{Ei}\left(-\gamma_1\varepsilon_1\right)}\exp\left(-\gamma_1 x\right), \quad x \geq \varepsilon_1,$$

$$f_2(x,\infty) = -\frac{1}{x\mathrm{Ei}\left(-\gamma_2\varepsilon_2\right)}\exp\left(-\gamma_2 x\right), \quad x \geq \varepsilon_2,$$

where ε_1, ε_2 are the initial lake areas for the main surface and for the surface of thermokarst depressions, respectively: γ_1, γ_2 are the average distribution density of the sources of stream channels for the main surface and for the surface of thermokarst depressions, respectively; and $\mathrm{Ei}(-x)$ is the integral-exponential function. The values of corresponding parameters of lake area distributions for the two types of surface should differ from one another.

The analysis of this modified base model suggests that distributions of thermokarst lake areas on the main surface (f_1) and in thermokarst depressions (f_2) can correspond to a special type of distribution, which is nominally called integral-exponential, and this can be one of the elements of empirical verification.

Comparison of empirical distributions of lake areas in the selected samples with the use of Smirnov's criterion made it possible to estimate the statistical significance of the difference between distributions of thermokarst lakes of the first and second types regardless of the hypothesis about belonging to one or the other type of distribution. The results of this estimate are presented in Table 1 and Fig. 4. The analysis shows that at seven out of eight sites, the differences between distributions of the two types of thermokarst lakes are significant at the 0.99 level.

The next stage was a comparison of empirical and theoretical distributions. Following the analysis of the model of the morphological pattern development for the thermokarst plains with fluvial erosion, integral-exponential distributions of lake areas should be observed. At the first step, the parameters of these distributions were estimated for each sample. The minimum value of parameter ε was taken for each of the samples, while parameter γ was found using the method of moments by numerical solution within a specially designed software module of the equation

$$-\frac{1}{\gamma\mathrm{Ei}(-\gamma\varepsilon)}\exp\left(-\gamma\varepsilon\right) = \overline{s},$$

where $\overline{s}$ is the average lake area.

Using the same module, the value of Pearson's criterion was calculated and compared with the critical value at a significance value of 0.99. The results of assessing the agreement between empirical and theoretical integral-exponential distributions using the Pearson criterion are given in Table 2. It can be seen that at the significance level of 0.99, the distribution of thermokarst lake areas within the main surface of thermokarst plains is consisted with the theoretical integral-exponential distribution at six out of eight

[3] For small key sites, the probability of having more than one source is much greater.

Table 1. **Comparison of empirical distributions of lake areas according to Smirnov's criterion**

District	Site number	Area, km^2	Sample size (number of lakes)		Maximum difference		Parameter p*
			on the main surface	on the surface of thermokarst depressions	negative	positive	
Yamal Peninsula	20	450	86	254	–0.012	0.227	$p < 0.005$
	25	202	131	116	–0.092	0.098	$p > 0.10$
	30	4419	260	132	0.00	0.261	$p < 0.001$
Tazovsky Peninsula	19	207	87	105	0.00	0.359	$p < 0.001$
Kolyma Lowland	21	1157	252	172	0.00	0.276	$p < 0.001$
	22	2867	113	183	0.00	0.348	$p < 0.001$
	28	1343	125	117	–0.012	0.245	$p < 0.005$
Parapolsky Dol	40	670	350	175	0.00	0.231	$p < 0.001$

* Difference in distributions is statistically significant at the 0.99 level in the case of $p < 0.01$.

sites. The distribution of thermokarst lake areas within thermokarst depressions also matches the theoretical integral-exponential distribution at six out of eight sites; in both cases, no correspondence is observed for site 30 (Penzhina Bay area).

In Fig. 4, graphs of thermokarst lake area distributions of the first and second types are provided; the difference between them and the correspondence of both graphs to the integral-exponential distribution are clearly seen.

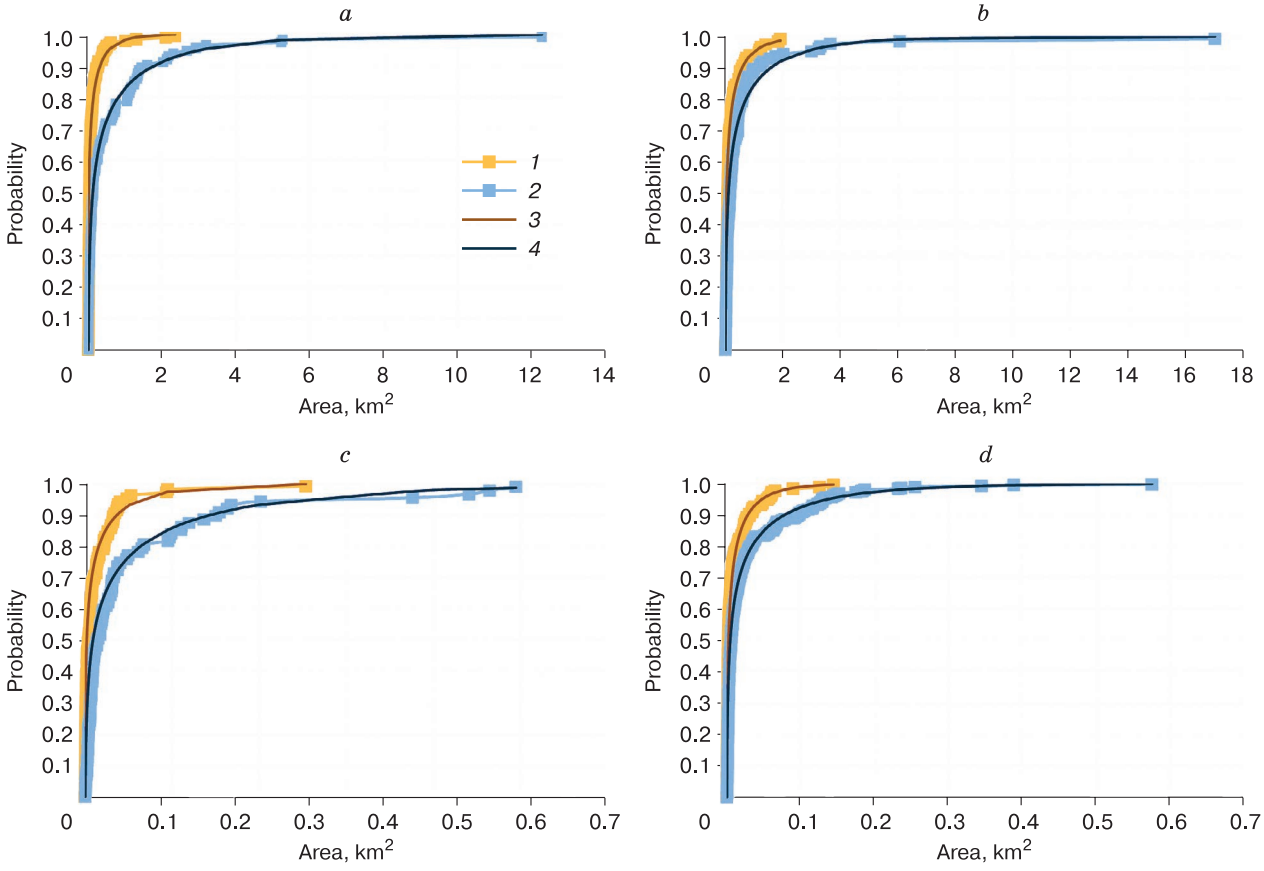

Fig. 4. Graphs of thermokarst lake area distribution at sites 22 (*a*), 28 (*b*), 19 (*c*), 40 (*d*).

1, *2* – empirical distribution of surface areas of type 1 and type 2 lakes, respectively; *3*, *4* – theoretical (integral-exponential) distributions of surface areas of type 1 and type 2, respectively.

Table 2. **Assessment of the agreement between empirical and theoretical integral-exponential distributions according to Pearson's criterion**

District	Site number	Average lake area, m^2	Sample size	Criterion value		ε, m^2	γ, km^{-2}
				Pearson	critical at the 0.99 level		
Main surface							
Yamal Peninsula	20	120 564	86	7.678	6.635	2112	5.483
	25	54 647	131	11.034	11.341	487	3.155
	30	31 296	260	22.570	13.277	194	5.021
Tazovsky Peninsula	19	51 774	87	5.537	9.210	473	3.271
Kolyma Lowland	21	300 137	252	5.413	15.086	6972	0.697
	22	638 574	113	4.870	11.341	7583	0.280
	28	568 958	125	2.200	6.635	6898	0.316
Parapolsky Dol	40	27 753	350	13.143	13.277	217	5.917
Surface of thermokarst depressions							
Yamal Peninsula	20	32 298	254	11.060	11.341	1307	7.573
	25	35 507	116	9.814	15.086	1519	5.416
	30	10 981	132	19.411	15.086	148	16.742
Tazovsky Peninsula	19	13 197	105	13.054	9.210	90	12.12
Kolyma Lowland	21	110 604	172	5.843	9.210	662	1.412
	22	115 790	183	3.589	9.210	1037	1.457
	28	211 069	117	4.341	11.341	3274	0.899
Parapolsky Dol	40	10 169	175	4.093	15.086	163	18.804

Note: γ is the estimate of the average density of the sources of stream channels; ε is the estimate of the initial size of the lakes.

Figure 5 shows the results of comparison of the parameters of both distributions for the same sites. The values of parameter γ, which, according to the model, reflects the average density of the sources of stream channels within the main surface and within thermokarst depressions are compared. Parameter ε as the minimum value for the sample is more susceptible to the influence of random factors (for example, it depends on sample size). Therefore, it was not specially analyzed.

The correlation coefficient between the values of γ_1 and γ_2 is 0.95. The values of this parameter for lakes on the main surface γ_1 are always less than those for lakes in thermokarst depressions γ_2.

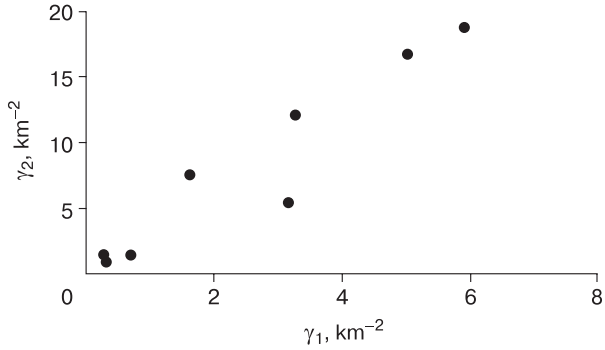

Fig. 5. Relationship between estimates of the average density of sources of stream channels for different types of surfaces of thermokarst plains with fluvial erosion.

γ_1 – main surface parameter value, γ_2 – thermokarst depression surface parameter value.

DISCUSSION OF THE RESULTS OF COMPARATIVE ANALYSIS

Analysis of the obtained results allows us to conclude that area distribution of thermokarst lakes forming on the surface of thermokarst depressions differs from that of thermokarst lakes on the main surface, This is illustrated by the discrepancy between the graphs: the graph of area distribution of type 1 lakes lies to the right of the graph of area distribution of type 2 lakes for all the sites. This is a consequence of the fact that the proportion of small lakes within lake clusters in thermokarst depression is significantly higher than that for small lakes on the main surface. The differences in distributions are statistically significant for all sites, except for site 25 (Yamal Peninsula).

Area distribution of thermokarst lakes forming on the main surface follows the integral-exponential distribution in 75% of the sites. As argued before [*Victorov et al., 2021*], this is a sign of dynamic equilibrium, some balance between the initiation and growth of the lakes, on one hand, and their drainage by erosional processes, on the other hand. This con-

clusion turns out to be valid provided that the model's assumptions are valid; in particular, the assumption about the ongoing process of the formation of new lakes. This assumption remains open to argument for the main surface, so the conclusion obtained is subject to further research and cannot be considered final.

The identified presence of integral-exponential distribution, although with other values of parameter γ for the lakes in thermokarst depressions, allows us to conclude that an analogous dynamic equilibrium is also established on this territory. This is also a consequence of the fulfillment of the model's assumptions, and in the given case the initiation of new lakes is explained by the appearance of new drained lake basins.

The difference in the values of parameter γ can be explained by the fact that within the area of thermokarst depressions, there are obviously more sources of stream channels owing to those that previously led to the formation of the existing thermokarst depressions; hence, parameter γ is higher. At the same time, at each site, the processes on the main surface and on the surface of thermokarst depressions occur within the same landscape – thermokarst plain with fluvial erosion and under uniform climatic conditions: the morphological parts of this landscape are linked by diverse interactions, including the movement of matter and energy. In our opinion, this circumstance explains good correlation between the values of parameter γ for lakes of the first and second types.

Analysis of the obtained results also allows us to conclude that the model of the development of the morphological pattern of thermokarst plains with fluvial erosion must consider the identified difference in the formation of thermokarst lakes on the main watershed surface and on the surface of thermokarst depressions.

CONCLUSIONS

This study allows us to make the following conclusions:

1. Comparison of area distributions of thermokarst lakes forming on the main surface of thermokarst plains with fluvial erosion and secondary lakes forming within the already existing thermokarst depressions shows the presence of statistically significant differences between them; therefore, the model of the development of the morphological pattern of thermokarst plains with fluvial erosion should be based on the existence of different conditions for the development of thermokarst lakes on the main surface of the plain and on the surface of thermokarst depressions, often forming clusters.

2. On each of the two types of surfaces within thermokarst plains with fluvial erosion, in a significant number of cases, integral-exponential distributions of the areas of thermokarst lakes are observed. Although they differ from one another, their existence can be interpreted as a sign of the establishment of dynamic equilibrium in the course of the development of thermokarst lakes, at least within the surface of thermokarst depressions.

3. Lake area distribution parameters for lakes on the main surface differ from those for lakes in thermokarst depressions; however, there is a good correlation between them.

Acknowledgements. *This study was supported by the Russian Science Foundation, project no. 18-17-00226P.*

References

Belshe F., Schuur E., Grosse G., 2013. Quantification of upland thermokarst features with high resolution remote sensing. *Environ. Res. Lett.* **8**, p. 035016. doi: 10.1088/1748-9326/8/3/035016.

Cael B., Seekell D., 2016. The size-distribution of Earth's lakes. *Sci. Rep.* **6**, p. 29633. doi: 10.1038/srep29633.

Chen M., Rowland J., Wilson C. et al., 2014. Temporal and spatial pattern of thermokarst lake area changes at Yukon Flats, Alaska. *Hydrol. Process.* **28**, p. 3. doi: 10.1002/hyp.9642.

Geocryological Map of the USSR, Scale 1:2 500 000, 1991. Moscow, GUGK, 16 p.

Grosse G., Jones B.M., Nitze I. et al., 2016. Massive thermokarst lake area loss in continuous ice-rich permafrost of the northern Seward Peninsula, Northwestern Alaska, 1949–2015. In: *XI Int. Conf. on Permafrost* (Potsdam, 20–24 June 2016): Abstracts, Potsdam, Germany, p. 739–740.

Jones B.M., Grosse G., Arp C. et al., 2011. Modern thermokarst lake dynamics in the continuous permafrost zone, northern Seward Peninsula Alaska. *J. Geophys. Res.: Biogeosciences* **116** (G2), 1–13. doi: 10.1029/2011jg001666.

Kravtsova V.I., Bystrova A.G., 2009. Changes in thermokarst lake size in different regions of Russia for the last 30 years. *Kriosfera Zemli* XIII (2), 16–26.

Lantz T.C., Turner K.W., 2015. Changes in lake area in response to thermokarst processes and climate in Old Crow Flats Yukon. *J. Geophys. Res.: Biogeosciences* **120** (3), 513–524.

Morgenstern A., Grosse G., Günther F. et al., 2011. Spatial analyses of thermokarst lakes and basins in Yedoma landscapes of the Lena Delta. *The Cryosphere Discuss.* **5**, 1495–1545. doi: 10.5194/tcd-5-1495-2011.

Muratov I., Ibraeva A., Timergazina L., Polishchuk Y., 2021. Remote study of thermokarst lakes in the Arctic tundra of Taimyr. *Yugra State Univ. Bull.* **17** (1), 62–71. doi: 10.17816/byusu20210162-71.

Olefeldt D., Goswami S., Grosse G. et al., 2016. Circumpolar distribution and carbon storage of thermokarst landscapes. *Nat. Commun.* **7**. doi: 10.1038/ncomms13043.

Polishchuk V.Yu., Polishchuk Yu.M., 2013. *Geosimulation Modeling of Thermokarst Lake Areas in Permafrost Zones*. Khanty-Mansiysk, UIP YuGU, 129 p. (in Russian).

Polishchuk Y., Bogdanov A., Muratov I. et al., 2018. Minor contribution of small thaw ponds to the pools of carbon and methane in the inland waters of the permafrost-affected part of western Siberian Lowland. *Environ. Res. Lett.* **13**, 1–16. doi: 10.1088/1748-9326/aab046.

Smith L.C., Sheng Y., Macdonald G.M., Hinzman L.D., 2005. Disappearing Arctic lakes. *Science* **308** (3), p. 14.

State Geological Map of the Russian Federation, Scale of 1:1 000 000 (third generation), Zapadno-Sibirskaya series, Q-43. St.-Petersburg, VSEGEI, 2015.

State Geological Map of the Russian Federation, Scale of 1:1 000 000. Koryaksko-Kurilskaya series, P-5. St. Petersburg, VSEGEI, 2016.

State Geological Map of the Russian Federation, Scale of 1:1 000 000 (new series), R-43-(45), R-(55)-57, R-(40)-42. St. Petersburg, VSEGEI, 2000.

Veremeeva A., Nitze I., Günther F. et al., 2021. Geomorphological and climatic drivers of thermokarst lake area increase trend (1999–2018) in the Kolyma Lowland Yedoma region, North-Eastern Siberia. *Remote Sens.* **13**, p. 178. doi: 10.3390/rs13020178.

Verpoorter C., Kutser T., Seekell D., Tranvik L., 2014. A global inventory of lakes based on high-resolution satellite imagery. *Geophys. Res. Lett.* **41** (18), 6396–6402. doi: 10.1002/2014GL060641.

Victorov A.S., 2005. Mathematical models of thermokarst erosion plains. In: *GIS and Spatial Analysis: Proc. of IAMG'05* (Toronto, Canada, August 21–26, 2005). Toronto, vol. I, p. 62–67.

Victorov A.S., 2006. *The Main Problems of Mathematical Morphology of Landscape*. Moscow, Nauka, 252 p. (in Russian).

Victorov A.S., Kapralova V.N., Orlov T.V. et al., 2016. *Mathematical Morphology of Landscapes in the Cryolithozone*. Moscow, RUDN, 232 p. (in Russian).

Victorov A.S., Orlov T.V., Kapralova V.N., Trapeznikova O.N., 2021. Modeling the ways of the morphological pattern development for thermokarst plains with fluvial erosion. *Earth's Cryosphere* XXV (1), 40–47.

Wei Z., Du Z., Wang L. et al., 2021. Sentinel-based inventory of thermokarst lakes and ponds across permafrost landscapes on the Qinghai-Tibet Plateau. *Earth and Space Sci.* **8**, p. 11. doi: 10.1029/2021EA001950.

Received March 24, 2022
Revised July 13, 2022
Accepted February 8, 2023

Translated by M.A. Korkka

EARTH'S CRYOSPHERE
SCIENTIFIC JOURNAL

Earth's Cryosphere, 2023, vol. XXVII, No. 2, pp. 56–66

CHRONICLE

MIKHAIL IVANOVICH SUMGIN – THE FOUNDER OF GEOCRYOLOGY
(on the 150th anniversary of the birth)

V.R. Alekseev

Melnikov Permafrost Institute, Siberian Branch of the Russian Academy of Sciences, Merzlotnaya St. 36, Yakutsk, 677010 Russia

E-mail: avr@crust.irk.ru

Information about the life and work of an outstanding scientist Mikhail Ivanovich Sumgin is presented. His contribution to the development of a young science of frozen rocks and related phenomena, geocryology, is discussed.

Keywords: *permafrost, cryolithozone, frozen rocks, perennial and seasonal frost, cryogenic processes and phenomena.*

Recommended citation: Alekseev V.R., 2023. Mikhail Ivanovich Sumgin – the founder of geocryology (on the 150th anniversary of the birth). *Earth's Cryosphere* XXVII (2), 56–66.

There are people, whose life, like a magnet, attracts us with apparent originality of actions, thoughts, and deeds. Even years after such person has left this turbulent, mysterious world, his life continues to attract people over again, sometimes as an example of service to a noble goal and sometimes simply as the behavior of an individual in the most difficult conditions of existence. They are people with an unshakable, iron will, obsessed with an idea or bright thoughts, capable of synthesizing their knowledge and putting it into practice. There are many such people in science. At all times, they have been followed, looked up to, and learned from. Such a person in permafrost science was Mikhail Ivanovich Sumgin (Fig. 1). The name of this man, an outstanding geographer, geologist, and engineer, occupies a strong place among the scientists, who have enriched Russian and world science. M.I. Sumgin's works have shaped the basis of many textbooks, projects, and engineering solutions and have been used in the construction methods and economies of nations living in cold regions of the globe. His books, articles, and ideas are still used today, not only to solve the current issues in the development of the North but also to assess the future development of our civilization under conditions of future climate change and the growing anthropogenic impact on the natural environment.

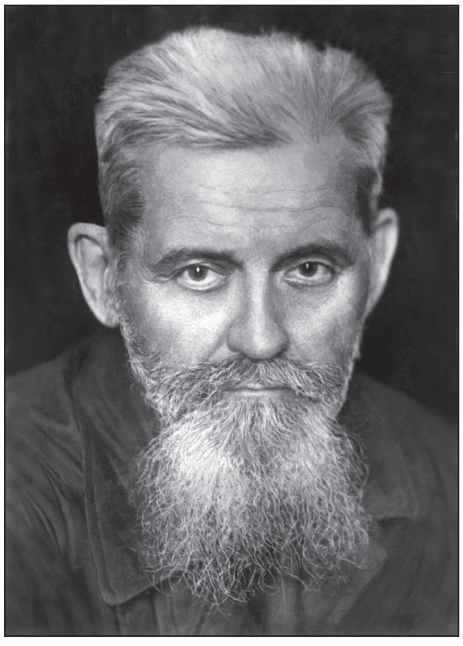

Fig. 1. Mikhail Ivanovich Sumgin (February 25, 1873–December 8, 1942).

THE BEGINNING OF LIFE JOURNEY

Mikhail Ivanovich Sumgin was born on February 25, 1873 into the family of a Mordovian peasant in Krapivki village, Lukoyanov Uyezd of the former Nizhny Novgorod Governorate. His father, Ivan Ignatyevich, an energetic and inquisitive man, became a volost clerk after finishing a parochial school.

It was the rarest case among illiterate people of the Erzya[1]. The mother of the future scientist, local

[1] Erzya is one of the ancient ethnic groups of the Mordovian people; among their representatives, there are many famous historical personas: Patriarch Nikon, Stepan Razin, Vladimir Lenin, Fyodor Chaliapin, Maxim Gorky, Lidiya Ruslanova, Vasilii Chapayev, etc.

beauty Anna Fedorovna Garankina, an intelligent and kind woman, could read, but she never learned to write. Misha's first teacher was his father. The boy inherited his curiosity, initiative, and practicality from him. The parents discovered their son's ability to learn and, despite financial difficulties, decided to give him an education. After graduating from a rural parochial school in the autumn of 1885, Misha entered the Lukoyanov secondary school, from which he graduated brilliantly two years later. Like his father, who had already died by this time, he became a clerk. He composed letters, petitions, and intercessions for peasants. He never took money following the example of his late parent. This fact raised reputation of the Sumgin family even more; the young clerk gained universal respect. In 1892, after the lean year with a bad harvest, misfortune came: his younger brother and sister died of scarlet fever, and his mother fell seriously ill. Misha was lucky; he survived. He continued his service, read a lot and educated himself.

The further life of the young man was largely determined by the fact that he met and communicated with kind and intelligent people. Not far from the village, where Misha lived, there was an estate of a relative of the famous artist, academician of painting V.I. Yakobi. The owner of the estate, Mrs. Yakobi, an educated woman, who voluntarily served as a local doctor, needed an assistant, who, in addition to the office business, would look after her son. Having heard from neighbors about the talented young man, she invited him to work, introduced him into her family, provided him with lodging, and allowed him to use their rich library. Sumgin spent four years in the family of V.I. Yakobi. Here he began to study French, Greek, and Latin and was determined to enter one of the Russian universities to become a "travelling professor" lecturing in villages and, thus, enlightening the illiterate underprivileged people.

However, several more difficult years had passed before he entered St. Petersburg University. It was necessary, at least for the start, to have some means of support, and his mother needed help. Leaving the Yakobi family, he went to Nizhny Novgorod and worked as a bath attendant, a barge loader, and a porter at a railroad station. It so happened that the young man met the famous statistician and journalist Nikolai Fedorovich Annensky, who was lived in an exile in the city on the Volga River and began to visit him. At the apartment of N.F. Annensky, he met the writer Vladimir Galaktionovich Korolenko. Misha impressed him with his stories, soulful character, biography, and attitude towards working people, especially the peasantry. N.F. Annensky and V.G. Korolenko appreciated the young man curiosity and recommended him to go to Moscow or Saint Petersburg, where he could enrich his knowledge in libraries and museums and to prepare for the university. N.F. Annensky wrote a recommendation letter to his brother, the director of the Tsarskoye Selo Gymnasium, asking him to help the talented young man. But there was still not enough money for the trip, Then his mother sold her only cow, and the assembly of Krapivki village handed the fellow countryman a kind of a referral certificate, which stated that "there are no obstacles to Sumgin's admission to a higher educational institution".

SAINT PETERSBURG: THE HARD WAY TO KNOWLEDGE

The capital greeted the young man unfriendly – there was nowhere to live, and it was difficult to find job. He spent some time sleeping under a bridge and at a train station. He managed to rent a small room in an attic and get a job at the Zincography Laboratory of Demchinsky. After a 12–14-hour workday he was exhausted. He had to get up early in the morning to study textbooks, but such studies were of little use. In the spring of 1894, he left the zincography business and began working as a self-employed man, which allowed him to change his work schedule and devote some of his free time to self-education. He loaded all sorts of things, carried boxes and suitcases at train stations, and sold tobacco, cigarettes, and matches.

One day he met V.I. Jacobi, member of the Academy of Arts, who, after hearing about the wanderings of his young friend, invited him to his studio. Sumgin posed for the artist in the costume of Emperor Alexander III for some time, read a lot, and prepared for exams. However, it did not last long. One of the visitors called Sumgin a "strange lackey", and he, offended, left the hospitable house. He began selling from a stall again, while loudly singing lines from the "Iliad" in Greek and the world-famous student song "Gaudeamus igitur" in Latin. Finally, fate smiled on the tall and handsome guy. On the bank of the Neva River, near the university building, he met one of the students, Vikarii Petrovich Samsel, who was greatly surprised by erudition of the unusual salesman. They became friends, and this friendship lasted for the rest of their lives.

V.P. Samsel created all possible conditions for systematization of the accumulated knowledge of M.I. Sumgin and actually prepared him to enter university. To begin with, in May 1895, Mikhail brilliantly passed the examinations for the full gymnasium course. Eight out of eleven subjects, including physics, mathematics, Greek, Latin, French, history, and geography, were rated "excellent" by the teachers of the capital's educational institution. This was a really big and well-deserved victory! Soon Michael became a student at the Faculty of Physics and Mathematics of St. Petersburg University.

There was an exciting new world of knowledge to explore. He studied avidly and enthusiastically. Chemistry, physics, astronomy, mathematical analy-

sis – everything was interesting. In addition to lectures, he attended scientific gatherings and meetings and was considered the best chess player at the faculty. He lived modestly. He rented a room on the Neva River embankment, where his hostess provided him with breakfast and dinner. At first, the scholarship was not given. He had to earn money by giving lessons and taking part in loading and unloading work at the seaport. Some of the money was sent to his mother in the village. In spite of the difficulties of everyday life, he graduated from the first year with honors. V.I. Jacobi continued to follow the progress of his fellow countryman. On his initiative, M.I. Sumgin was exempted from tuition fees as "extremely poor", and soon he was awarded the Rybin scholarship established by one of the city's benefactors "for success and exemplary conduct".

Misha had a smooth temper, sincerity, goodwill, and extremely hard-working nature. This captivated people around him. A lot of friends appeared; he earned attention and respect of teachers and professors. They predicted him a great future in science and promised to leave him at the university after graduation. Dreams of education were rapidly coming true.

No one knows how the future fate of Mikhail Sumgin would have turned out. Surely, he would have become a major scientist in the field of physical and mathematical sciences, just not a permafrost scientist. If not for one "but". The political destiny of Russia had been bothering him for a long time. He wanted to devote himself to the struggle for "the happiness of people". Communicating with leading intellectuals of St. Petersburg, attending student gatherings, reading forbidden literature, Mikhail Sumgin entered the spirit of freedom-loving ideas of that time. The ideology of populism, the struggle for the truth and for the overthrow of monarchy were closest to him. When M.I. Sumgin was in his third year of the university, the police became aware of his illegal activities. His rented apartment was searched and a forbidden brochure was found. A successful student was arrested, deprived of his scholarship, and expelled from the university.

The hard days began again. He had to change cheap housing and to live by casual earnings. Mikhail went to his mother in the village of Krapivki for the summer. In the autumn, he returned to the capital on the advice of friends and submitted a petition for reinstatement to the university. The petition was supported by professors K.A. Posse, O.D. Khvolson, and I.I. Borgman. On October 28, 1898, M.I. Sumgin returned to his classrooms and settled in the apartment of Professor N.A. Gezakhus, which offered him the perfect conditions for continuing his studies. What more could a poor student dream of? The exciting prospect of mastering the knowledge accumulated by mankind was once again at hand. But one cannot hide from fate, one cannot run away...

UNDER POLICE SUPERVISION

In February 1899, significant events occurred in St. Petersburg: students, preparing for a political demonstration, disrupted classes. A conflict with gendarmes took place, many young people were beaten, some were arrested and imprisoned. Among the victims, M. Sumgin was one of the first to be taken, because he was under suspicion. As a result, he was exiled to Nizhny Novgorod under police supervision and was deprived of the right to enter any institution of higher education in Russia.

Mikhail did not stay in Nizhny Novgorod for long. At the end of June 1899, investigators found him in Samara, to where he had gone illegally. The Samara period of Sumgin's life lasted with some interruptions for eight years. He worked in the statistics department of the zemstvo office, traveled extensively through villages and settlements and did not miss the opportunity to conduct revolutionary propaganda among the local population. Science took second place. He joined the Socialist-Revolutionary Party (SRP) illegally established in 1902. The political positions were close to him as a representative of the working peasantry. The time was uneasy; turbulent meetings, strikes, protest demonstrations, clashes with the police covered almost the entire country. The emotionally charged atmosphere increased dramatically after defeat of Russia in the Russian–Japanese War. The year 1905 was fateful for Mikhail Ivanovich. The police did not stop surveillance looking for a reason to bring him to trial. And such a reason was found. On December 18, Sumgin published the "Invitation to the Samara Peasant Congress" in the city newspaper, which the authorities considered as a call for a general protest against the tsarist autocracy. M.I. Sumgin was arrested and spent more than a year in prison. In December 1906, he was sentenced to three years of exile in Tobolsk Gubernia.

In January 1907, at the request of his friends, the exile to Tobolsk Gubernia was replaced by deportation abroad for two years. In the case of an earlier return to Russia, he was promised the full extent of his punishment. He was arrested and transported under guard to Odessa. Then, he was free to go to France, to Paris. Life in the "Capital of the World" was exciting, but did not suit Mikhail Ivanovich. He was not picky, could work, spoke French, and could adapt to any living conditions. But he was homesick! He felt nostalgia for his homeland and for his deed, which was taken away from him... and for his wife Liza Ovsyanaya, a graduate of the Institute of Noble Maidens, who, after his arrest, went to the future famous soil scientist Professor F.A. Petrov. Sumgin could not stand it and six months later returned to Russia illegally.

The joyful exhilaration of the struggle, the secret meetings, the hopes... All this did not last long. In March 1908, the police raided the secret house in

Kostroma, where the Socialist Revolutionaries were meeting. Again, he was arrested and imprisoned for six months; then, he was exiled to the remote Siberian village of Morozovka, 30 versts from Tobolsk. His mood dropped. Health deteriorated rapidly. Dark days came. There was no work in the village. Fishing and gardening on a small plot of land allotted by locals helped out in the first year. Then, he was transferred to the abandoned village of Alysanovo even further from the gubernia center – the authorities carefully protected the peasants from the influence of political exiles. Idleness, mental breakdown, stomach disease, rheumatism of the legs, and other misfortunes almost brought him to the grave. But something unexpected happened. A quick zig of fate brought him out of dead-end and determined the direction of his entire future life.

ON THE AMUR AND ZEYA RIVERS

In the summer of 1910, the expedition of the Pereselencheskoye (Resettlement) Department of the Ministry of Land Management and Agriculture of Russia worked in Irtysh Region. One of the teams was headed by an energetic young man, Professor Nikolai Ivanovich Prokhorov (1877–1930), the future founder of cryopedology (permafrost soil science) and road soil science. He paid attention to the educated settler and inspired him to study the virgin nature of the Far East. At the request of N.I. Prokhorov, M.I. Sumgin was included in the Zeya soil team after the end of his exile. He was appointed the head of the newly organized Bomnak weather station. This was a period, when the settlement of the Amur region dramatically intensified because of the railroad construction and the development of gold mining industry. It was believed that the Amur Region would become a kind of a locomotive for economic development in the east of Russia. According to the decree of the emperor, the Amur Comprehensive Expedition under the guidance of the Governor-General N.L. Gondatti was created to study the nature, assess land, and determine the possibilities for wide-scale colonization. The Zeya soil team of N.I. Prokhorov was part of it.

On March 14, 1911, Mikhail Sumgin, inspired by freedom and the opportunity to engage in science, left Tobolsk and went to the Amur region. The Bomnak weather station was located on the right bank of the Zeya River, about 230 km upstream from the merchant town of the same name. The water level in the Zeya River was very low in that year. Steamboats were anchored at piers, so it was not possible to reach the place of destination quickly. Sumgin had to spend more than a month at the Pikan agroclimatic station. And that was helpful. Mikhail Ivanovich met and made friends with young employees V.N. Aleksakhin and P.I. Koloskov, who also recently arrived in the Amur Region and launched a wide range of experimental work. While waiting for the steamboat, M.I. Sumgin studied in detail the instrument base and methods of meteorological, soil-permafrost, and other stationary observations. He arrived in Bomnak already with a fully prepared research program. In addition to studying climatic features of the area, the program included the issues related to the water and ice regime of rivers, freezing and thawing of soils, assessment of wetlands, etc. To his great joy, M.I. Sumgin met his friend, Valerian Gavrilovich Petrov, member of the Socialist-Revolutionary Party, who was also exiled to Siberia in Bomnak. The last time they saw each other was on walks in Samara prison.

M.I. Sumgin stayed in Bomnak for about a year. N.I. Prokhorov appreciated his enthusiasm and interest in science and offered to head the newly organized Meteorological Bureau of the Amur Region, which was in charge of the observation stations of the Resettlement Department. In Blagoveshchensk, Mikhail was literally transformed. The best qualities of this talented extraordinary person were clearly revealed. Everything that had been hiding in his rebellious, restless soul in recent years suddenly erupted into a cascade of deeds and accomplishments. The Meteorological Bureau quickly turned into a kind of a research center under the leadership of M.I. Sumgin. The center was small in number of staff, but very effective in terms of its results with its own journal, traditions, and development prospects. It was the weather service not only for the Amur Region, but for the entire Russian Far East. Suffice it to say that the number of weather stations in this vast territory doubled during the period from 1913 to 1916.

Here, in the Amur Region, Mikhail Ivanovich Sumgin became infected with an interest in the "Siberian Sphinx". Already in Bomnak, he tried to find out the causes of permafrost formation through observations of soil temperature at experimental sites with different types of vegetation, peat layer, and snow cover. He discovered many amazing things while hiking in the valleys of local rivers and creeks, especially during a trip in January 1912 on a reindeer sledge b to the mouth of the Kupuri River (about 160 km along ice and coastal areas of the Zeya River). In Blagoveshchensk, M.I. Sumgin studied all the available literature on frozen soils, from the work of A.F. Middendorf to the articles of V.B. Shostakovich and I.A. Lopatin. Even letters and petitions of the first explorers of the 17th century (V.D. Poyarkov, E.P. Khabarov, V. Yuriev and others) were not ignored. It turned out that this "unusual" natural phenomenon, known to science since the time of M.V. Lomonosov, had been studied insufficiently. There was not even a substantiated map of the permafrost distribution. Dozens, hundreds of issues about the origin, history of development, properties, nature and forms, and behavior of frozen ground and soils under the in-

fluence of natural factors and human activity came up before the inquisitive physicist-meteorologist.

M.I. Sumgin decided to study the Siberian phenomenon thoroughly. First of all, he organized systematic observations of freezing and thawing of soils at the sites of existing and newly organized stations. Then, he began to collect data on the distribution of permafrost in the Amur Region by bits and pieces. He used a proven method of questioning of the population in addition to personal observations during inspections and business trips. His questionnaire was addressed mostly to people involved in mining work at gold mines. This method proved to be justified. A year later, Mikhail Ivanovich had material, which, along with the previously known data, allowed him to prepare and publish a special paper "Geographical distribution of permafrost in the Amur region" [*Sumgin, 1914*]. This paper provided information on long-term freezing of rocks at 71 points, analyzed the conditions and causes of the permafrost formation, determined the southern boundary of the permafrost distribution, and raised the question of organizing a special permafrost station. This work became a milestone in the history of permafrost science. The time of systematic accumulation and analysis of geocryological data, necessary for formulating the principles of the organization and development of a new scientific field, can be counted from this paper.

The life of Mikhail Ivanovich in Blagoveshchensk developed rapidly and interestingly. Long explorer's trips, meetings, processing observational and experimental data, preparing scientific articles and essays, editing collections, and friendly business meetings took up all his time. There was no time to be bored. He still lived alone, without a family, but he did not feel lonely.

IN THE FLAME OF REVOLUTIONS

Nearly five years passed like this. The fatal year of 1917 came for Russia. M.I. Sumgin once again could not stand it and immediately after the February events left for his homeland in Lukoyanovsky district and became involved into the political struggle. The Socialist-Revolutionaries did not forget the merits of their colleague to the party and elected him to the Central Committee, where he headed the Peasant Department. Sumgin represented the Socialist-Revolutionary Party at the First All-Russia Congress of Soviets of Peasant Deputies held in Petrograd from May 4 to May 28, 1917. At this congress, the Socialist Revolutionaries succeeded in carrying out their proposals for support of the Coalition Provisional Government on the matter of war and peace, national policy, etc. Solving the land question was postponed until the Constituent Assembly, but the resolution included the provision "All lands without exception must go under the jurisdiction of Land Committees". M.I. Sumgin played an important role in the preparation of this decision. In November, Mikhail Ivanovich was elected a member of the Constituent Assembly, the representative body of Russia, which had to adopt a constitution. However, on January 6 (19), the Constituent Assembly was dismissed by the Decree of the Council of People's Commissars.

Sumgin fell into the millstone of two revolutions, which almost took his life. In March 1917, in Nizhny Novgorod, the post of governor with all attributes of the old government, including chancellery, board, servants, etc., was eliminated. Instead of the former governing structure, the Executive Provincial Committee of the Provisional Government headed by the gubernia commissar was established. At the end of July 1917, Mikhail Ivanovich was elected to this high position. He held it until the beginning of 1918. It was a very difficult, unpredictable, and bloody time. Events developed rapidly and were mostly spontaneous. The chaos of authority unleashed pogroms of estates, land seizures, robbery and murder throughout the gubernia. M.I. Sumgin, extremely concerned about the current situation, could do nothing to normalize it.

The situation in the country was critical. According to the Social Revolutionaries, the Bolsheviks could not cope with the situation. Something had to be done. In February 1918, the Central Committee of the Socialist-Revolutionary Party (SRP) discussed the need for terror. V.M. Chernov, Minister of Agriculture in the Provisional Government of A.F. Kerensky, was especially passionate in defending this way. Mikhail Ivanovich Sumgin was categorically against it, considering this method of political struggle impossible, including the struggle against the Bolsheviks and the Soviets. He did not manage to defend his point of view, and left the Central Committee in protest. Then, he left the Socialist-Revolutionary Party; the break was based on fundamental positions. Mikhail Ivanovich stepped back from political activity deciding to devote himself entirely to science. However, he did not manage to return to his old occupation right away. He went to his homeland, took up farming, prepared and read reports for the locals, and worked with young people.

After the murder of V. Volodarsky and M.S. Uritsky, the attempted murder of V.I. Lenin, and a number of other anti-Bolshevik acts, many members of the SRP were persecuted because of their "counter-revolutionary essence". In 1919, members of the Central Committee of the SRP were arrested. The district government was also going to arrest M.I. Sumgin, but he was warned, and he escaped to the village of Sarbaevo in Simbirsk Gubernia under the name of Petr Ivanovich Demin. There he worked as an accountant and rural e teacher for two years.

MOSCOW: THE BIRTH OF SCIENCE

It was disgusting and offensive for him to live under someone else's name, because he had committed no crime. In the hope of being officially legalized, Mikhail Ivanovich moved to Moscow in 1922. He worked as a janitor, as an office clerk in knitwear warehouses, and as a head of the fire statistics section. He lived in the countryside or in a small janitor's closet under the stairs. In his free time, he visited libraries, where he collected materials on the permafrost distribution and on cryogenic phenomena in Russia, enjoying silence and comfort of reading-rooms. Sometimes, he met with his old friend Vicary Samsel, in whose family he found comfort and understanding. But there was no peace of mind, because every day he could be arrested and charged in the case of terrorist activities of the SRP, of which he had once been a member of the Central Committee. At the end of March 1925, the question of his legalization based on the application submitted long ago was finally resolved. M.I. Sumgin visited the office of V.R. Menzhinsky, Deputy Chairman of the Joint State Political Directorate. A conversation took place in the presence of F.E. Dzerzhinsky, during which Mikhail Ivanovich confirmed his decision not to engage in politics. He kept this promise until the end of his life.

In the same year, 1925, he met with a colleague from the Amur business P.I. Koloskov, who at that time headed the Far Eastern Geophysical Observatory and appeared in Moscow as a delegate to the Geographical Congress. Pavel Ivanovich warmly supported Sumgin's desire to create a large generalizing monograph on permafrost and in 1927 published it in Vladivostok [*Sumgin, 1927*] at the expense of the Observatory and even paid the author a small fee. It was a success! The great Russian scientist V.I. Vernadsky said about the publication of Sumgin's book: "The appearance of this work should be considered the starting point for the formation of permafrost science".

Indeed, this book by Sumgin was the first theoretical and regional work on the study of frozen rocks. It summarized all the data known at that time about the geographic distribution of permafrost, its thickness, temperature regime and physical properties, and provided two permafrost maps, which differed dramatically from the previously created cartographic schemes by G.I. Vild, V.B. Shostakovich, and L.A. Yachevsky. In this work, M.I. Sumgin developed the scientific terminology of permafrost studies, evaluated the role of cryogenic processes in human economic activity, and outlined a broad program for studying permafrost. The confident ascent of M.I. Sumgin to the heights of new knowledge began owing to the publication of this book. He himself and many Russian scientists and engineers were the fathers of this new knowledge.

During his work on the monograph, M.I. Sumgin established contacts with institutions interested in solving the problems of growing construction on permafrost. The Leningrad Research Road Bureau of the Central Administration for Road Transport (subsequently People's Commissariat for Railway Transport – PCRT) was one of such organizations. At that time, specialists were focused on stability of a roadbed in harsh climatic conditions. Soil heave, subsidence, and phenomena of icing created extremely unfavorable and sometimes catastrophic situations on the roads. The Bureau proposed M.I. Sumgin to organize a permafrost laboratory to develop methods to control dangerous cryogenic phenomena and to study the structure and physical and mechanical properties of frozen rocks. This initiative of road workers was greatly stimulated by the Fifth International Road Congress held in Milan in September 1925. The congress was accompanied by an exhibition of achievements in road construction. Mikhail Ivanovich sent his report "Roads and Permafrost Soils in the USSR" and two maps "Permafrost Distribution in the USSR" and "A Schematic Map of Permafrost according to the Types of its Geographic Distribution" to Italy. The materials were submitted on behalf of the PCRT and the Department of Local Transport. The "exhibits" made a stunning impression. Since then, M.I. Sumgin's authority as a permafrost scientist constantly grew and did not weaken until the end of his life, not only in Russia but also in many other countries.

In 1927, M.I. Sumgin moved to Leningrad, where he served as a head of the Road Geophysics Department at the Road Bureau of the PCRT. His talent of a scientist and an organizer, an experimenter and a teacher of new scientific disciplines was revealed even more vividly. On the basis of experiments carried out in laboratory conditions, he developed a number of theoretical concepts, which helped to explain many phenomena in frozen grounds and soils. Soil heaving, moisture migration during freezing and thawing of moistened mineral mass, behavior of thin films of water on the surface of rock particles, delayed movement of the freezing front (a so-called zero curtain), formation of ice inclusions of various shapes and sizes, and other cryogenic phenomena. became understandable in a first approximation. Compared to the research of S. Taber [*Taber, 1916, 1917*], a great step forward was made in the field of studying the mechanics of frozen rocks. This work was very important for calculating the bearing capacity of foundations of the engineering structures designed on permafrost soils. The experiments were carried out by M.I. Sumgin with the help of a talented young engineer N.A. Tsytovich, with whom he worked in creative collaboration for many years. Together they created the fundamental work "Foundations of the Mechanics of Frozen Soils" [*Tsytovich, Sumgin, 1937*], which gained world significance and determined the priority of Russian science in the field of engineering geocryology.

Sumgin suggested a number of ideas about the possibility of controlling permafrost processes; in particular, about the use of natural cold to strengthen the foundations, the creation of artificial structures made of ice and frozen soils, the construction of underground warehouses and storage facilities, and the building of dams and temporary winter roads. He initiated a special study of icings on the newly built Amur–Yakutsk Highway. For this important work, M.I. Sumgin invited his friend V.G. Petrov, who brilliantly fulfilled his task. In 1930, M.I. Sumgin edited Petrov's monograph "Icings on the Amur–Yakutsk Highway", which became a classic monograph on the subject, and also prepared several albums of magnificent author's photographs. Articles about the features of the distribution, origin, and development of dangerous icing phenomena appeared in the scientific and industry journals; ideas about the possibility of controlling icings on roads, railroads, and in populated areas of the permafrost zone were clearly stated.

By the early 1930s, M.I. Sumgin published about 30 works, in which he clearly and understandably revealed the functions of permafrost and seasonally freezing rocks and soils as the most important elements of the geological and geographical environment. The great role of permafrost in the organization of the national economy and in the development of nature became so obvious that the specific large-scale studies of the permafrost distribution, structure, and properties became an urgent issue. The accumulated information no longer satisfied the growing demands of practice. The circle of people involved in studying cryogenic phenomena on the vast permafrost territory also expanded. For example, Professor N.I. Prokhorov, who served as a scientific secretary of the newly established Soil Science Institute named after V.V. Dokuchaev, initiated studies of permafrost soils at the agronomical station on the Kola Peninsula. P.I. Koloskov intensified the experiments and tests on thermal reclamation of soils and grounds in the Far East. Permafrost on the Arctic coast of the country was studied extensively. There was a need to create a coordinating center that would determine the strategic positions, tasks, and methods of expeditionary and stationary research. M.I. Sumgin dreamed about this for a long time. He came to the conclusion that it would be most reasonable to establish such a center within the structure of the USSR Academy of Sciences.

M.I. Sumgin shared his thoughts with Academician V.I. Vernadsky, who actively supported the idea. At the end of December 1929, the General Meeting of the USSR Academy of Sciences decided to create a Commission for the Study of Permafrost headed by the famous geologist and geographer Academician Vladimir Afanasyevich Obruchev. Mikhail Sumgin was appointed Scientific Secretary and then Deputy Chairman of the Commission. Sumgin became a soul and an actual head of the new structure. Professors N.I. Prokhorov, A.V. Lvov, A.A. Grigoriev, B.N. Gorodkov, V.B. Shostakovich, A.A. Petrovsky and the future famous scientists N.A. Tsytovich, N.I. Tolstikhin, A.V. Liverovsky, M.Y. Chernyshev, A.M. Chekotillo, and others became members of the coordination center (Fig. 2). Since that moment, the life of

Fig. 2. Active members of the Commission for the Study of Permafrost, Academy of Sciences of the USSR.
From left to right: N.I. Tolstikhin, A.V. Liverovsky, M.I. Sumgin, P.N. Kapterev. Far right standing N.A. Tsytovich (Moscow, 1934).

M.I. Sumgin found new breath and meaning. He became the initiator, conductor, and ideological inspirer of the unique works focused on the integrated study of the unique phenomenon of nature, permafrost.

THE GOLDEN DECADE

The Permafrost Commission started extensive regional and theoretical research and soon outgrew its capabilities. In 1936, it was reorganized into the Committee for the Study of Permafrost (CSP). By that time, Mikhail Ivanovich was awarded the degree of Doctor of Geological Sciences without defending his dissertation. In 1939, the CSP was transformed into a full-fledged academic structure – the V.A. Obruchev Institute of Permafrost Science of the USSR Academy of Sciences. Mikhail Ivanovich took the position of a deputy director for the scientific research. In fact, until the end of his days, he acted as the head of the institute (formally, the director was Academician V.A. Obruchev). Outstanding scientists, who eventually created their own scientific schools – N.A. Tsytovich, V.A. Kudryavtsev, P.I. Koloskov, M.M. Krylov, V.P. Dadykin, and others – started working in this institute. The new academic institution included the Department of General Permafrost Science with an Agrobiological Direction, the Department of Engineering Permafrost Science, Permafrost Laboratory, Administrative and Economic Department, and the Igarka and Anadyr permafrost stations.

Sumgin impressed people by his bubbling energy and breadth of outlook. He created an excellent school of Soviet permafrost scientists in a relatively short using his attractive power and ability to group people of different ages and different specialties around him. Most of them were young people (geographers, geologists, engineers), who grew up under his unflagging attention and care – N.A. Grave, S.P. Kachurin, V.A. Kudryavtsev, A.I. Popov, V.K. Yanovsky, I.Y. Baranov, V.F. Tumel, P.I. Melnikov, I.D. Belokrylov, etc. M.I. Sumgin prepared and delivered (for the first time in the history of education) a course of lectures on permafrost science; special courses were introduced on his initiative in a number of higher educational institutions of the country. He also established the first permafrost graduate school. The formation of the school of Soviet permafrost scientists was stimulated by the organization of annual scientific meetings, seminars, public speeches on permafrost studies, and even a weekly tea party, at which current issues and tasks of upcoming research were actively discussed.

Mikhail Ivanovich paid much attention to organize field works in different areas of permafrost distribution. In 1931, he organized two small expeditions to the European North (to the basins of the Pechora and Usa rivers) and to the Angara region (in the area of the proposed cascade of future hydroelectric power plants). Then, he initiated expeditionary works in other regions of the country. He supervised the Yakut Expedition, which studied the permafrost-hydrogeological conditions of the Yakutsk artesian basin, giant ice fields in the northeast of the USSR, permafrost soils, agriculture, and construction conditions in the Yakut ASSR (Fig. 3). In the Far East (in the area of the future Baikal-Amur Mainline), 10 permafrost

Fig. 3. M.I. Sumgin with the staff of the expedition of the Council for the Study of Production Forces, Academy of Sciences of the USSR in Yakutsk (1939).

teams worked to study the geographic distribution of frozen rocks and their engineering and geological properties. To clarify the southern boundary of permafrost, studies were carried out on the Kola Peninsula, in the basins of the Severnaya Dvina and Pechora rivers, and in the Urals. M.I. Sumgin was eager to visit almost every established expedition. He participated in studying the cryogenic structure and temperature regime of soils, in identifying peculiarities of the occurrence and properties of ground ice, and in solving specific practical problems faced by explorers, designers, and builders. He advised, lectured, and selflessly passed on his experience and knowledge, inspiring those around him with interest in the phenomena of permafrost.

While writing his first book, Mr. Sumgin thoroughly substantiated the necessity of organizing permanent observation points – special research stations – in the permafrost zone. This idea was not new. It had been discussed by the Russian Geographical Society since the 1890s. During the Amur Expedition, permafrost stations were supposed to be established in the Upper Amur region, but World War I and the bloody confrontation of the divided Russian society interfered.

Sumgin developed two variants of the program of permafrost stations considering them to be a kind of experimental and expeditionary bases for the future fundamental research. The minimum program involved studying patterns of the geographical distribution of permafrost, processes of seasonal freezing and thawing of rocks, conditions and factors of the development of dangerous cryogenic phenomena, and physical and mechanical properties of frozen soils and ice. These fields of research had to provide the choice of optimum methods and techniques for engineering development of the area, to identify opportunities and ways of thermal reclamation of cold soils, to solve the problems of water supply, etc. In addition to the aforementioned aspects, the maximum program included the extensive theoretical and experimental work, on the basis of which the crucial issues of the economic development of the entire frozen zone of the lithosphere could be solved.

The establishment of the first permafrost station in the Amur Region in Tygan-Urkan settlement or at Skovorodino station (formerly Rukhlovo) was to be discussed in April 1926 in Khabarovsk at the meeting on the development of productive resources of the Far East. It was planned to create a special committee of representatives of the interested institutions, leading scientists and engineers who possessed the necessary information. Unfortunately, M.I. Sumgin was unable to participate in that meeting, and the question of organizing the permafrost station was temporarily dismissed. However, M.I. Sumgin did not despair. Together with N.A. Tsytovich, he compiled a detailed instruction for the study of permafrost for construction purposes at reference stations [*Sumgin, Tsytovich, 1931*]. He started negotiations on the development of the stations with the heads of interested institutions, primarily with those who had encountered negative forms of permafrost. At the same time, he actively promoted his idea in articles, lectures, and during numerous meetings with the heads of industrial organizations.

As a result, research permafrost stations (RPS) began to appear "like mushrooms after the rain". In 1927, Skovorodino Permafrost Station began operating within a system of the People's Commissariat for Railway Transport. In the following year, the Leningrad Engineering and Construction Institute (LECI) opened the station in Petrovsk-Zabaikalsk. In 1931, a permafrost station was established in Bratsk under guidance of the Central Institute for Geological Prospecting. By the beginning of the war, there were more than ten such stations in the USSR: Igarka (IRPS, 1930), Anadyr (ARPS, 1935), Vorkuta (VRPS, 1936), Yakutsk (YRPS, 1941), as well as stations on Spitsbergen, in Ust-Port, in Amderma, etc.

The programs of these stations with a wide range of geological-geographical and engineering tasks were always prepared by Mikhail Ivanovich or under his control. One of these scientific cells eventually turned into the world-famous Permafrost Institute of the Siberian Branch of the Academy of Sciences of the USSR (Yakutsk). Today, it bears the name of its founder, Academician Pavel Ivanovich Melnikov. M.I. Sumgin visited practically all permafrost stations and expeditions, where he held consultations and unique seminars on research of cryogenic phenomena in the field. The most important area of Sumgin's activity was studying the physical and mechanical properties of frozen and freezing rocks. This work was carried out according to the original methodology both at permafrost stations and in laboratories of Moscow and Leningrad. The tested methodology was introduced at the first opportunity into the programs of the construction and geological exploration departments of higher educational institutions. M.I. Sumgin himself often conducted classes with students or disclosed methodological approaches in his lectures and speeches.

Sumgin initiated many scientific discussions and conferences on permafrost. Instructions and programs for studying frozen rocks were prepared, ambitious experiments and tests were conducted, and works were published under his supervision. Under his editorship, almost every year, materials of various geocryological studies were published: from 1932 to 1940, 10 issues of Proceedings of the Commission on Permafrost Study and the Committee on Permafrost Study were published. He himself followed the motto "Not a day without a line". In a decade, M.I. Sumgin published over 50 detailed articles and four monographs (two of them co-authored). Several all-time

popular books on permafrost [*Sumgin, 1931, 1938; Sumgin, Demchinsky, 1940*], written in a lively, fascinating, and accessible manner, as well as the world's first textbook "General Permafrost Science" [*Sumgin et al., 1940*] prepared in collaboration with his students and colleagues N.I. Tolstikhin, V.F. Tumel, and S.P. Kachurin were published. These books, rich in interesting information, still have not lost their educational and scientific significance (Fig. 4).

Sumgin worked hard and enthusiastically. That is why his creative legacy is unusually large. He not only skillfully, comprehensively and timely generalized the incoming information on the distribution and specific features of the development of permafrost but also created and constantly improved the theory of many cryogenic processes and tried to present his conclusions in mathematical terms and immediately put them into practice. M.I. Sumgin substantiated the hypothesis of the origin of permafrost, introduced the concepts of degradation and aggradation of permafrost, developed some elements of the theory of the icing formation processes, proposed a number of constructive methods to control harmful cryogenic phenomena, laid the foundation for the physics and mechanics of permafrost soils, suggested the idea and created the project of a museum-refrigerator in the thickness of permafrost, etc. The list of Sumgin's scientific works on permafrost issues significantly exceeds 100 titles.

The 1930s were fundamental for permafrost science. A giant breakthrough in the accumulation of knowledge about the frozen layers of the earth took place: the conceptual and terminological apparatus of the new scientific field was formed; maps of the permafrost distribution were compiled; physical and mechanical properties of frozen soils were studied; basic principles of the design, construction, and operation of engineering structures in the permafrost zone were formulated; and much, much more. Permafrost science became on a par with fundamental natural science disciplines, such as soil science, climatology, geobotany, geomorphology, and others. General recognition of the achievements of the young science was largely ensured by the solution of pressing geocryological engineering problems. All this happened on the initiative, under the leadership, and with direct participation of Mikhail Ivanovich Sumgin.

Fig. 4. Covers of M.I. Sumgin's books on permafrost science, climatology, and geophysics.

PERSONAL QUALITIES OF M.I. SUMGIN

Sumgin was an outstanding person not only for his scientific and organizational abilities but also for his excellent spiritual qualities. Everyone who knew him enthusiastically noted sensitivity, responsiveness, crystal honesty, and good-nature of "Uncle Misha" (as his colleagues and friends respectfully called him). He was a modest, unassuming man, who professes a kind of personal asceticism. He did not have large savings, rich apartment, expensive furniture, or expensive clothes. He had books, magazines, and files of notes and documents. These were his main possessions. He bequeathed books to his brainchild, the Permafrost Institute of the USSR Academy of Sciences, and most of his savings were used to pay prizes for the best scientific work in the field of geocryology without mentioning his name. As for ideas, intellectual property, projects and plans, they are all in his articles and books. After the death of Mikhail Sumgin, there were no unfinished manuscripts left.

MOSCOW–TASHKENT: THE LAST DAYS OF LIFE

World War II abruptly changed plans and lives of many people and the entire country. From the very beginning, the Permafrost Institute o of the USSR Academy of Sciences paid much attention to defense issues, designing military airfields, warehouses, underground communications. In the war years, the tasks expanded and became particularly relevant in connection with the creation of defensive line. M.I. Sumgin spent almost all his time at Bolshoi Cherkassky Lane 2. Despite worsening illness, he often traveled to the sites, advised and gave instructions. During the first German air raid on Moscow,

Mikhail Ivanovich received a contusion from a bomb that exploded nearby. The injuries aggravated his already painful condition. By decision of the Presidium of the USSR Academy of Sciences, the heads of many institutions together with their families were evacuated to the deep rear – it was necessary to preserve the potential of science. M.I. Sumgin was sent to the north, to Vorkuta, but then, given his state of health, he was sent to Tashkent together with the staff of the Soil Science Institute of the USSR Academy of Sciences, which was headed by his friend A.A. Rode. Already on the way to Tashkent, M.I. Sumgin began to make plans for his activities at the new site of his settlement. He decided to study the seasonal freezing of soils in the plains of Central Asia and Kazakhstan, as well as to reveal patterns of the permafrost distribution in the Pamir and Tien-Shan mountains. Having arrived in Tashkent, he outlined dozens of sites for personal visits, developed the program of field research, and with the onset of winter began to observe cryogenic processes in the vicinity of the city. However, his health condition worsened. "The disease comes in by poods and comes out by zolotniks", he wrote in one of his letters. Nevertheless, M.I. Sumgin continued to work. Weak and exhausted, he wrote letters almost every day, got acquainted with the reports of the permafrost teams and stations, wrote reviews and notes, and read a lot. Already quite helpless, he prepared a large article "Prospects for Studying Permafrost in the Yakut Republic" and a generalizing work "Permafrost Science" for the collection "Advances in Geological and Geographical Sciences over 25 Years". In these works, he summarized the results of his studies of permafrost and outlined the ways for further research. Both articles were published after Mikhail Ivanovich's death.

M.I. Sumgin tried to behave like a healthy person for a long time, did not surrender to the disease, was cheerful, dreamed of creating a general monograph in two volumes: general and engineering permafrost science, but the disease worsened every day. Friends and colleagues helped with food and medicines. But Mikhail Ivanovich could not be saved. He died on December 8, 1942. He was buried at the Botkin Cemetery near Tashkent.

Science, like life itself, does not die and does not stand still. The ideological and informational foundations of permafrost science shaped by M.I. Sumgin have turned into a powerful branch of natural science, without which no practical issue of developing the cold regions of the globe can be resolved today. Numerous students and followers continue the work of M.I. Sumgin. His image is embodied in the works of writers, artists, and sculptors. A peninsula in the southwestern part of the Franz Josef Land Archipelago, a crater on the planet Mars with a diameter of 22 km, a glacier in the Buordakh massif near the Peak Pobedy (Chersky Ridge), a stream in the vicinity of the village of Bomnak in the Amur region, a school in his native village of Krapivki were named after M.I. Sumgin. The best students of the Permafrost Department of the North-Eastern Federal University (Yakutsk) and of the Geocryology Department of Moscow State University were awarded the M.I. Sumgin scholarship. Seminars, meetings, and conferences are regularly held in memory of the outstanding permafrost researcher. The scientific feat of Mikhail Ivanovich Sumgin has become a source of inspiration and a role model for many people.

References

Sumgin M.I., 1914. Geographic distribution of permafrost in the Amur region. *Izvestiya Meteorol. Bureau of the Amur region* **2**, 1–30.

Sumgin M.I., 1927. *Soil Permafrost within the USSR*. Vladivostok, Far East Geophysical Observatory, 372 p. (in Russian).

Sumgin M.I., 1931. *Permafrost*. Leningrad, Izd. Akad. Nauk SSSR, 85 p. (in Russian).

Sumgin M.I., 1938. *Conquering the North in the Area of Permafrost*. Moscow; Leningrad, Izd. Akad. Nauk SSSR, 155 p. (in Russian).

Sumgin M.I., Demchinsky B.N., 1940. Permafrost Area. Moscow; Leningrad, Izd. Glavsevmorputi, 238 p. (in Russian).

Sumgin M.I., Kachurin S.P., Tolstikhin N.I., Tumel V.F., 1940. *General Permafrost Science*. Moscow; Leningrad, Izd. Akad. Nauk SSSR, 340 p. (in Russian).

Sumgin M.I., Tsytovich N.A., 1931. Temporary Instructions for the Study of Permafrost at Reference Stations for Construction Purposes. *Byull. Leningrad State Institute of Constructions (LOGIS)*, No. 7, 73 p. (in Russian).

Taber S., 1916 June. The growth of crystals under external pressure. *Amer. J. Sci.* 41, 532–556. doi: 10.2475/ ajs.s4-41.246.532.

Taber S., 1917 Apr. Pressure phenomena accompanying the growth of crystal. In: *Proc. Natl. Acad. Sci. USA* **3** (4), 297–302. doi: 10.1073/pnas.3.4.297.

Tsytovich N.A., Sumgin M.I., 1937. *Foundations of the Mechanics of Frozen Soils*. Moscow; Leningrad, Izd. Akad. Nauk SSSR, 432 p. (in Russian).

Received March 23, 2023
Revised March 28, 2023
Accepted April 13, 2023

Translated by V.A. Krutikova